DEVELOPMENT OF AFATINIB LIPID NANOPARTICLES TARGETING NON SMALL CELL LUNG CANCER

ALANOOD SUNHAT ALMURSHEDI

A thesis submitted in partial fulfilment of the requirements of Liverpool John Moores University for the degree of Doctor of Philosophy

2018

Acknowledgments

Published Papers and Conferences

Parts of the theses have been published in ISI Scientific journal:

1. Almurshedi, A.S., Radwan, M.A. Omar, S., Badran, M., Elsaghire, H., Saleem, I.Y., Hutcheon, G.A. A novel pH-sensitive liposome to trigger delivery of afatinib to cancer cells: Impact on lung cancer therapy. Journal of Molecular Liquids. 2018, 259(1): p. 154-166.

Parts of the theses have been presented in international conferences

1. A. S. Almurshedi, M. A. Radwan, S. Omar, M. Alkatib, Saleem I.Y, G.A. Hutcheon. Development of A Novel Pulmonary Liposomal Delivery System for Afatinib to Treat Non-Small Cell Lung Cancer: *In Vitro* Characterization. 43rd Controlled Release Society Annual Meeting, 17-20/7/2016, Seattle, Washington, U.S.A.

Table of contents

List of Figures

List of Tables

List of abbreviations

AFT	Afatinib
CAP1	Adenylate cyclase-associated protein 1
CH	Chitosan
CHEMS	cholesteryl hemisuccinate
CL	Cationic liposomes
CNCMPs	The spray dried PSL NPs using LEU and CH
d_{ae}	The theoretical primary aerodynamic diameter
DDS	Drug delivery system
DOPC	1,2-dioleoyl-sn-glycero-3-phosphocholine [18:1]
DOPE	dioleoylphosphatidyl-ethanolamine
DOPS	Dioleoylphosphatidylserine
DOTAP	1,2-dioleoy-3-trimethylammonium-propane Chloride salt
DPIs	Dry powder inhalers
DPPC	Dipalmitoylphosphatidylcholine
DSPC	1,2-distearoyl-sn-glycero-3-phosphocholine[18:0]
EE%	Encapsulation efficiency %
EGFR	Epidermal growth factor receptor
FDA	Food and Drug Administration
FPD	The fine particle dose
FPF	Fine particle fraction
HEPES	HEPES 4-(2-hydroxyethyl)-1-piperazineethanesulfonic acid
HER2	Human epidermal growth factor receptor 2
HPLC	High performance liquid chromatography
HSPC	hydrogenated soya phosphatidylcholine
IC_{50}	The concentration of drug needed to inhibit 50% of cells
ICH	International Conference on Harmonization guidelines
LDHA	Lactate dehydrogenase-A
LEU	L-leucine

LOD	limit of detection
LOQ	limit of quantification
LUVs	large unilamellar vesicles
MLVs	multilamellar vesicles
MMAD	Mass median aerodynamic diameter
MTT	3-4, 5-dimethylthiazol-2-yl-2,5-diphenyl tetrazolium bromide
NCMPs	Nanocomposite microparticles
NGI	Next Generation Impactor
NL	Nontargeting liposomes (Control)
NPs	Nanoparticles
NSCLC	Non small cell lung cancer
PC	Phosphatidylcholine
PCA	Principal Component Analysis
PDI	Polydispersibility index
PE	Phosphatidylethanolamine
PG	Phosphatidylglycerol
pMDIs	Pressurized metered dose inhalers
POPC	1-palmitoyl-2-oleoyl-sn-glycero-3-phosphocholine
PSL	pH-sensitive liposomes
RH	Relative humidity
SCF	Supercritical fluids
SCLC	Small cell lung cancer
SD	Spray drying
SUVs	small unilamellar vesicles
TEM	Transmission electron microscopy
TKI	Tyrosine kinase inhibitor
Tm	transition temperature

Abstract

Lung cancer is the most common cause of cancer-associated mortality in males and females globally. Widespread research is currently focused on the development of novel approaches for targeting non small cell lung cancer with different therapeutic nanotechnologies. In this study, a sensitive and selective HPLC method was developed for the quantification of afatinib (AFT) in formulations. Novel drug delivery systems based on cationic (CL) and pH-sensitive liposomes (PSL) for AFT were developed, with different ratios of lipid to AFT, using a film hydration method. The obtained liposomes had a small particle size of less than 50 nm with a low polydispersibilty index and acceptable zeta potential. The highest Encapsulation Efficiency (EE%) of AFT reached 43.20%, 50.20%, and 52.01% for NL (Non targeting liposomes), PSL, CL, respectively at the 1:0.5 ratio of AFT: lipids. The *in vitro* release study confirmed that all formulations had sustained release profiles in pH 7.4. However, in acidic pH values, PSL exhibited fast release. The stability study, conducted at 4°C and 25°C for 1 month, showed that the characteristics of liposomes in liquid form did not change significantly over this period. *In vitro* cytotoxicity studies revealed high antitumor activity of PSL on all cell lines at 0.75 μM concentration after 24 h exposure, based on using the Annexin V assay. A proteomics study identified 12 proteins which can be used as biomarkers capable of prediction of treatment response and choice of therapy for two different types of human NSCLC cells (H-1975 and H-1650).

Spray drying was used to produce nanocomposite microparticles (NCMPs) using L-leucine and coated using different ratios of chitosan for the optimized PSL NPs. The particles had a corrugated surface except at high CH ratios, where more homogenous and smooth particles with some small indentations were obtained. The powder properties showed good flow properties and reproducible size. Coated NCMPs showed a delayed drug release profile compared to PSL NPs and the best correlation with the Higuchi model. A stability study at 40°C/ 75% ± 5% relative humidity (RH) showed large changes in the drug content for all coated NCMPs powders. Analysis of the *in vitro* aerosolization performance demonstrated a mass median aerodynamic diameter (MMAD) of 3.24 – 5.85 μm and fine particle fraction (FPF%) of 54.20-33.66%. The particle size of the reconstituted powders was < 100 nm, which is within the size range to be effectively taken up by tumor cells. Assessment of the stability of spray dried liposomes after 3 months of storage at 40 °C/75% RH, showed that fusion

and aggregation of the liposomes occurred in all samples tested. The C1NCMPs (lipid: LEU: CH ratio of 1:1.5:0.5) exhibited the highest FPF (51.2%) and fine particle dose (FPD) (40.0 µg of AFT) indicating deep lung deposition. Further cell viability studies of C1 NCMP, at a concentration of 0.75 µM on H-1975 NSCLC cell line showed a good toxicity profile comparable to PSL nanoparticles (NPs). The obtained data indicates that pulmonary delivery of PSL NCMPs is a potential new clinical strategy for better targetability and delivery of AFT for the treatment of lung cancer.

Chapter 1

General Introduction

1.1. Introduction

1.1.1. Lung cancer

Lung cancer is responsible for 1.38 million annual mortalities worldwide [1]. It is the most common cause of cancer associated mortality in males and the second in females after breast cancer [2]. In the Kingdom of Saudi Arabia, the rate of lung cancer has increased significantly in recent years, accounting for 3.7 % of all newly diagnosed cancers. This is mainly due to the increased prevalence of cigarette smoking among Saudi men and women. Recently, the Saudi Cancer Registry has reported that lung cancer ranked the fifth most common in males and fifteenth in females [3]. Of the 3.7 % of those with lung cancer, 326 (74.9 %) were males and 109 (25.1 %) females, with a male to female ratio of 3:1 [4, 5]. Alamoudi also reported that lung cancer was the most common cause of hospitalization in Saudi male patients admitted with respiratory diseases [5]. In the United Kingdom, lung cancer is among the most frequently diagnosed types of cancer and accounts for 20% of new cancer cases (34,000 new patients) annually [6].

Lung cancer is commonly related to smoking and is thus often classified as a social disease with an associated stigma attached. The majority (85 %) of cases of lung cancer are due to long-term tobacco smoking. These cases are often caused by a combination of genetic factors and exposure to radon gas, asbestos, second-hand smoke, or other forms of air pollution. Contrary to popular belief, lung cancer also affects non-smokers and about 10–15% of cases occur in people who have never smoked [7]. For example, in women only 65% of cancer deaths are a result of smoking, with lung cancer killing more women than breast, ovarian and uterine cancers combined. Regardless of cause, death from lung cancer is high; with less

than 10% of those diagnosed surviving for 5 years [8]. This may partly be due to the length of time between the onset of cancer symptoms and the patient's presentation to health care, leading to more late-stage diagnosis and therefore, less eligibility for potentially curative treatment.

The most common symptoms of lung cancer are dyspnea, cough (including coughing up blood), chest pain, and weight loss. Clinically, lung cancer is divided into two main types according to the characteristics of the disease and its response to therapy (Figure 1- 1).
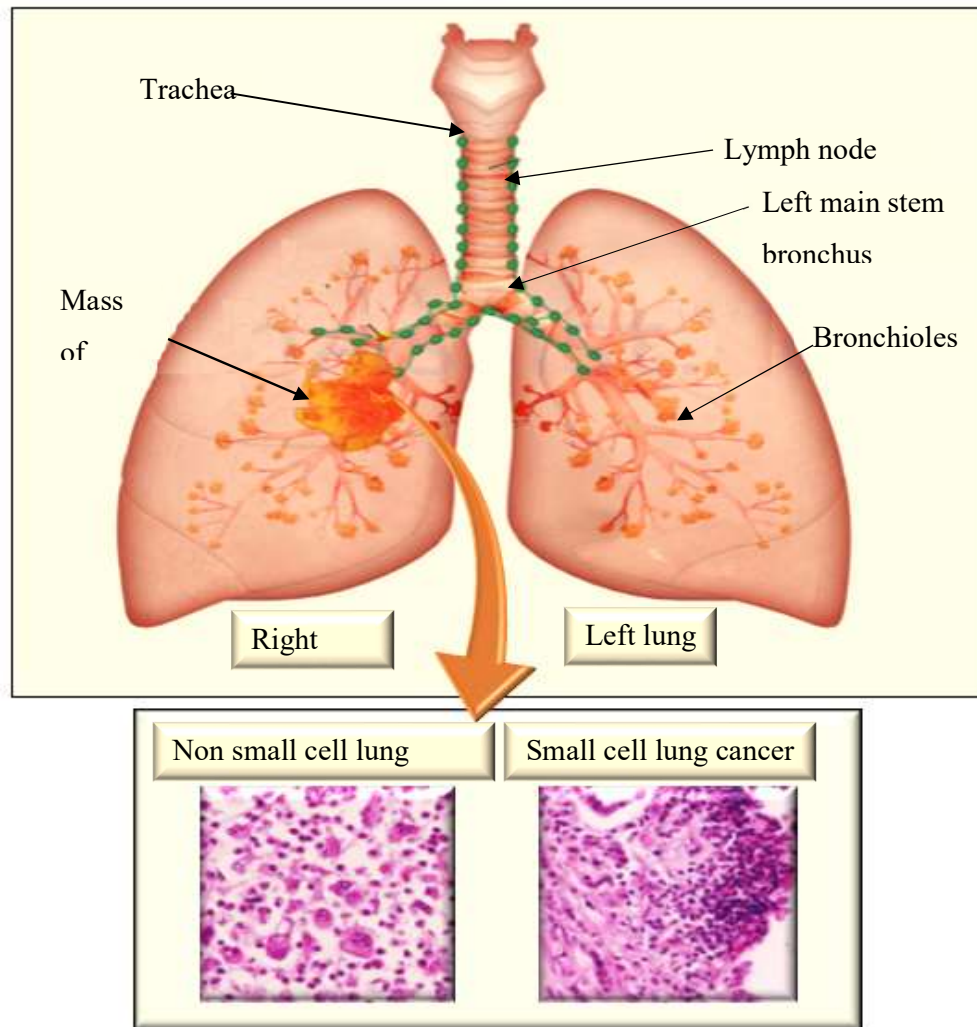
Figure 1- 1: The structure of the lung and histological photographs of non small cell lung cancer (left bottom) and small cell lung cancer (right Bottom) [9]**.**

Non small cell lung cancer (NSCLC) can be located in the mid-chest, but it is also found in other parts of the lung. According to the current World Health Organization classification [9], NSCLC is classified into the following histological types:

1. Squamous carcinoma, the most common type, found in the central or inner parts of the lung and/or along the trachea, accounting for 35% of all NSCLC. The cells are well differentiated and metastases occur comparatively late.

2. Adenocarcinoma, accounts for approximately, 27% of lung cancers and is associated with brain and bones metastases. It is the most common type of lung cancer in people working with asbestos and is also common in non-smokers, older people and women.

3. Large-cell carcinoma, which accounts for 10% of all lung cancers. It is less well differentiated than the first type and metastasizes earlier.

In the same classification, small cell lung carcinomas (SCLC) is typically more centrally located in lungs and includes the following histological types: typical carcinoid tumor, atypical carcinoid tumor and large cell neuroendocrine carcinoma. Accounting for about 85% of all lung cancer cases, NSCLC is the most common of the two types while the remaining 15 % are small cell lung cancer [10]. Clinical staging and identification of the histological type are essential to finding the best therapeutic strategy for treating such patients. Therefore, the classification of lung cancer into SCLC and NSCLC was necessary for treatment of patients with lung cancer in hospital routine practice. However, for clinical treatment, NSCLC sub classification by molecular factors and immunohistochemistry has become mandatory. Explanations for this are; better understanding of cancer biology, favored

efficacy or toxicity of novel drugs in subtypes of NSCLC, and the demonstration of therapeutically related driver mutations in subcategories of NSCLC [11].

1.1.1. Management of NSCLC

Surgery is the treatment of choice in the early stages of NSCLC. Unfortunately, surgery is only accessible to a few patients because around 70% of patients with NSCLC will present with advanced tumors. Patients with more advanced stages of disease are treated with chemotherapy, radiation therapy, or chemoradiotherapy [12]. Chemotherapy has a significant role in treating patients with both SCLC and NSCLC. For patients with early-stage NSCLC, chemotherapy can be used either before surgery is carried out or following surgery to help treat the patient and improve long-term survival rates. However, conventional chemotherapy is highly non-specific in targeting the drugs to the cancer cells causing undesirable side-effects to healthy tissues such as neurotoxicity [13] and bone marrow suppression [14, 15].

New technologies and understandings can now be used to discover targets for innovative drugs. Fortunately, over the past decade, there have been major advances in the understanding of the pathogenesis and management of lung cancers, leading to a remarkable evolution in diagnosis, improved staging and new therapeutic options. Therefore, many genes and proteins, including small-molecule signal transduction inhibitors implicated in tumour growth, are now potential clinical targets and are being developed for the treatment of cancer. The tyrosine kinases, an example of such targets, are enzymes that phosphorylate proteins leading to the activation of signal-transduction pathways which play an important role in different biological processes, including cell growth, differentiation, and death. Therefore, the discovery of frequent molecular alterations in NSCLC, particularly epidermal growth factor receptor (EGFR) mutations, has led to a new treatment paradigm that includes targeted agents.

EGFR is a transmembrane glycoprotein which widely expressed (40-80%) in NSCLC. [16].

One of the signaling pathways often dysregulated in malignant epithelial cells is the Erb family of receptor tyrosine kinases, also known as the HER family, and their associated ligands. They comprise four structurally related transmembrane receptor tyrosine kinases (Figure 1- 2); epidermal growth factor receptor (EGFR; ErbB1), human EGFR 2 (HER2; ErbB2), ErbB3 and ErbB4. The activation of these receptors leads to phosphorylation of tyrosine kinase in EGFR proteins, which in turn triggers multiple signal transduction cascades [17]. The resulting phosphotyrosine residues are significant components of multiple downstream signaling processes necessary to activate cell proliferation and other cell responses, including angiogenesis, cell migration, and decreased apoptosis, all of which can lead to tumor growth [18].

Knowing the role of the EGFR receptor signaling cascade in cancer led to the development of new agents designed to specifically target these receptors. Significant progression was made in the treatment of NSCLC following the observation that mutations in the kinase domain of EGFR strongly linked with sensitivity to EGFR tyrosine kinase inhibitors (TKIs) [19].

Recently, numerous EGFR targeting agents have been approved for the treatment of NSCLC. Erlotinib and gefitinib, the first-generation small-molecule EGFR-TKIs, bind reversibly to the kinase domain and efficiently inhibit both wild-type and mutated EGFR. These drugs cause notable improvements in progression-free survival in comparison to conventional chemotherapy. However, primary and acquired resistance against first-generation EGFR-TKIs usually occurs within a year [20]. The problems with resistance to first-generation EGFR-TKIs supports the need for development of new strategies for such patients. These include agents which can form

irreversible covalent bonds to the EGFR TK domain (in contrary to first-generation TKIs that act through competitive binding with ATP to induce reversible inhibition), so theoretically extending inhibition of signaling. Also, many of the new drugs are designed to block other EGFR family members, leading to inhibition of similar signaling pathways which may be involved in resistance [21]. Afatinib (AFT) targeting of several members of the EGFR family, is one such strategy[22].
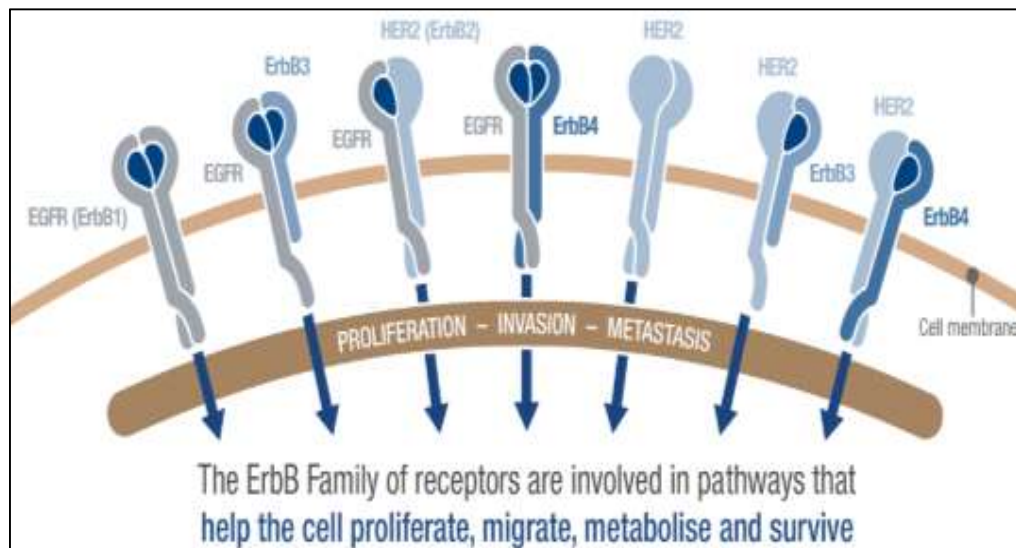
Figure 1- 2: Signal transduction. Adapted with permission from [15].

1.2. Afatinib

Afatinib (AFT) is a novel, potent, irreversible small-molecule tyrosine kinase inhibitor (TKI). In July 2013, the U.S. Food and Drug Administration (FDA) approved AFT as an oral once-daily tablet (produced as the dimaleate salt, Gilotrif; Boehringer Ingelheim) for the first-line treatment of patients with metastatic NSCLC and EGFR mutation [23]. It is an aniline–quinazoline derivative (Figure 1- 3). Gilotrif

tablets are available in 40 mg, 30 mg, or 20 mg of AFT (equivalent to 59.12 mg, 44.34 mg, or 29.56 mg AFT dimaleate) [24]. The suggested dose of AFT is 40 mg once daily; but a maximum of 50 mg/day or a minimum of 20 mg/day, can be prescribed based on tolerability [25]. At the approved AFT dose of 40 mg, there is low AFT– drug interaction potential. Afatinib pharmacokinetics are not affected by commonly co-prescribed medicines such as cytochrome P450 inducers or inhibitors and acid-reducing agents, but concomitant treatment with strong inducers or inhibitors of P-gp can affect the pharmacokinetics of AFT, and consequently caution is advisable with this combination. Treatment is continued until disease progression or undesirable toxicity occurs [26].
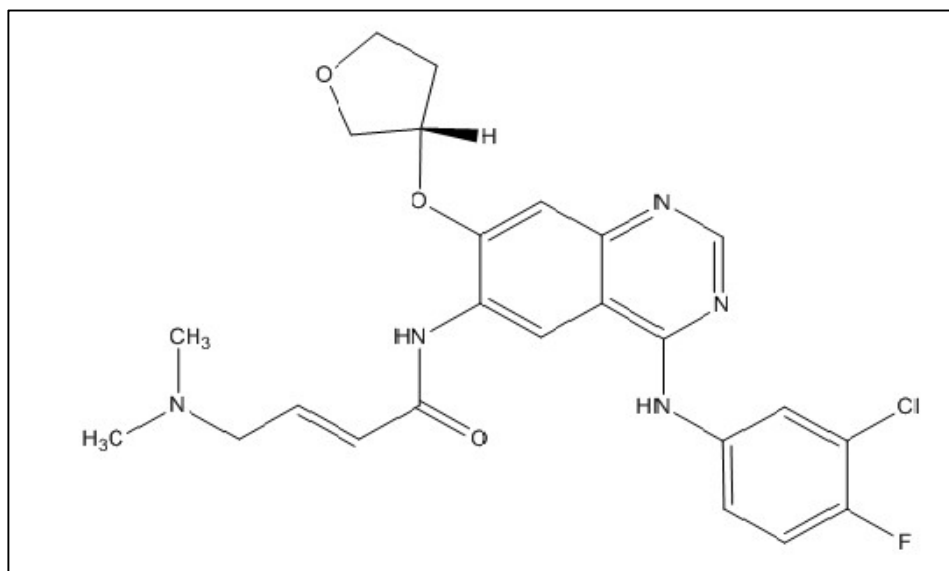
Figure 1- 3: Chemical structure of afatinib

1.2.1. Mechanism of action

Afatinib binds irreversibly to the intracellular kinase domains, inhibiting tyrosine kinase autophosphorylation, and subsequently preventing intracellular signaling. By targeting the ErbB family of receptors (Figure 1- 2), AFT has broader antitumor activity against receptors with acquired mutations that are resistant to the first generation of TKIs [27]. The irreversible binding of AFT, unlike other compounds which are reversible, provides a sustained, selective, covalent and complete ErbB family blockade. This means that AFT may provide the benefit of enhanced inhibition of tumor cell proliferation and effectiveness across a wide range of cancers compared to first generation of EGFR TKIs, which offer single, reversible, receptor blocking [28].

1.2.2. Pharmacokinetics

After oral dosing, AFT reaches peak plasma concentrations within 2 to 5 h, in patients with solid tumours (Table 1- 1) [29]. The absolute bioavailability of AFT in humans has not been studied but the relative bioavailability was 92% after a single dose of a 20 mg tablet compared with an oral solution and was ≈ 95 % plasma protein bound *in vitro* [10]. Afatinib has a large volume of distribution, with a mean value of 2,870 L reported at steady state in patients receiving AFT 40 mg once daily [29]. Furthermore, patient age, weight, gender or ethnicity do not have a clinically related effect on the clearance or exposure of AFT [30]. A high fat meal has a moderate effect on AFT exposure and thus, AFT should be taken without food. There is inter-patient variability in AFT plasma concentrations in patients receiving the drug [31].

Table 1- 1: Pharmacokinetic parameters of 40 mg Afatinib after multiple once-daily doses in cancer patients [29-30].

Parameter	Afatinib
Usual starting dose (mg/day)	40
T_{max} (h)	$2-5$
V_d (L)	2870
Protein binding	95
$t_{1/2}$ (h)	37
F absolute	Not known
CL (mL/min)	$1070-1390$
Metabolism	Minimal hepatic metabolism
Renal excretion	$< 5\%$
Accumulation	2 to 3-fold
Food effect	AUC $\downarrow$ 39%

1.2.3. Safety and tolerability of afatinib

Clinical studies indicate that AFT is well tolerated with most adverse effects stated as mild-to-moderate. The most common gastrointestinal problem is diarrhea, but nausea, vomiting, mucositis and fatigue were also detected, similar to those reported with other TKIs and were commonly self-limiting or effectively controlled by suitable medication. Regardless of the adverse events reported, only 8% of patients treated with AFT discontinued the treatment [32].

Afatinib demonstrated effective inhibition of wild-type EGFR, HER2, and ErbB4 at low nano-molar concentrations, while reversible TKIs erlotinib and gefitinib only

inhibited EGFR [33]. In comparison with erlotinib and gefitinib, AFT was also active against NSCLC cells that overexpress HER2. Afatinib induced apoptosis and inhibited cellular growth in several tumor cell lines, and caused tumor shrinkage in xenograft models of many cancer types, including NSCLC, colorectal cancer, pancreatic cancer, and head and neck squamous cell cancer [34]. Afatinib also confirmed good activity in preclinical models of tumor cells resistant to reversible EGFR inhibitors, demonstrating that irreversible ErbB family blockade was effective in patients with reversible EGFR-TKI-resistant illness [34, 35].

Also, AFT inhibited EGFR harboring L858R/T790M at low nano-molar concentrations (half maximal effective concentration (IC50), 9–10 nM. Moreover, AFT inhibited cell growth in cultured lung cancer cells (IC50, 99 nM) and a lung cancer xenograft model harboring L858R/T790M. In addition, AFT is active *in vitro* and *in vivo* in the presence of "secondary" mutations; a mechanism responsible for 50%–60% of cases of resistance. A study of xenograft models showed that AFT has a broad spectrum of antitumor activity *in vivo* demonstrating an improvement in overall survival as a first line treatment as compared to conventional chemotherapy. In patients with lung squamous cell cancer, AFT established an important increase in overall survival and progression-free survival compared with erlotinib [36].

Taken together, the potent activity and the irreversible inhibition of signaling from all ErbB family receptor dimers formed by EGFR, HER2, and ErbB4, and preclinical antitumor activity of AFT, provides biological validation of the effectiveness of AFT in clinical studies. Therefore, AFT is considered as a new treatment choice for lung cancer patients hence there is an urgent need to develop novel and innovative technologies to overcome the side effects and for better targeting to fight this fatal cancer.

1.3. Nano-scale drug delivery systems

Nanotechnology includes the creation and use of materials, devices or systems at nanoscale (3-200 nm), that can be fabricated using a variety of materials [37]. Advances in nanotechnology have contributed to recent innovations for cancer treatments, including diagnostic techniques, by enabling interactions with cells at a molecular level. Frequently, it costs less to develop new ways of administering existing drugs with improved efficacy and bioavailability, reduced dosing frequency and lower side effects, than to develop new drugs [38, 39].

Multifunctional and smart nanomaterials are multipurpose carriers for different biomedical applications such as tumor targeting [40], and drug delivery [41]. Cancer nanotechnology has the potential to offer new opportunities for personalized oncology in which therapy is based on each individual's molecular and cellular profile [42].

Nanoparticles (NPs) are emerging as a new class of therapeutics for cancer. NPs are solid, colloidal particles containing macromolecular materials with a size range from 10 nm to 100 nm. Nanoparticles can be designed to help therapeutic drugs easily cross biological barriers, enable molecular interactions, and to detect molecular changes. Generally, the drug is entrapped, dissolved, adsorbed, attached and/or encapsulated into or onto a nano-matrix [43]. Compared to microparticles, nanoparticles have a larger surface area with modifiable optical, electronic, magnetic, and biologic properties. Additionally, new methods of administration can be explored by including the existing drug in a new drug delivery system (DDS) [44].

There is now extensive interest in formulating anticancer drugs for pulmonary delivery, inspired by the potential utility of the lung as a portal for the administration of drugs to treat both lung disease and for systemic delivery [45]. Using dry powder inhalation (DPI) for targeted pulmonary delivery is an attractive choice that can be

optimized for inhalation to create a flexible platform that can accommodate wide range of active pharmaceutical ingredients and medical conditions [46]. Even though some chemotherapeutics can be delivered directly through the pulmonary or intratracheal route [47], most anticancer drugs cannot be inhaled in their traditional form and need a specific DDS to enable deposition directly into the lungs [48]. Recently, several different DDS have been developed for the inhalation of different classes of drugs but not all have been effective because of their limited capability to specifically target tumor sites. For example, in cancer chemotherapy, many drugs kill normal cells as well as the cancer cells. Another difficulty includes premature drug loss through fast clearance from the blood stream and metabolism. Thus, there is a growing need for development of drug delivery strategy that selectively targets tumor cells and direct local delivery. Moreover, the development of new DDS is a continuous procedure, starting from the early research to product development, passing through all stages of clinical trials and finally resulting in commercial utilization [49].

Nano-sized systems have received significant attention as pharmaceutical carriers with a varied range of applications, including vaccine adjuvants, carriers in medical diagnostics and analytical biochemistry, support matrices for chemical ingredients and solubilizing agents for various materials. Moreover, attention has been given to their role as an interface between the patient and the drug, and can be administered through different routes (oral, intravenous, transdermal or inhalation) [44]. The DDS can be successfully formulated and enhance the therapeutic efficacy of a great number of pulmonary anticancer drugs [49]. This holds considerable promise for improving the treatment of many diseases by minimizing nonspecific toxicity and enhancing the efficacy of therapy. Therefore, nanocarriers are considered as new, "smart" DDSs

which can be targeted towards specific sites and organs and triggered to release the drug whenever needed [50]. These DDS are created from materials that are sensitive to a wide range of external stimuli, including light, ultrasound, electrical and magnetic fields, and specific molecules [51]. The most studied DDS are nanocarriers which are mostly associated with drugs that are pharmacologically potent but could not be administered as a "free" drug owing to high toxicity or low bioavailability[52]. Nanocarrier systems are known to increase drug bioavailability and therapeutic efficiency and decrease nonspecific toxicity of potent anticancer drugs [53]. In addition, their biocompatibility, and ability to deliver the drug into the target tissue using low drug doses make nanocarriers an ideal delivery vehicle [54] . Therapeutic strategies to effectively target tumor sites can be classified into two different strategies: passive targeting and active targeting [55].

1.3.1. Passive targeting

Passive targeting takes advantage of the enhanced permeation and retention (EPR) of tumor tissue. This EPR results in higher local permeability and retention of drug loaded particles and allows the possibility of targeting cancer cells in which the fast and newly growing cancerous tissue interrupts the structure of normal tissue and vessel walls, which in turn, can be easily accessible to toxic chemotherapeutic drugs. Some drugs can be administered as prodrugs or inactive drugs, which once exposed to the tumor environment, can be switched on to become highly active [56]. The passive cancer targeting potentially benefits from imperfect vasculature and poor lymphatic drainage produced by angiogenesis in tumor tissues. The accumulation of drug loaded particles in the tumor tissues could be enhanced by optimizing the properties and features of the particulate carriers, such as surface charge, chemistry, and particle size [57].

1.3.2. Active targeting

A molecular targeting moiety can be used to precisely target biomarkers or receptors on the tumor cells, thus enabling better accumulation of the drug in the tumor tissue. Active cancer targeting has been extensively studied using DDS to target tumor cells and decrease the systemic toxicity [58]. This strategy can be used to direct nanoparticles to cell surface carbohydrates, receptors, and antigens. Active targeting can also use targeting ligands on the surface of nanoparticles towards membrane receptors on cancer cells causing enhanced cellular uptake of nanoparticles[56].

1.4. Inhalation therapy for lung cancer

Administration of drugs to the lung by aerosolisation has been used for many years to treat mainly localized disease conditions within the bronchi. The pulmonary route of administration can distribute therapeutic agents to the tumor sites while minimizing their distribution in the systemic circulation. Systemic drug delivery is less successful because only a limited amount of the chemotherapeutic drugs arrives at the lung tumors, even when administered at high dose. A more promising therapeutic index can be attained for lung treatment when drugs are administered locally by inhalation rather than by other routes.

Pulmonary delivery is a non-invasive route, with the advantages of; site-specific delivery, good permeability of the pulmonary epithelium, lower enzymatic activity compared to the gut, a large surface area, a very thin absorption membrane, and massive vascularization (5 L/min), which rapidly distributes molecules throughout the body [59]. Compared to other delivery routes the greatest advantages of pulmonary administration are the improved bioavailability of drugs in the lung due to higher absorption rates, decreased drug doses and a fast onset of action. Therefore, inhalation

therapy has been used to treat local lung diseases such as microbial infections and asthma along with systemic diseases like diabetes and it plays a significant role in gene delivery [60]. Also, inhalation therapy can help in the fight against cancer by delivering drugs locally to the tumor cell in lungs [61]. However, the delivery of anticancer agents by inhalation can be limited due to [49, 62]:

1) The short residence of the inhaled drug in the lung and the potential for systemic adverse effects.

2) The low aqueous solubility of drugs which may lead to local irritation and inflammation in the lung airways.

3) The poor intracellular penetration of some drugs to treat intracellular pathogens.

4) The inability of drugs to target tumor cells and tissues selectively.

The development of novel approaches for targeting lung cancer with different therapeutic carriers is of great importance. Carriers providing sustained drug release in the lungs could improve therapeutic outcomes of inhaled medicines. Their objectives are to keep the drug load within the lungs for an extended period of time and to increasingly release the drug locally at therapeutic levels. Sustained therapeutic drug concentrations should improve local therapeutic efficacy and decrease systemic adverse effects as the bio distribution through the systemic circulation is minimized. In addition, a sustained-release inhaled formulation could avoid peaks in local drug concentrations that could be toxic to the pulmonary tissue. This is mainly relevant for chemotherapeutic drugs.

1.5. Liposomes

Liposomes are small spherical vesicles, formed with one or more lipid bilayers constituted of amphiphilic lipids and may include cholesterol. Usually, liposomes are

used to deliver hydrophobic or hydrophilic drugs through inclusion in either the lipid bilayer itself or encapsulation in the inner aqueous core, respectively (Figure 1- 4). Liposomes can take the form of a wide variety of structures, but all consist of one or more lipid bilayers enclosing an aqueous space [63]. Liposomes can be made using different lipids; neutral, anionic or cationic, from natural or synthetic sources, and most include cholesterol (CH) or surfactants. The most commonly used lipids are the lecithins: phosphatidylethanolamine (PE), phosphatidylcholine (PC), phosphatidylglycerol (PG), phosphatidylinositol, phosphatidylserine and sphingomyelin. Most of these lipids exist naturally in the lung therefore have good biocompatibility [64]. Liposome properties can be determined by lipid composition, surface charge, size, lamellarity and the technique of preparation. There are different techniques for liposomal preparation, which result in vesicles that may be small or large unilamellar vesicles, or multilamellar vesicles [65] .
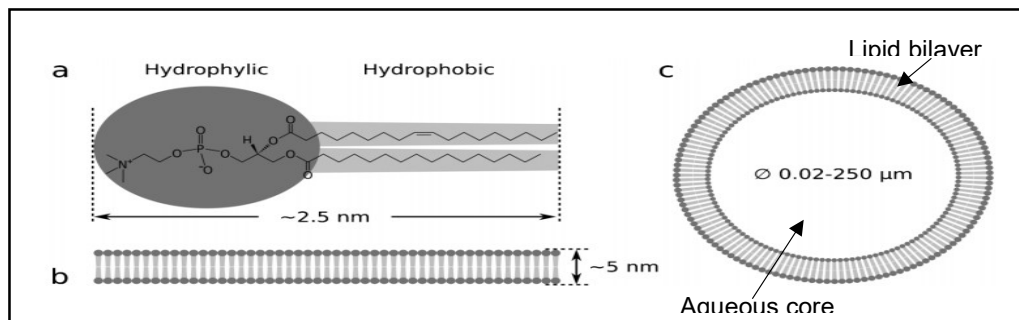
Figure 1- 4: (a) The structure of one POPC (1-palmitoyl-2-oleoyl-sn-glycero-3-phosphocholine) lipid molecule, showing the hydrophilic head and hydrophobic tail. POPC is a naturally-occurring lipid and is commonly used in the production of synthetic liposomes. (b) The heads and tails of the lipid interact to self-assemble into a membrane structure, and (c) a lipid vesicle. Adapted with permission from The Royal Society of Chemistry [63]. Copyright 2013.

1.5.1. Classification of Liposomes

Liposomes can be classified according to their size, formation method or the number of bilayers in the vesicle. Based on the number of bilayers, they are often split into small unilamellar vesicles (SUVs; 25-100 nm), large unilamellar vesicles (LUVs; 0.1-1 μm), and multilamellar vesicles (MLVs; 0.1-20 μm) (Figure 1- 5) [65]. MLVs are usually made using a thin-film hydration method, the most common method. Other methods include, organic solvent injection [66], reverse-phase evaporation [67], and dehydration-rehydration [68]. All the liposome preparation techniques involve 4 basic steps as illustrated in Figure 1- 6. Techniques such as sonication, membrane extrusion, homogenization and/or freeze-thawing are used to control the size and size distribution. Furthermore, oligolamellar vesicles (0.1-1 μm) have been reported; these are liposomes containing two or three bilayers which can be produced using a reverse phase evaporation technique [67] or an ethanol-based proliposome technology [69]. For the pulmonary delivery of liposomes, MLVs are usually prepared by the traditional thin-film hydration technique, followed by either sonication to produce SUVs, or membrane extrusion to get smaller MLVs or LUVs [70].
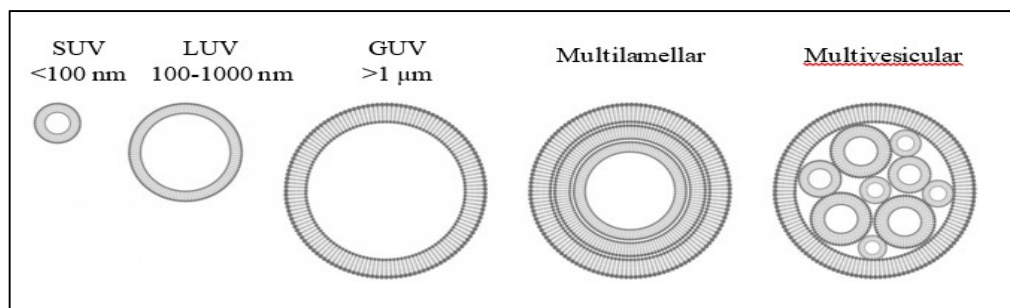
Figure 1- 5: A schematic representation of vesicle size and lamellarity classification system of liposomes. Small unilamellar vesicles are <100 nm in diameter and large unilamellar vesicles are between 100 and 1000 nm. Multilamellar vesicles have more than one membrane layer, and can encapsulate smaller vesicles. Adapted with permission from The Royal Society of Chemistry [63]. Copyright 2013.
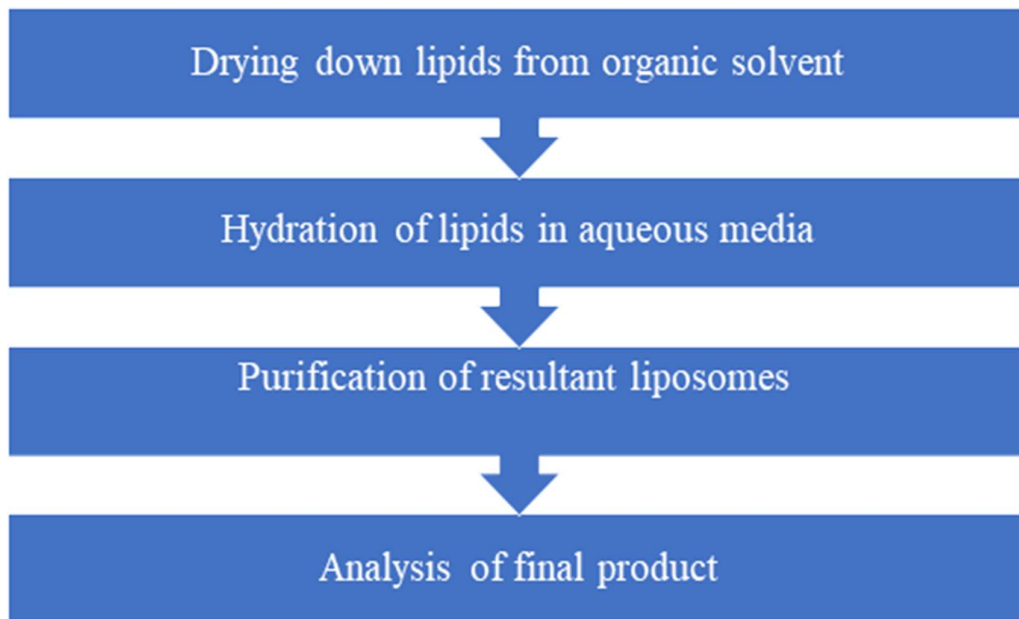
Figure 1- 6: Common Steps in liposomes preparation

1.5.2. Types of liposomal drug delivery systems

Liposomal DDS have been reported to improve the administration of chemotherapeutic agents in the treatment of lung cancer and inhibition of metastases when compared to other routes of administration [71]. Liposome encapsulation can increase the antitumor efficacy of the incorporated drugs by providing more selective delivery or targeting to the tumor tissue, while in other cases, toxicity is decreased by avoidance of critical normal tissues [72].

Due to extensive developments in liposome technology, a number of FDA approved nano-formulations of drugs for different diseases, are available on the market for human use (Table 1- 2) or are under different phases of clinical trials. Treating cancer was the utmost widely explored area in terms of clinically approved products utilizing liposomes. The first nano-sized liposomal based product was Doxil® (1995) for the

treatment of patients with ovarian cancer and AIDS-related Kaposi's sarcoma. Doxil® has a prolonged circulation time, better release and accumulation in the tumor site, which increased drug efficiency and decreased adverse effects. Later, DaunoXome® was developed for the delivery of daunorubicin, for the management of advanced HIV-associated Kaposi's sarcoma [73].

Liposomal formulations are also available for conventional chemotherapeutic drugs such as platinum derivatives [74]. In patients with NSCLC, clinical trials have shown reduced toxicities following administration of liposome formulations of cisplatin, but without significant improvements in efficacy relative to free drug [75].

Lipoplatin (Regulon, Inc.) is one of the most promising liposomal platinum drug formulations under clinical trial. Pre-clinical studies of Lipoplatin in animals reported that it has lower side effects, and remarkably lower nephrotoxicity compared to cisplatin [76]. SPI-77 (Alza Pharmaceuticals) is another liposomal cisplatin formulation. Preclinical studies in tumor-bearing mice indicated higher antitumor activity in contrast to cisplatin with higher cumulative doses of SPI-77 being well tolerated [77].

There are four main variations of liposomal delivery systems: conventional liposomes, ligand-targeted liposomes, sterically-stabilized liposomes, and a combination of the above. The first generation is the conventional liposomes which consist of a lipid bilayer that can be composed of anionic, cationic, or neutral phospholipids and cholesterol.

Table 1- 2: Therapeutic areas covered by liposomes-based products.

Area	Clinical Products	Active Agent	Indication
Cancer therapy	Doxil®	Doxorubicin	Ovarian, breast cancer, Kaposi's sarcoma
	DaunoXome®	Daunorubicin	AIDS-related Kaposi's sarcoma
	Depocyt®	Cytarabine/Ara-C	Neoplastic meningitis
	Myocet®	Doxorubicin	breast cancer
	Mepact®	Mifamurtide	High-grade, resectable, non-metastatic osteosarcoma
	Marqibo®	Vincristine	Acute lymphoblastic leukaemia
	Onivyde™	Irinotecan	metastatic adenocarcinoma of the pancreas
Fungal diseases	Abelcet®	Amphotericin B	Invasive severe fungal infections
	Ambisome®	Amphotericin B	Presumed fungal infections
	Amphotec®	Amphotericin B	Severe fungal infections
Analgesics	DepoDur™	Morphine sulfate	Pain management
	Exparel®	Bupivacaine	Pain management
Viral vaccines	Epaxal®	Inactivated hepatitis A virus	Hepatitis A
	Inflexal®V	Inactivated hemaglutinine of Influenza virus strains A and B	Influenza
Photodynamic therapy	Visudyne®	Verteporphin	Choroidal neovascularisation

Research on the clinical significance of conventional liposomal delivery showed improvement of the therapeutic index of encapsulated drugs, such as doxorubicin. The toxicity of drugs *in vivo* was also reduced by alteration of the pharmacokinetics and biodistribution, improving drug delivery to diseased tissue in contrast to free drug.

To enhance liposome stability and improve the blood circulation time, sterically-stabilized liposomes were developed. The hydrophilic polymer, polyethylene glycol, has proved to be the best choice to obtain sterically-stabilized liposomes. The formation of a steric barrier enhances the efficiency of encapsulated drugs by minimizing *in vivo* opsonization with serum components, and the fast recognition and uptake by the reticuloendothelial system which decreases the side effects [78].

Ligand-targeted liposomes have the potential for site specific delivery of drugs to selected cell types or organs *in vivo*, which are characterized by selective expression or over-expression of specific ligands at the site of disease [79]. Several types of ligands are available, such as carbohydrates, antibodies, and peptides/proteins. Monoclonal antibodies, used to create immunoliposomes, are some of the most versatile ligands that can be attached to liposome surfaces. Monoclonal antibodies are used owing to their stability and higher binding affinity due to the presence of two binding sites on each molecule [80].

Steric stabilization strongly affects the pharmacokinetics of liposomes, with reported half-lives ranging from 2 to 24 h in rodents (mice and rats) and as high as 45 h in humans, based on the characteristics of the coating polymer and particle size [81]. Whilst coating liposomes with polyethylene glycol results in extended circulation times, generally, as a drug delivery platform, liposomes provide a more dynamic and adaptable technology for improving the systemic effectiveness of therapeutics in many diseases [82].

Of late, liposome research has focused on the development of strategies to increase the activity of conventional liposomes to facilitate intracellular delivery of the encapsulated molecules. This resulted in the development of an improved form of liposomes called pH-sensitive liposomes (PSL). These liposomes are stable at physiological pH (pH 7.4) but undergo destabilization and acquire fusogenic characteristics upon acidification, leading to the release of their contents into the cytosol. Different types of PSL have been reported in the literature, based on the mechanism of triggering pH sensitivity [83-85].

Commonly established methods include blending PE or its derivatives with compounds containing an acidic group (e.g. carboxylic group) that functions as a stabilizer at neutral pH [86]. Different studies describe the use of synthetic fusogenic peptides/proteins, and novel pH-sensitive lipids either included or encapsulated in the lipid bilayer and attachment of pH-sensitive polymers with liposomes [87, 88]. Liposomes need to be stable in biological fluids and have long circulation times when administered intravenously, allowing them to reach target cells (such as tumor cells) and mediate cytoplasmic delivery [85]. The use of lipids with high transition temperatures, such as hydrogenated soya PC (HSPC), distearoylphosphatidylcholine (DSPC), the incorporation of cholesterol and lipid conjugates, such as phosphatidylethanolamine–poly(ethylene glycol), has led to a significant decrease in leakage of the encapsulated drugs through the circulation or in the extra-cellular environment [89]. These lipids also reduce non-specific interactions between the liposomes and serum proteins (opsonins), therefore, avoiding liposome clearance by the cells of the RES. Moreover, the usage of liposomes of size < 150 nm can lead to the increase of the circulation time [90].

1.5.3. Advantages of liposomes for inhalation

Local application of liposomes has been extensively investigated, including the pulmonary path for controlled delivery of drug to the lung. The development of liposomal formulations for aerosol delivery has expanded the potential for more effective utilization of an array of potent and effective drugs. Liposomal aerosols in pulmonary therapy are believed to overcome some of the problems associated with conventional chemotherapy due to their capability to: (1) act as a solubilization matrix for agents with different solubility, whether hydrophobic, hydrophilic or a combination of both; (2) act as a biodegradable sustained release reservoir; and (3) enable intracellular delivery of drugs, specifically to alveolar macrophages [91]. Consequently, liposomes can improve pulmonary residence time, prolong local therapeutic drug levels, reduce pulmonary toxicity, and result in high intracellular drug concentrations. Cumulatively, this will result in a decreased systemic spill-over of drugs and an increase in their potency. Moreover, liposomes are considered promising nanocarriers because of their good structure compatibility with lung surface cells since they are prepared with PLs endogenous to the lung as surfactants [92].

The success of liposomes as DDS is reflected in the number of liposome-based formulations that are commercially available or are currently under clinical research [73]. There are many disease states which could potentially benefit from treatment with aerosolized liposome-encapsulated drugs. A number of possible therapies employing inhaled liposomes have been investigated. The majority of studies focus on the potential for targeting the lung with drugs for a local effect. Cancer was the most extensively researched area in respect of clinically approved liposome products [73, 93]. Some drugs with advantageous local effects may have toxic systemic effects and their pulmonary absorption would be undesirable. (e.g., cytotoxic anti-cancer

drugs). Therefore, drug formulation plays an important role in creating an effective inhalable treatment. It is important have a drug that is pharmacologically active, but also efficiently delivered into the lungs to the appropriate site of action and will remain in the lungs until the desired pharmacological effect occurs [73].

Many studies have shown the high biocompatibility and biodegradability of liposomes as drug carriers in inhaled formulations (Table 1- 3) [71]. Historically, liposomes were recommended as surfactant replacement therapy in patients with respiratory distress syndrome. More recently, pulmonary surfactants based on mixtures of phospholipids have been commercialized (e.g. Survanta ®) as prophylaxis against respiratory distress syndrome in neonates [94]. Myers et al., have shown that chronic inhalation of HSPC liposomes caused no histologic changes of the lung or untoward effects on general health or survival of animals [95]. Prolonged nebulization of higher concentrations of HSPC (up to 150 mg/ml), acted as a local sustained release reservoir, and were safe and nonirritating to the lung of sheep. Also, several studies using human volunteers have confirmed the safety of liposomal formulations for inhalation [71, 73, 96]. Drugs encapsulated in liposomes are safe for pulmonary delivery since liposomes can control the drug release, hence decreasing the local drug concentration available to exert side effects [97]. Early studies showed the safety of drugs in liposome formulations given by inhalation. *In vitro* assessment of transferrin-conjugated doxorubicin-loaded liposomes showed greater cytotoxicity toward cancerous human pulmonary epithelial cell lines (Calu-3 cell line, A549 cell line, and 16HBE140 cell line) in comparison to non-cancerous human AT I/AT II cells in primary culture [98]. This study suggested that such DDS might have the potential to selectively deliver cytostatic drugs to sites of lung cancer by inhalation.

Table 1- 3: *In vivo* studies of aerosolised liposomal formulations for treating lung cancer [71].

Therapeutic agent	Delivery device	Major ingredient	Subject	Mass median aerodynamic diameter (μm)	Study phase	Reference
Cisplatin	PARI LC Star jet nebulizer	DPPC	Human	3.7	Phase I	[99]
9-nitro-camptothecin	AeroMist nebulizer	DLPC	Human	1–3	Phase I/II	[100], [101]
	AeroTech II nebuliser	DLPC	Animal (mice)	1.2–1.6	–	[102], [103]
	AeroMist nebulizer	DLPC	Animal (mice)	1.2	–	[104]
Interleukin 2	Puritan Bennett twin jet nebuliser	DMPC	Human & Animal	2.0	Phase I	[105], [106]
Paclitaxel	AeroMist nebulizer	DLPC	Animal (mice)	2.2	–	[107, 108]
Doxorubicin	Collison nebuliser connected to four-port, nose-only exposure chambers	DLPC	Animal (mice)	–	–	[48]
Doxorubicin	Collison jet nebulizer	EPC-Chol, DSPE-PEG	Animal (mice)	–	–	[109]
Camptothecin	Aerotech II nebulizer	DLPC	Animal (mice)	1.6	–	[110]

DPPC = dipalmitoylphosphatidylcholine; DLPC = dilauroylphosphatidylcholine; DMPC = dimyristoylphosphatidylcholine; EPC-Chol = egg phosphatidylcholine with cholesterol; DSPE-PEG = pegylated distearoyl phosphatidylethanolamin

Zhang et al. studied the *in vitro* release, *in vivo* distribution (in mice) and severity of damage (in rat lungs) following intratracheal instillation of 9-nitrocamptothecin (9-NC) liposomes. The results showed that 9-NC liposomes act as local sustained release reservoir and were safe and non-irritating to the lungs [111].

The safety of drugs in liposome formulations given by inhalation is not limited to anticancer agents. Many early studies have demonstrated the safety of liposomes for pulmonary administration of antimicrobial agents, genes, and antidiabetic drugs. For example, no adverse effects on the function or histology of the lungs were reported once liposome-pDNA complexes were aerosolized to the lung [112]. Steroids are usually used as anti-inflammatory agents in prophylaxis for asthma. Researchers have demonstrated that beclomethasone liposome aerosol was well tolerated when given in therapeutic doses to humans [113].

1.6. Physicochemical characteristic of pulmonary liposomes

The pulmonary administration of liposomal formulations is very promising, offering the benefit of improved drug concentrations at the site of action. Nevertheless, specific care must be given to the stability of liposomes, as they may be exposed to physical and chemical changes which can result in leakage of the encapsulated agents. Several parameters are key to the successful generation of stable liposome aerosols [114].

1.6.1. Phospholipid Composition and Mean Size of Liposomes

The lipid composition and mean size of liposomes have been found to affect the stability of liposomes during nebulization. Niven and co-workers studied the parameters that influence the release of carboxyfluorescein from liposomes after nebulization. They showed that a reduction in liposome mean size from 5 to 0.2 μm led to a lower release

rate of carboxyfluorescein from liposomes prepared with a lipid mixture of soy phosphatidylcholine and dipalmitoyl phosphatidylglycerol [115]. Also, Taylor et al, came to a similar conclusion in their studies on size reduction of liposomal vesicles, prepared with cholesterol and phosphatidylcholine by extrusion techniques [116]. The phospholipid composition controlling the rigidity of liposomal membranes is a significant parameter that affects the leakage of encapsulated drugs from the liposome vesicle, mainly when the temperatures through nebulization are higher than the phase transition temperature (*Tm*) of the phospholipid mixture. Different studies have shown that nebulization of liposomes at temperatures above the *Tm* of the phospholipids resulted in an increased release of encapsulated drug and increased rigidity of the bilayer, either by insertion of cholesterol or by using more rigid phospholipids, leading to the formation of liposomes which were more resistant to nebulization [117].

1.7. Technical concerns of using aerosolizable particles for pulmonary delivery

Nanoparticles are attractive for pulmonary delivery due to their important and unique features, such as their surface to mass ratio which is larger than that of other particles and their ability to adsorb and carry other compounds. However, NPs, in dry form do not deposit efficiently in the deep lungs leading to the exhalation of most of the inhaled dose. To solve this problem, particulate systems combining NPs into micron-scale structures have been developed; such as agglomerated NPs, embedding NPs within an inert 'microcarrier', porous nanoparticle-aggregate particles [118] and nanocomposite microparticles (NCMPs) [119] as a dry powders. These systems are designed to dissolve upon contact with lung lining fluids hence releasing the NPs with encapsulated drug from

the inert carrier [120]. Consequently, in order to increase the amount of drug deposited in the lung, and hence the amount of drug offered for absorption, it is essential to overcome the natural defense barriers of the lung [121].

1.7.1. Particle Deposition in the Lung

There are three main deposition mechanisms, inertial impaction, gravitational sedimentation, and Brownian diffusion that cause deposition of particulate matter in the lung. Inertial impaction arises after a particle travelling in an air stream is unable to follow a change in direction and the momentum of the particle causes it to remain in the original direction of motion, and impact on the respiratory airway's wall. This mechanism occurs in the upper respiratory tract and is accountable for the deposition of large and/or dense particles (e.g., particles >5 µm in diameter) travelling at a high velocity. While, very small particles (e.g., particles <1 µm in diameter) will typically deposit through the mechanism of Brownian diffusion, as a result from the random motions of the particles produced by their collisions with gas molecules and this motion can lead to contact and deposition in the alveolar region, where there is very low airflow. Particles of an intermediate size (1–5 µm) will evade deposition by inertial impaction and will instead deposit by gravitational sedimentation, where the settling rate is dependent on the particle size, density, in addition to its residence time in the airway. This mechanism occurs in the central and peripheral regions of the lung. Therefore, for effective pulmonary deposition, the aerosol must include particles 1–5 µm in diameter. Moreover, central and peripheral deposition can be improved by patient breathing techniques, such as a slow, deep breath followed by a breath hold, to maximize deposition by gravitational sedimentation and Brownian diffusion and minimize deposition by inertial impaction [79, 122, 123].

1.7.2. Clearance Mechanisms

After the deposition of inhaled drugs inside the lung, there are several physiological barriers to overcome before absorption can take place in the respiratory epithelium, and consequently drug action, can occur. The first barrier is a thin layer of mucus, about 5 µm deep that covers the walls of the tracheobroncial airways. The function of this mucus, in addition to hydrating the pulmonary epithelium, is removal of entrapped particulate matter via mucociliary clearance. Although the unciliated alveolar airways are not covered in mucus, phagocytic macrophages exist in this region, engulfing particulate matter and transported to the ciliated areas of the respiratory tract for elimination by mucociliary clearance. Also, mast cells present in the tracheobroncial and respiratory airways release protease enzymes, and several other enzymes, such as esterases, peptidases, are present in the lung and exist as an extra barrier to susceptible compounds [124, 125].

1.8. Methods of preparation of liposomal dry powders for inhalation

1.8.1. Freeze-drying

Freeze drying is a two-step procedure; first freezing of the sample then removing the water by sublimation under vacuum. This method can prevent hydrolysis of the lipids and physical degradation of the vesicles during storage. On the other hand, the freeze-drying method itself can affect the final product and consequently influence the liposome stability and induce changes in the vesicle size and loss of the encapsulated drug. The freezing rate is a very important step and the impact of slow and quick freezing was

reviewed by Van Winden et al. [126] who demonstrated that successful drug retention during freeze drying is mostly dependent on the lipid bilayer composition. Moreover, a slow freezing rate is advantageous. This is can be explained by the improved membrane recovery from deformations during slow freezing. These deformations are due to the osmotic pressures, which are formed by freeze-concentration. Finally, the resultant dried powder must be processed, usually by jet milling, to decrease its particle size so that it is suitable to use for DPI. However, the frictional contact between particles during jet milling can lead to liposomal disruption. Moreover, freeze-drying is an energy and time-consuming technique. Excipients such as disaccharides can been added to protect the liposomes [127].

1.8.2. Spray drying

Spray drying (SD) is a one-step technique which transforms liquid feedstock into a dried particulate. The liquid feedstock can be a suspension, solution or emulsion. The first step in SD is the atomization of the liquid through a nozzle followed by the sprayed gas mixing in the drying compartment. The droplet size reduces with evaporation until the droplets eventually turn into particles. The dried particles are then separated from the gas by a cyclone [128]. One advantage of SD compared to other drying methods is the possibility to design the resulting product in terms of shape, particle size, moisture content, and density. This offers a way to produce microparticles appropriate for the pulmonary delivery of drugs since pulmonary deposition patterns are highly dependent on particle size due to the complex anatomy of the lungs that is significant for the particle movement patterns in the airways (Figure 1- 7) [129].

Goldbach et al. studied the SD of liposomes to produce particles appropriate for pulmonary delivery. Atomization was achieved by a rotary atomizer and a pneumatic nozzle and produced particle sizes of 3.5 μm and 7.1 μm. The liposome mean size was not affected by the SD process, the phospholipids were not oxidized or hydrolyzed [130] and SD had no effect on the encapsulated drugs. Goldbach and others found only a slight decrease in the size of redispersed powders, when atropine sulphate liposomal dispersions were spray dried in the presence of 10% lactose [130].
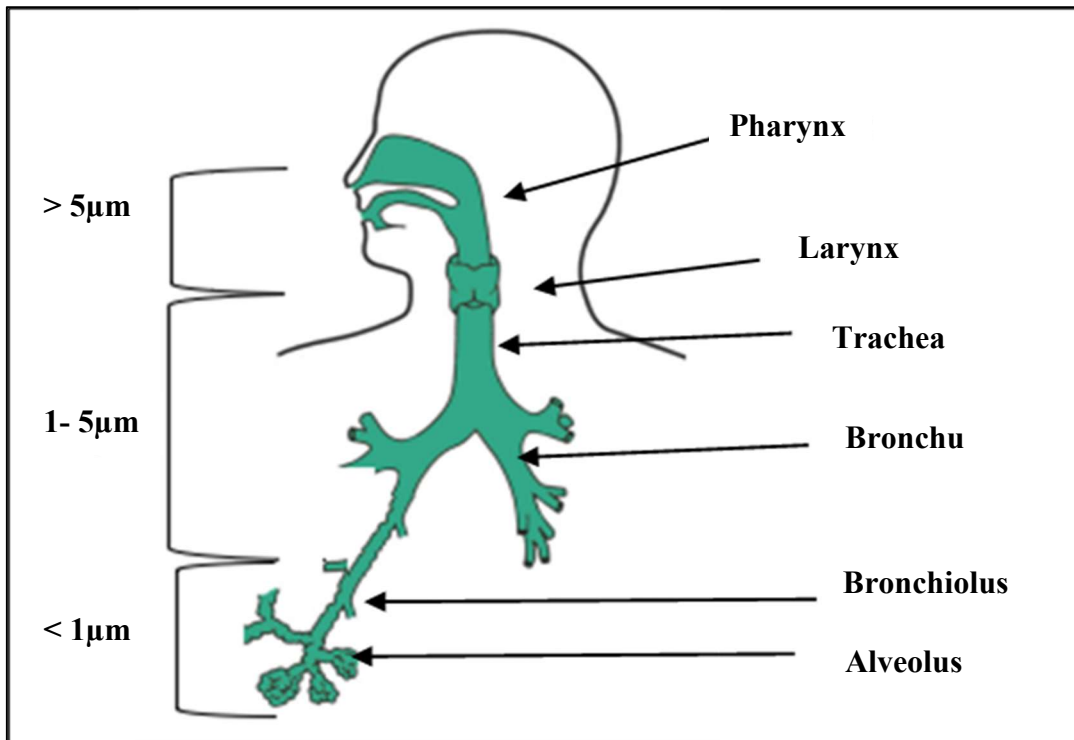
Figure 1- 7: A diagram of the effect of aerosol particle size on the site of deposition in the airways.

32

1.8.3. Spray freeze drying

The spray freeze-drying process can be divided into two separate steps: spray-freezing into a cryogenic liquid and lyophilization. Spray freeze-drying has been used to produce dry forms of poorly water-soluble drugs and to transform suspensions of liposomes into dry-powders using adjuvants such as lactose, sucrose, and mannitol. One example is the production of a liposomal powder formulation containing ciprofloxacin for pulmonary drug delivery where, after reconstitution of the powder, spontaneous *in vitro* formation of liposomes in pulmonary fluid occurred. The main advantage of this process is the improved mass median aerodynamic diameter (MMAD) [131]. The limitations of the method are the use of expensive cryogenic fluids, which can be technically impractical, and it is a time consuming and expensive method [132].

1.8.4. Supercritical fluid

Supercritical fluids (SCF) are compressed liquids or gases above their critical temperatures and pressures and have the combined advantages of both gases and liquids. Supercritical fluids have many attractive properties such as providing mild conditions for pharmaceutical processing, which is advantageous for labile drugs[133]. Moreover, simple and convenient SCF processes have been used to produce liposomes eliminating the problems involved in conventional preparation. Commonly used SCF include carbon dioxide, propane, nitrous oxide, acetone, propane, chlorodifluoromethane, diethyl ether, water, or mixtures. The SCF used in most studies is carbon dioxide because it is cost effective, nontoxic, nonflammable and has an accessible critical point of 31°C and 74 bar that makes it appropriate for processing thermolabile agents. [134]. There are several studies reporting the preparation of liposomes using SCF-CO_2 [135]. Liposomes

formulations were produced using CO_2 as a substitute for organic solvents by depressurizing the supercritical phase into water. At pressures over 200 bar, spherical liposomal vesicles with good uniformity were attained [136]. Cyclosporin A and Amphotericin B liposomes are the main DDS formulated using SCF [134]. Frederiksen et al [137] used SCF-CO_2 to prepare liposomes containing lipid and cholesterol dissolved in organic solvent, into the aqueous phase, which produced small unilamellar vesicles 20–50 nm in size. Otake et al [138] developed an enhanced supercritical reverse-phase evaporation process to evade the use of organic solvent in liposome formulation and improve the stability and drug-loading efficiency.

1.9. Aerosol delivery device options

There are three different categories of inhalation technologies including nebulizers, metered dose inhalers (PMDIs), and DPIs.

1.9.1. Nebulizers

There are three types of commercially available nebulizers: air jet, ultrasonic, and vibrating mesh. Air jet nebulizers depend on compressed gas passing through a nozzle to produce a negative pressure above the nebulizer fluid, which causes liquid filaments to form and collapse into aerosol droplets due to the liquid's surface tension [139]. Ultrasonic nebulizers use a piezoelectric crystal which vibrates at high frequency under the nebulizer fluid in order to create a fountain of liquid that releases aerosol [139, 140]. The third type, namely vibrating-mesh nebulizers, has lately been commercialized. Mesh nebulizers use micropump technology for aerosol production. They force liquid medications through several apertures in a mesh to produce an aerosol. As small and portable nebulizers that are powered by either rechargeable battery or electricity, they

have silent efficient operation, short treatment times, and minimum residual volume. Advantages of mesh nebulizers include consistent and improved aerosol generation efficiency, a mainly fine-particle fraction reaching into the peripheral lung, and the capability to nebulize low drug volumes [141-143].

The size of the pore, in the aerosol chamber and the reservoir, in addition to the output rate of mesh nebulizers, can be adjusted for different drugs in order to improve aerosol drug delivery to patients[144]. Comparisons of ultrasonic and mesh nebulizers confirmed similar drug delivery in simulated ventilator-dependent patients [143].

1.9.1.1. Aerosolisation of Liposomes

One of the parameters that affects the suitability of liposomes for inhalation is the method of application. Most liposomal formulations are nebulized to produce an inhalable aerosol cloud using different types of nebulizers. However, effective drug delivery might be affected by disintegration and instability of the liposomes by the high shear forces applied by the nebulizers leading to fragmentation of the liposomal bilayers and leakage of encapsulated drug [145].

An important issue for nebulization of liposomes is the lipid concentration and the corresponding aerosol output rate. Different studies have shown a direct correlation between droplet size, phospholipid concentration and viscosity, when using air-jet nebulizers for aerosolizing liposomes. A decrease in the aerosol output rate was detected when the liposomal size was greater than 2.5 μm. Increasing the liposomes mean size decreased the number of liposomes in the aerosolized droplets [115]. Thus, the nebulization of large liposomes will decrease the total liposomal aerosol output and influence the stability of the encapsulated drug [116]. Elhissi et al, found that MLVs

entrapping salbutamol sulphate were unstable during jet nebulization and stability was not enhanced when vesicles were extruded before nebulization [146]. The use of very viscous fluids led to termination of nebulization in the Omron Micron Air whereas in the Aeroneb Pro, an irregular aerosol generation was observed [147].

Liquid liposomal formulations are associated with some stability issues during aerosilization. Physical instabilities such as aggregation and fusion affect the properties of liposomes and may cause leakage of the encapsulated drug [148]. Therefore, to overcome these problems, dry powder formulations have been developed for pulmonary drug delivery. Several strategies have been used to increase the stability of liposomes which are freeze-drying (lyophilization), and spray drying technologies.

Several nebulizers have been tested to report their suitability for pulmonary administration of liposomes. With air-jet nebulizers, the droplet size is affected by the pressure of the compressed air and the structure of the nebulizer. Jet nebulizers have been shown to be effective for aerosol droplet deposition in lung tissues. Mostly, the size of the droplets in which the liposomes are dispersed is a significant issue in lung deposition. The mass median diameters (MMDs) generally range from 2 to 5 μm, will be deposited into the lower respiratory tract or the alveolar system, with an air pressure of 20 to 30 psi [146].

With ultrasonic nebulizers, aerosols are produced using high frequency ultrasound waves. The higher the frequency, the smaller the droplet size because of the heat generated through the process of atomization. During this process, the stability of labile agents can be negatively affected or encapsulated materials could be released from liposomal formulations [149].

The vibrating mesh technology is appropriate to nebulize sensitive agents such as peptides, proteins, nucleic acids or liposomal formulations, as high temperatures are minimized in contrast to ultrasonic nebulizers. This is owing to the lower operating frequency and since the energy needed for the nebulization is used [147].

Mesh nebulizers have demonstrated higher efficiency than jet nebulizers and can deliver higher drug doses to patients. Though human studies with mesh nebulizers are limited, *in vitro* studies confirmed approximately 2-3 times higher lung deposition with mesh nebulizers in contrast to jet nebulizers [150, 151]. Owing to the higher efficiency of mesh nebulizers, the doses of drug formulations may need to be adjusted to avoid the development of side effects because of overdose. Thus, patients need to be be monitored during treatment for clinical responses and side effects.

Elhissi et al have shown that an ethanol-based method to producing liposomes can be used to prepare a salbutamol sulphate formulation with improved drug output and inhanced fine particle fraction (FPF) compared to a conventional solution of the drug when nebulization was performed using the vibrating mesh nebulizer [152].

The vibrating-mesh nebulization using the customized large aperture mesh nebulizer had a less disruptive effect on liposomes and produced a higher output rate in comparison with the air-jet nebulizer [146].

1.9.2. Pressurized-metered dose inhaler

pMDIs are robust devices containing a drug dissolved or dispersed in a liquefied propellant that upon actuation with coordinated inspiration delivers a precise dose, generally with an aerodynamic particle size of less than 5 microns. The propellant rapidly

evaporates due to its high vapor pressure, leaving an accurate dose of the aerosolized drug particles to be inhaled by the patient.

They are inexpensive and pocket-sized devices but are not very efficient. They are associated with poor lung deposition and hence are generally only appropriate for molecules that are potent at low doses [132]. An approach to delivering liposomes using pMDIs was testified by dissolving the phospholipid in chlorofluorocarbons (CFC) propellant in which drugs like Salbutamol and co-solvents like ethanol are included. However, there are concerns about using pMDIs clinically, due to the limited dose reaching the deep lung and environmentally, because CFCs contributed to the depleting the ozone layer. The ozone-depleting effect of CFCs resulted in the introduction of safer alternative propellants, namely hydrofluoroalkanes, in which phospholipids have very limited solubility. However, lipid-based formulations for use in pMDIs have been made by dispersing phospholipids in PEG-phospholipids followed by the delivery of the subsequent *in situ* formation of liposomes in the aqueous environment of the impinger [154]. Furthermore, the development of liposomal formulations for delivery via pMDIs has major limitations such as complicated formulation, stability, and poor FPF of the aerosolized dose [153]. Moreover, the inclusion of co-solvents in phospholipid formulations may be deposited in the lung, also contributing to limitations of pMDIs [153, 154].

1.9.3. Dry Powder Inhaler

Among the three categories of inhalation technologies, dry powder inhalers (DPI), are the most extensively studied for the treatment of several lung diseases and pathological conditions. Each type of delivery device has unique strengths and weaknesses therefore

DPIs were introduced to overcome some of the weaknesses associated with nebulizers and pMDIs [155]. DPIs stand out because of the stability of drugs and formulations [156]. DPIs are portable, breath actuated devices that need minimal patient coordination between breathing and actuation. Although, Nebulizers have been used extensively for the delivery of liposomes [92, 157], liposomal DPIs have many advantages for pulmonary administration with respect to; reduced toxicity, increased potency, controlled delivery, uniform, local drug deposition, high dose capacity, propellant-free nature, patient compliance, and stability [154]. Using powdered medicines offers a benefit especially for the delivery of poorly water-soluble, peptide and protein drugs [158].

The preparation of liposomes for DPI has been investigated using several drying technologies such as freeze drying, SD, or spray freeze drying. For any of these technologies, the challenge is to stabilize the liposome vesicles to prevent agglomeration or membrane rupture, minimize release of the encapsulated drug throughout the processing steps, and ensure that the vesicle structure is maintained upon hydration in the lung fluid. One approach that avoids drying of liposomes, and therefore, their potential rupture, is to generate the liposomes *in situ* in the airways of the lung from the individual dried components (e.g., lipids, drug and a powder dispersing agent such as lactose). It is expected that hydration of the powdered lipid particles would occur in the aqueous fluid of the lung following inhalation of the proliposome powder [159]. Although the encapsulation efficiency after reconstitution was 100% for the cationic CM3 peptide and 96% for ciprofloxacin, this approach may not be possible for every liposomal product [98].

Another approach is SD of agents in liposome formulations of small aerodynamic size particles (i.e. high FPF), and it was predicted that the rehydration of liposomes would occur after the deposition of the powder in the aqueous environment of the lung. Joshi et al studied the delivery of liposomal budesonide and liposomal ketotifen DPI by blending the lactose carrier with preformed liposomes. They found that DPI of liposomes was successful when delivered as an aerosolized DPI to the required site in the lungs [160, 161].

Liposomal dry powders of N-acetylcysteine were developed for pulmonary administration. Liposomes were spray dried using lactose (10%, w/w) as a drying adjuvant. Liposomal dry-powders recovered the nanometric size of the original dispersion after their redispersion in aqueous medium and the powders presented aerodynamic diameters of about 7 μm and respirable fractions above 30%, indicating suitable properties for pulmonary use [162].

The formulation of liposomes as dry powder for inhalation is a promising method for NSCLC treatment.

1.11. Thesis Aim and objectives

To design, formulate and characterize nanocomposite microparticles encapsulating AFT as a treatment for NSCLC by dry powder pulmonary delivery.

To meet the aim of the thesis a systematic study was designed considering the following objectives:

1) 1) Optimization of AFT loaded liposomes NPs prepared by the thin film hydration technique.

   a. Optimization of NPs in term of lipid ratios, size, zeta potential, and encapsulation efficiency.

   b. Development and validation of an HPLC method for *in vitro* analysis of AFT.

   c. Evaluation of the stability of the liposomal dispersion.

2) Investigation of the toxicity and efficacy of the optimized liposomal NPs.

   a. Evaluation of the cytotoxicity of the optimized AFT-liposomal NPs formulations on NSCLC cells.

   b. Investigation of the therapeutic effect of AFT in lung cancer cells using proteomic analyses.

3) Incorporation of NPs into NCMPs via spray drying

   a. Optimization of NCMPs formulations in term of size, zeta potential, morphology yield% comparing different carrier materials.

   b. Assessment of the *in vitro* aerosolisation properties, release and lung cell toxicity.

   c. Assessment of the stability of NCMPs.

Chapter 2
Formulation and *In Vitro* Characterization of Afatinib Loaded Liposomes Nanoparticles

2.1. Introduction

Liposomal drug delivery systems have been reported to improve the administration of chemotherapeutic agents in the treatment of lung cancer and inhibition of metastases when compared to other DDS [71]. Liposome encapsulation can increase the antitumor efficacy of the incorporated drugs by providing more selective delivery and/or targeting to the tumor tissue, while in other cases, toxicity is decreased by avoidance of critical normal tissues [72].

The physicochemical properties of liposomes can highly affect their *in vivo* stability and kinetics. An important parameter that influences passive targeting through the enhanced permeability and retention (EPR) effect is the size of the liposomes. The accumulation of liposomes in the tumor depends on the size of the endothelial gaps lining the tumor capillaries. To apply the EPR effect, the liposomes should generally be <200 nm [163].

The composition and charge on the surface of liposomes are other parameters that influence passive targeting. Cationic vesicles have been shown to provide higher encapsulation efficiencies due to electrostatic interactions [54]. Cationic liposomes (CL), prepared from at least one cationic phospholipid enable cellular uptake by electrostatic absorptive endocytosis due to the negative charge on the cell membrane [164]. Although these liposomes have the capability of intracellular delivery, they are associated with drawbacks such as rapid clearance from the reticuloendothelial system (RES) and cytotoxicity [165, 166]. The toxicity associated with the use of cationic lipids can severely limit clinical applications [167].

Another approach to improve therapeutic efficiency of conventional liposomes is the use of local triggers such as enzymes or pH for site-specific release of therapeutics from

liposomes or the use of specific lipid compositions [168]. The use of pH-sensitive liposomes (PSL) is one strategy to increase the activity of conventional liposomes. These liposomes are destabilized in the acidic environment of the endocytotic pathway as they contain pH-sensitive lipid components. Therefore, the encapsulated drug is delivered to the intracellular bio-environment by destabilization or fusion with the endosomal membrane. PSL are usually composed of a neutral cone-shaped lipid dioleoylphosphatidyl-ethanolamine (DOPE) and a weakly acidic amphiphile, for example cholesteryl hemisuccinate (CHEMS) [169]. The fusogenic performance of these liposomes is due to the DOPE present in the lipid layer that does not form a bilayer structure, once dispersed in aqueous media, but forms a hexagonal structure. Other lipids such as *N*-succinyl-DOPE [170], or dioleoylphosphatidylcholine (DOPC) [171] can also be incorporated to induce pH sensitivity. All these lipids have a negatively charged group, which can be neutralized on the acidic endosome, resulting in destabilization, fusion with endosomal membrane and content release [172]. PSL rapidly become destabilized on acidification in the tumor tissue and the applications of PSL can be restricted because of their recognition by the phagocytes of the RES resulting in a very short circulation half-life of these carriers. To overcome RES uptake and prolong circulation time, the inclusion of PEGylated phospholipids in liposome composition is recommended. Moreover, the development of nano-size liposomes can contribute to an increase in circulation time and enhance the uptake by target cells [173]. The therapeutic effectiveness of PSL supports their commercial utility especially in cancer treatment [85]. A bio-distribution study comparing PEGylated (stealth) PSL containing cisplatin and free cisplatin in solid tumor bearing mice was reported. The results showed that stealth PSL enhanced the

bioavailability of cisplatin in the tumor and retention of stealth PSL by the kidney indicated the usefulness of this carrier to reduce cisplatin toxicity [174].

Depending on the application of the liposome, a variety of production methods may be used to attain the desired properties. Size, lamellarity and the homogeneity of the liposomal formulation are all end goals that impact the choice of preparation method. The most widely used method is the thin-film hydration method, also named hand shaking method or Bangham method [175]. For preparing liposomes, phospholipids are distributed in a thin film on the surface of glassware by dissolving a mixture of phospholipids in an organic solvent, typically chloroform, and later evaporating the solvent. The addition of an aqueous buffer under conditions of agitation or vortexing results in the production of liposomes. The temperature needs to be kept above the phase transition temperature of the phospholipids. Most liposomes are then extruded through membranes under pressure in order to get a homogenous size distribution [70]. Liposomes with diameters between 100-200 nm are most desirable as in this size range they are able to accumulate in the affected tissues. This size range of liposomes also does not induce an immune response but are of sufficient size to carry an appropriate concentration of the desired drug [176, 177].

Simple approaches to decreasing liposome size include vortexing of the rehydrated lipid film or sonication. Two different sonication devices can be used. Probe sonication is one choice, but has a crucial disadvantage in that metal parts from the probe tip can end up in the liposome formulation [178]. An alternative is the use of a bath sonicator [179]. Homogenization can also be used to reduce the liposome size. Brandl et al., produced small unilamellar vesicles with a narrow size distribution and a size of 25 – 50 nm using

a high-pressure homogenizer [180]. The French press extrusion is another approach to generating liposomes of a definite size. Hamilton et al., used a French pressure cell to extrude liposomes at 20 000 psi through a small orifice. After only a single pass, 70 % of the liposomes built a homogenous population [178].

On a laboratory scale, there are two commonly used techniques: the sonication techniques described above and filter extrusion using polycarbonate membranes with defined pore sizes. This method has several advantages; it yields liposomes with relatively homogeneous size distributions and is reproducible. A liposome suspension is extruded many times through a membrane with a defined pore size. In order to achieve a smooth extrusion, the temperature of the liposome dispersion must be above the phase transition temperature of the phospholipids or the membrane will clog and break. Berger et al., reported that extrusion through big filter pores (e.g. 800 nm) results in vesicles smaller than the filter pore size. Another determining factor is the number of extrusions [181]. With increasing extrusions through the same membrane, the size distribution becomes more uniform. A disadvantage of classical extrusion procedures is the limited batch size [182].

2.2. Aim

This study aims to formulate and evaluate liposomes nanoparticles (NPs) encapsulating afatinib (AFT) into CL and PSL compared to NL (control liposomes) for the design of an efficient anticancer delivery system. The main objectives of research were: to optimize liposome formulations in terms of; lipid ratio, particle size, polydispersibilty index, zeta potential, AFT encapsulation efficiency, and liposome stability. To achieve this, a liquid chromatography (HPLC) assay was developed for AFT quantification.

2.3. Materials and methods

2.3.1. Materials

AFT (99.8% purity) was purchased from Green Stone Swiss Co., Limited. 1,2-distearoyl-sn-glycero-3-phosphocholine [18:0] (DSPC), 1,2-dioleoyl-sn-glycero-3-phosphoethanolamine [18:1] (DOPE), 1,2-dioleoyl-sn-glycero-3-phosphocholine [18:1] (DOPC), and Cholesteryl hemisuccinate (CHEMS), was purchased from Avanti Polar Lipid. 1,2-dioleoy-3-trimethylammonium-propane Chloride salt (DOTAP) were kindly gifted by Avanti Polar Lipid. Phosphate buffered saline powder, pH 7.4, HEPES (4-(2-hydroxyethyl)-1-piperazine ethane sulfonic acid), Triton X-100, Triethylamine, Sodium hydroxide pellets, and Tween 80 were purchased from Sigma-Aldrich, Saint Louis, USA. All other reagents and chemicals were of analytical grade.

2.3.2. Methods

2.3.2.1. Preparation of conventional liposomal nanoparticles

Afatinib loaded liposomes NPs were prepared by a thin film hydration method [183] (Figure 2- 1). To prepare conventional non-targeting liposomes (NL), a mixture of 1, 2-distearoyl-sn-glycero-3-phosphocholine [18:0] (DSPC): 1,2-dioleoyl-sn-glycero-3-phosphoethanolamine [18:1] (DOPE) and 1,2-dioleoyl-sn-glycero-3-phosphocholine [18:1] (DOPC) at a molar ratio of 3: 3: 10 were dissolved in 1 ml of chloroform. This solution was mixed with the phospholipid (PL) mixture in AFT: total lipid molar ratios of (0.25:1, 0.5:1, 0.75:1, 1:1, 1.25:1, and 1.5:1). Chloroformic solutions were evaporated using a Buchi® rotary evaporator at a temperature just above the phase transition

temperature(T_m) (55 °C) to form a thin dried film. The lipid film was hydrated with buffer (pH 7.4). The mixture was incubated for 10 min in a water bath at a temperature above the T_m at 55 °C with intermittent vortexing to produce multilamellar vesicular liposomes and to ensure that all the lipids were dispersed in the buffer. For preparation of small multilamellar liposomes, liposomes were sonicated (for 30min) using an Ultrasonic cleaner® bath sonicator at + 55°C. Unloaded liposome (free) were prepared (without AFT) as control.

2.3.2.2. Size Reduction of Liposomes by extrusion

The resulting liposomal dispersions were filter-extruded through a polycarbonate TrackEtch Nuclepore membrane (Whatman, UK). Up to 1 mL of liposomes formulations were passed back-and-forth five times through double stacked membranes with 200-nm polycarbonate membrane filters. The extrusion was done by hand with a syringe extruder (Liposo-Fast™ Avestin Inc., Ottawa, Canada) (Figure 2- 2). To allow the formation of smaller vesicles, this was followed by extrusions through 100-nm polycarbonate membrane filters and the procedure was repeated 21 times. During all the extrusions, the temperature was maintained at least 10 °C above the glass transition temperature of the DSPC (55°C). The resultant products were stored in the fridge at 4°C overnight prior to characterization.

2.3.2.2. Preparation of targeting AFT-loaded liposome nanoparticles

Cationic and pH-sensitive phospholipids were produced using the same thin film hydration method except 3 of the 10 parts of DOPC in the total liposomes composition were replaced by either 1,2-dioleoy-3-trimethylammonium-propane chloride salt

(DOTAP) or cholesteryl hemisuccinate (CHEMS) for the development of cationic and

pH sensitive liposomes, respectively as shown in Table 2- 1.
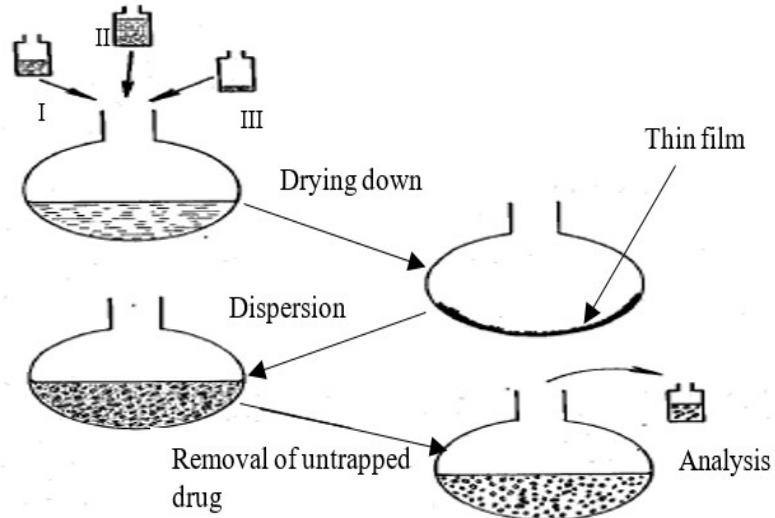
Figure 2- 1: Thin film hydration method (I & II phospholipid solutions and III is drug).

Figure 2- 2: Mini-Extruder. The polycarbonate membrane and filter supports are placed between two Teflon internal membrane supports. 1.0 ml Hamilton syringes are connected to the extruder outer casting. Photo of liposome dispersions: Left (A): crude liposomes Right (B): after extrusion through 0.1 μm membrane.

Table 2- 1: Compositions of different types of liposomes.

Phospholipids	Amount required (µmol/mL)		
	NL	PSL	CL
DSPC	3	3	3
DOPC	10	7	7
DOPE	3	3	3
CHEMS	-	3	-
DOTAP	-	-	3

NL: Non-targeting liposomes; PSL: pH-sensitive liposomes; CL: Cationic liposomes; DSPC: 1,2-distearoyl-sn-glycero-3-phosphocholine [18:0]; DOPC: 1,2-dioleoyl-sn-glycero-3-phosphocholine [18:1]; DOPE:1,2-dioleoyl-sn-glycero-3-phosphoethanolamine [18:1]; CHEMS: Cholesteryl hemisuccinate; DOTAP:1,2-dioleoy-3-trimethylammonium-propane Chloride salt (DOTAP)

2.3.3. Physicochemical characterization of liposomal nanoparticles

2.3.3.1. Determination of particle size, polydispersity and Zeta Potential

The mean vesicle size, size distribution and zeta potential were characterized by dynamic light scattering (DLS) at 25ºC with a fixed angle of 137° using a Zetasizer Nano ZS (Malvern Instruments Ltd., UK). The liposomes were appropriately diluted with purified and filtered water (0.2 µm pore size) prior to the measurements. The mean vesicle diameters were the averages of five measurements. All measurements were done in triplicate.

2.3.3.2. Transmission electron microscopy

The liposomal formulations were examined by transmission electron microscope (TEM) using a JEM-2100 electron microscope (Jeol, Tokyo, Japan). Briefly, a drop of liposomal formulation was applied to a copper coated carbon grid, and the excess was removed using filter paper, and then examined under the electron microscope.

2.3.3.3. Determination of Encapsulation Efficiency

Due to the poor solubility of AFT, the free AFT occurred in two forms in the external phase of the liposomal dispersion; free undissolved and free dissolved AFT. The free undissolved AFT was separated from the liposomes using light centrifugation. Meanwhile, the supernatant (encapsulated and free dissolved AFT) were filled into centrifuge tubes and ultra-centrifuged (Sorvall™ WX Ultra80 Floor Ultracentrifuge, T-890 Fixed Angle Rotor, Thermo Electron Corporation) at 40000 rpm at 4 ∘C for 30 min. The clear supernatant which contained the free dissolved AFT was collected. The total AFT is the sum of both encapsulated and free AFT. The concentration of AFT within the liposome was determined after dissolving and disrupting the liposomal dispersion in methanol and triton x-100 using a vortex mixer, followed by centrifugation for 15 min. The clear supernatant which contained the AFT was then transferred to a new tube and kept at 4 ∘C until analysis. The drug encapsulation efficiency (EE%) was calculated by using the following formula:

$$EE \% = \frac{\text{AFT}_{total} - AFT_{free}}{\text{AFT}_{total}} \times 100 \qquad \text{Eq. 2.1}$$

2.3.4. HPLC Assay for Afatinib

A simple, rapid and sensitive analytical method was developed and validated for AFT quantification. The developed method was characterized by the ease of sample preparation and the small sample volume required and validated for linearity, precision and accuracy.

2.3.4.1 HPLC method

A stock solution of AFT was prepared in methanol at a concentration of 1 mg/mL and stored in 4.0 mL amber glass vials at -20°C. Serial dilutions in mobile phase were performed in the range of 0.01 to 25 µg/ml to produce a standard calibration curve using HPLC analysis. A Waters Breeze2TM HPLC system (Waters Corporation, Milford, U.S.A) was equipped with an automated sampling system (Waters^{TM} 2695 Plus Autosampler, USA) at 4°C and a photodiode array detector (WatersTM 2998, USA), "Breeze2 (WaterTM)" software and a reversed-phase C18 column (WaterTM, 3 x 150 mm, 3.5 µm particle size) coupled with a C18 guard cartridge (4×2.0 mm) and maintained at 50°C. The mobile phase consisted of A: 0.1% triethanolamine and 1% acetonitrile in HPLC water (pH= 6), and B: acetonitrile and 10% methanol at a flow rate of 1 mL/min. The injection volume of each AFT sample was 10 µl and detected by the UV detector at 253 nm. All the operations were carried out at room temperature. A daily standard calibration curve (n=3) ranging from 0.01 to 25 µg/ml was prepared to determine the unknown AFT concentrations for entrapment efficiency and drug release.

2.3.4.2. Assessment of Linearity, Accuracy and Precision

Validation of the HPLC method was conducted according to the International Conference on Harmonization (ICH) guidelines [184] considering: linearity, accuracy, precision, specificity, limit of detection (LOD), limit of quantification (LOQ) and robustness. Six standard calibration lines were prepared at different times during 3 months to evaluate the linearity, precision, accuracy, and stability of the method.

Linearity was assessed by calculating a regression line by plotting the peak area of AFT vs. the AFT concentration ranging from 0.01 to 25 µg/ml.

The accuracy was determined via the analysis of multiple replicates (n = 6) of AFT concentration. The accuracy of the method was expressed in term of bias.

The precision of a quantitative method was determined by repeatability as intra-day precision by an analysis of three replicates of AFT concentrations over the same day. Inter-day precision was determined by the analysis of three replicates of various AFT concentrations over three different days. The results were expressed as the relative standard deviation (RSD%).

Low, medium, and high concentration quality control (QC) samples at concentrations of (100, 1,000 and 10,000 ng/ml AFT, respectively) were analyzed, on three distinct occasions within at least 3 months, as described above.

The LOD and LOQ were determined from the calibration curve obtained using six replicates that were closest to the LOQ. The following equations were used:

$$LOD = 3.3\ \sigma/S \qquad\qquad\qquad \text{Eq. 2.2}$$

$$LOQ = 10\ \sigma/S \qquad\qquad\qquad \text{Eq. 2.3}$$

LOD and LOQ were determined based upon the slope (S) of the calibration curve and least standard deviation obtained from the response (σ). It has a low limit of quantitation (10 ng/ml) with satisfactory specificity, no matrix interference was observed. These findings demonstrated that the assay has good selectivity.

2.3.5. *In vitro* Drug release

The *in vitro* release of AFT from NL, CL, and PSL (optimized formulations) was evaluated using a Franz diffusion cell system (FDC-6, LOGAN, Instruments Corporation, USA). The experiments were conducted in PBS buffer (pH 7.4 and 5.5) with 0.2% Tween 80 to maintain sink condition. The cellophane dialysis membranes (molecular weight cut off: 12-14 KDa) were soaked before use in distilled water at room temperature for 12 h prior to use to ensure wetting. An aliquot of 100 µL liposome suspension was added into donor chambers, ensuring there were no air bubbles under the membrane. The receptor compartment consisted of PBS (pH 7.4) and pH 5.5 for PSL at 37 °C and stirred at 150 rpm. Samples of 500 µL were withdrawn at various time intervals up to 24 h, and replaced immediately with an equal volume of fresh PBS at 37 °C. The amount of AFT in each sample was analyzed by HPLC. The experiments were performed in triplicate.

2.3.5.1. Kinetic Modelling

The *in vitro* AFT release data were fitted to various kinetic equations, including zero order, first order, Higuchi's model and Korsmeyer Peppas plot and R^2. Then, n values (diffusion exponent) were calculated for each linear curve obtained by the regression analysis of each kinetic equation [185].

2.3.6. Stability testing

Liposomal formulations were stored in glass vials at 4±1 °C and 25°C ± 2°C over a period of one month. The stability was evaluated by measuring the average particle size, zeta potential and PDI and AFT content after storage for one month. The physicochemical stability of the freshly prepared formulation (at day 1) was used as control and AFT content (at day 1) was normalized to 100%.

2.3.7. Data and statistical analysis

Quantitative data were expressed as the mean ± SD of at least three replicates. The Student's t-test and one-way analysis of variance (ANOVA) using IBMSPSS Statistics 21 was used to assess multiple comparisons between different methods and times. The level of confidence was set as 95%.

2.4. Results

2.4.1. Liposome size, polydispersibility index, and zeta potential determination

The obtained liposomes were characterized in terms of mean particle size, PDI and zeta potential values using DLS and electrophoretic light scattering. The particle size of the liposomes ranged from 42 to 57 nm and values of PDI were less than 0.2, which indicate a narrow size distribution and no aggregation. The zeta potential values increased with increasing AFT: lipid ratios, until the ratio was 0.5:1 (Figure 2- 3). The AFT-containing liposomes exhibited more positive zeta potential than liposomes without AFT, which suggests that the addition of AFT increased the zeta potential of liposomes. In case of the

NL, the positive zeta potential was low and after the incorporation of AFT, increased by approximately two-fold until a ratio of 0.5:1 of AFT: lipid. CL were more positive, with zeta potential ranging from 38.9 mV for the blank to 48.4 mV for the ratio of 0.5:1. However, PSL were negatively charged due to CHEMS and zeta potential decreased with increasing the drug to lipid ratios (Figure 2- 3).
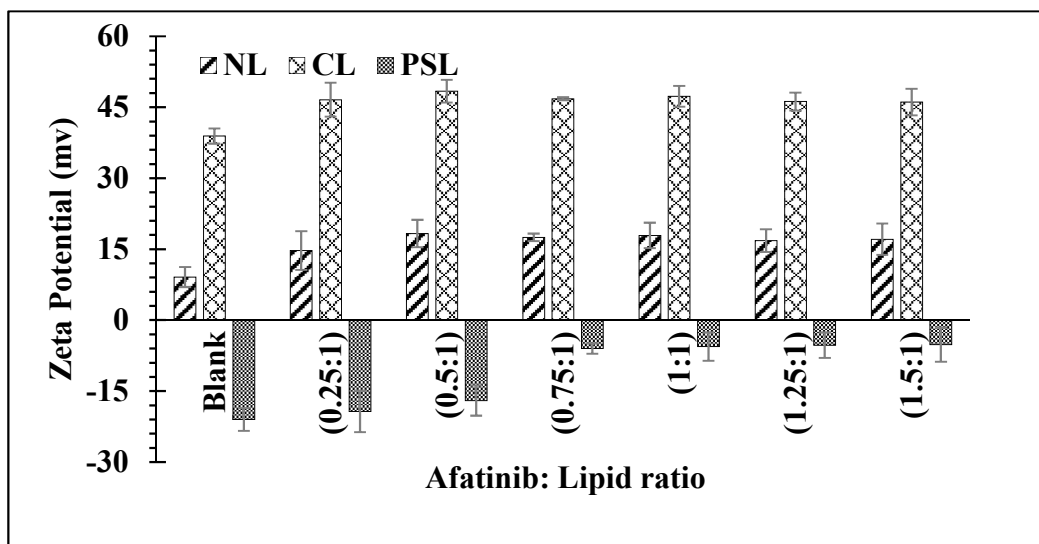
Figure 2- 3: Zeta potentials of NL (Non-targeting liposomes), CL (Cationic liposomes), and PSL (pH-sensitive liposomes) at different lipid to AFT ratios.

2.4.2. Transmission electron microscopy

Transmission electron microscopy images of PSL are presented in (Figure 2- 4) showing that PSL were uniform, homogenous and spherical shape liposomes with smooth surface and had a multilamellar structure that was clearly visible inside PSL. The liposomes observed under TEM were <50 nm which was in good agreement with the dynamic light scattering measurements.
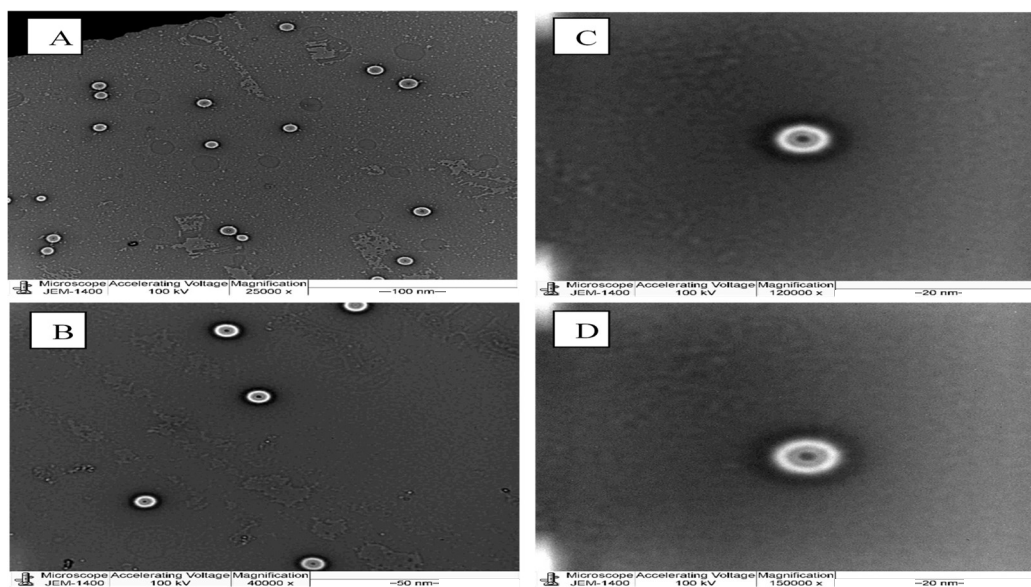
Figure 2- 4: TEM micrographs of the pH sensitive liposome at AFT:lipid ratio of 0.5:1 (PSL), at A) 25,000×, B) 40,000× C) 120,000 x, and D) 150,000 x magnifications power.

2.4.3. Chromatographic Analysis of Afatinib

The maximum UV absorbance for AFT was determined to be 206 and 253 nm which is in contrast to values reported in the literature of 252, 258 or 268 nm [186-188]. The detection wavelength of 253 nm was used for a better quantification of AFT in the HPLC in this study due to the higher peak area. As shown in Figure 2- 5, the average retention time was 2.4 min, with no interfering peaks in either chromatogram A (the blank) and chromatograms B and C (AFT) indicating the specificity of the HPLC assay method. During the *in vitro* studies, there was no interfering peaks from the NP ingredients co-eluted with the AFT peak, which further confirmed the specificity of the method.

2.4.3.1 Method validation

A calibration curve of the peak area of AFT vs. concentration in the range of 0.01 to 25 µg/ml was produced. The regression equation of the line was $y = 355.74x + 1.6229$) with a correlation coefficient (r^2) of 0.9999 (Figure 2- 6).

The analytical method was validated in terms of linearity, precision, and accuracy. Linearity was assessed using a calibration curve to investigate the ability of the method to get a proportional response to the different concentrations. Based on concentrations from 0.01 to 25 µg/mL, the linearity was evaluated in triplicate, and a calibration curve constructed.

The LOD was determined to be 5 ng/ml and the LOQ was 10 ng/ml, with the corresponding CV values of 1.8 and 0.926 %, respectively (Table 2- 2). For precision and accuracy of sample analysis, AFT standard solutions of three replicates were prepared in triplicate and analyzed on the same day (repeatability) or in three different days (intermediate precision). Table 2- 3 shows that the precision did not exceed the required RSD value with a maximum value < 1.98 %. Analysis of variance of the data indicated no significant difference (p =0.401) in the slopes, intra- and inter-day of the calibration curves. The results confirmed the reproducibility of the assay with an accuracy of >99.9 %. The method was found to be robust, since small variations in the method conditions had a negligible effect on the chromatographic behavior of the AFT. The results also indicated that changing the HPLC system or the C_{18} column had no effect on the analysis of AFT. Even a small change in the mobile phase composition did not significantly change the peak area of the drug used for this method.
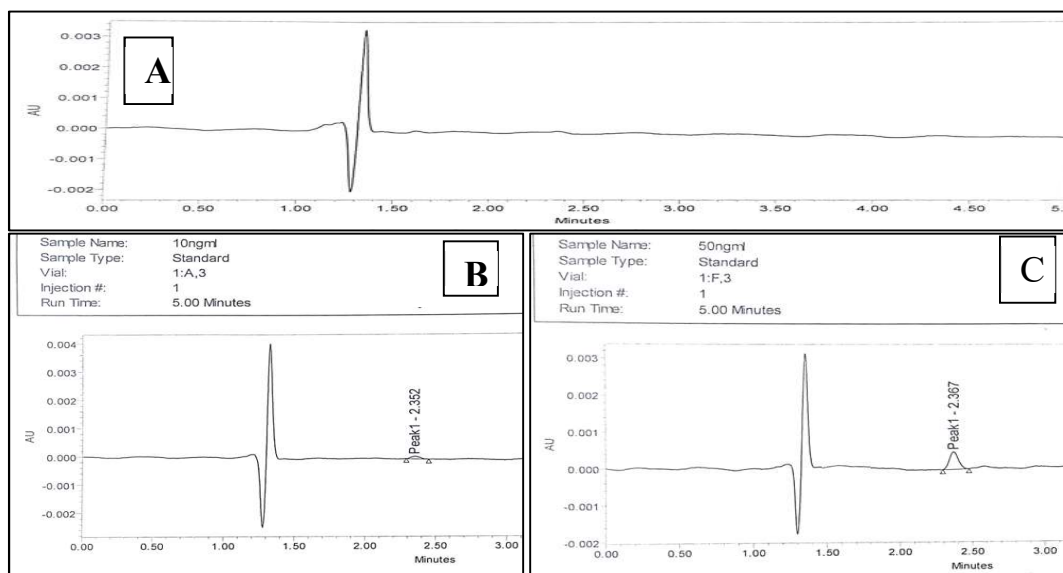
Figure 2- 5: HPLC chromatograms of the mobile phase (chromatogram A), and HPLC chromatograms of the mobile phase containing (B) 10 ng/ml and (C) 50 ng/ml afatinib.
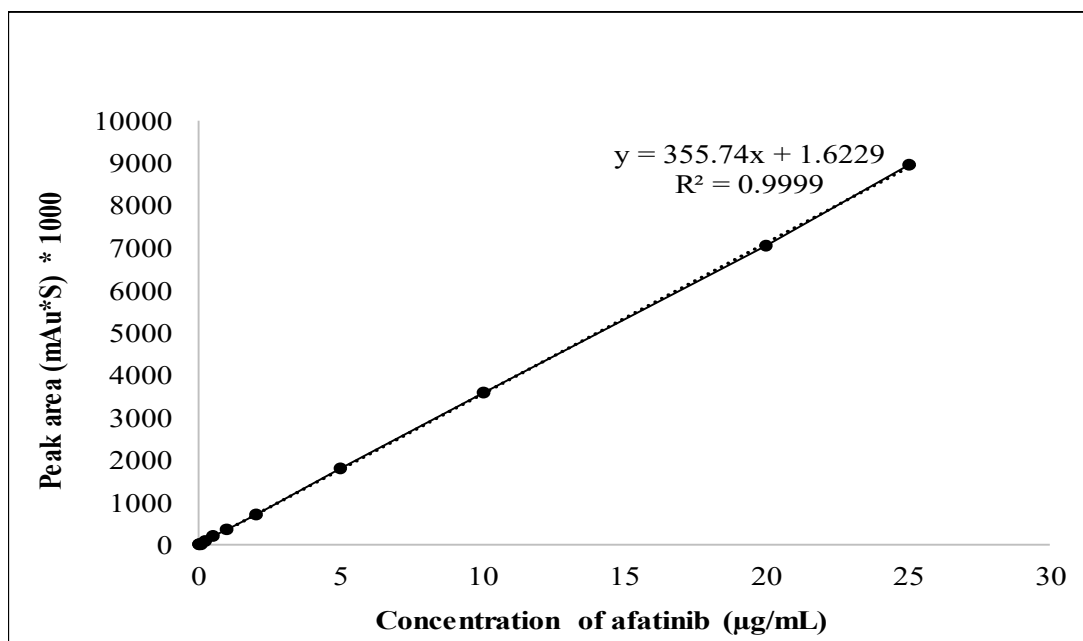
Figure 2- 6: Standard calibration curve of afatinib solution in methanol at λ 253 nm (n = 6).

Table 2- 2: Precision of the developed method for analysis of afatinib.

Concentration (µg/ml)	Mean ± SD[a]	Precision RSD[b] (%)	Accuracy (%)
Inter day			
0.1	99.98 ± 1.98	1.98	99.9
1	1000.72 ± 0.49	0.05	102
10	10000 ± 113.26	1.13	100.1
Intra-day			
0.1	100 ± 1.06	1.07	99.86
1	1000 ± 0.29	0.03	100.5
10	10000 ± 60.08	0.6008	100.2

a Standard deviation of the mean
b Relative standard deviation

Table 2- 3: Inter day and Intraday accuracy determination of afatinib (n = 6).

Nominal (µg/mL)	Concentrations Mean ± SD	CV%
0.01	0.01 ± 6.09	0.9266
0.05	0.05 ± 6.40	0.8051
0.1	0.1 ± 5.71	1.7143
0.25	0.25 ± 1.76	0.7076
0.5	0.5 ± 5.70	1.1404
1	1 ± 1.77	0.1763
2	2 ± 4.03	2.3016
5	5 ± 5.65	1.0731
10	10 ± 3.76	1.3577
20	20 ± 3.83	0.1992
25	25 ± 2.55	0.1102

SD: standard deviation; CV: Coefficient of variation percentage

2.4.4. Encapsulation efficiency of AFT in liposomes

The effect of the lipid to AFT ratio on the encapsulation of AFT is indicated in Figure 2-7. As the AFT: lipid ratio increased, the EE% was increased to a certain extent and then decreased in all tested formulations. The highest values of encapsulated AFT were with AFT:lipid ratio of 0.5:1 where the EE% values were 43, 50, and 52 % for NL, PSL, and CL respectively. As expected, the amount of AFT in the liposomes increased with increasing AFT ratio. After reaching the maximum encapsulated amount of AFT in liposomes, EE values decreased with additional AFT. However, the amount of undissolved drug increased ($P < 0.05$) significantly, thereby notably decreasing the EE% values. As the amount of undissolved drug increased and were present as free crystals that were visible in TEM-images (Figure 2- 8). According to the obtained results, AFT: lipid ratio 0.5:1 was selected for further studies due to the high EE% in all tested liposomes. In contrast, PSL at a lipid to drug ratio of 1:1 showed the lowest EE%.

//////
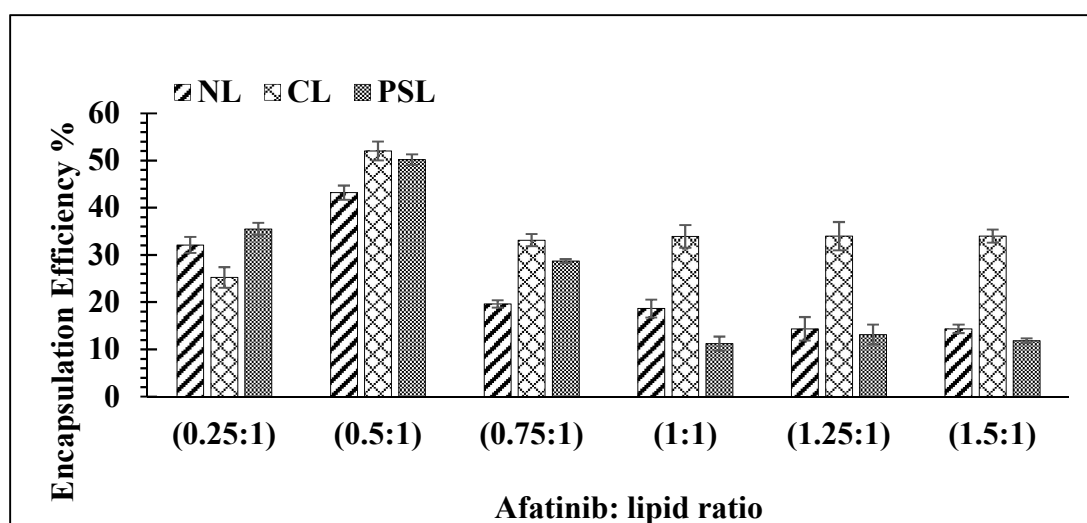
Figure 2- 7: Encapsulation efficiency % of NL (non-targeting liposome), PSL (pH sensitive liposome) and CL (cationic liposome) with different drug: lipid ratios.
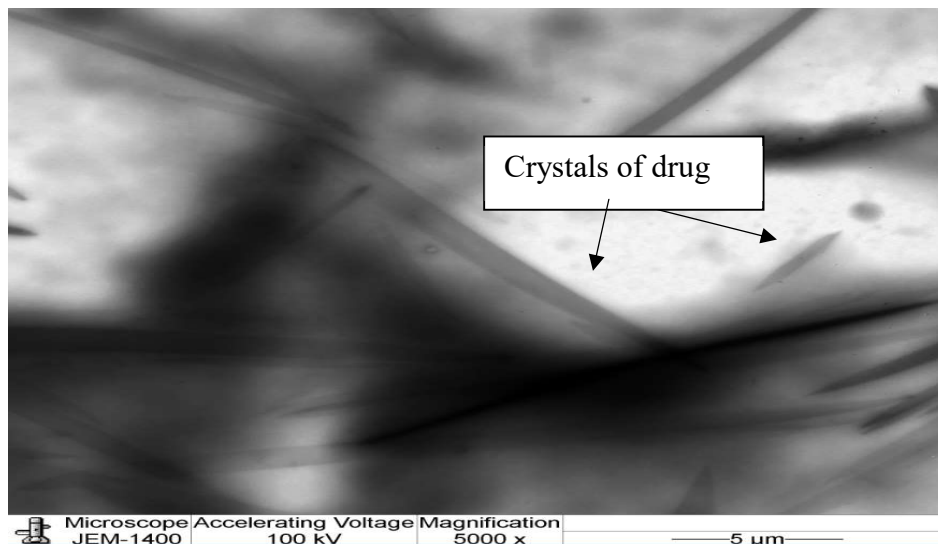
Figure 2- 8: Free afatinib crystals present in the suspension of PSL (pH sensitive liposomes) formulated at a AFT: Lipid ratio of 1.5:1.

2.4.5. *In vitro* Release of AFT

To evaluate the *in vitro* drug release of AFT from CL and PSL compared to NL, NPs were incubated in PBS solutions (pH 7.4) at 37°C (Figure 2- 9). Moreover, to determine the pH sensitivity of PSL, AFT release behavior at pH 5.5 was also investigated, and pH 5.5 was selected to mimic the tumor pH (Figure 2- 9) as weakly acidic environments are present in the endosomal and lysosomal compartments of tumor cells [189]. The AFT release rate was relatively slow in neutral pH 7.4, only reaching 59.5%, 35.4% and 28.6 % for CL, NL, and PSL, respectively within 24 h. These data revealed that the liposomes exhibited significantly sustained release profiles and AFT was successfully loaded into the liposomes. However, the cumulative release of AFT in PSL at pH 5.5 reached 101 % in 4 h, presenting a burst release phenomenon.
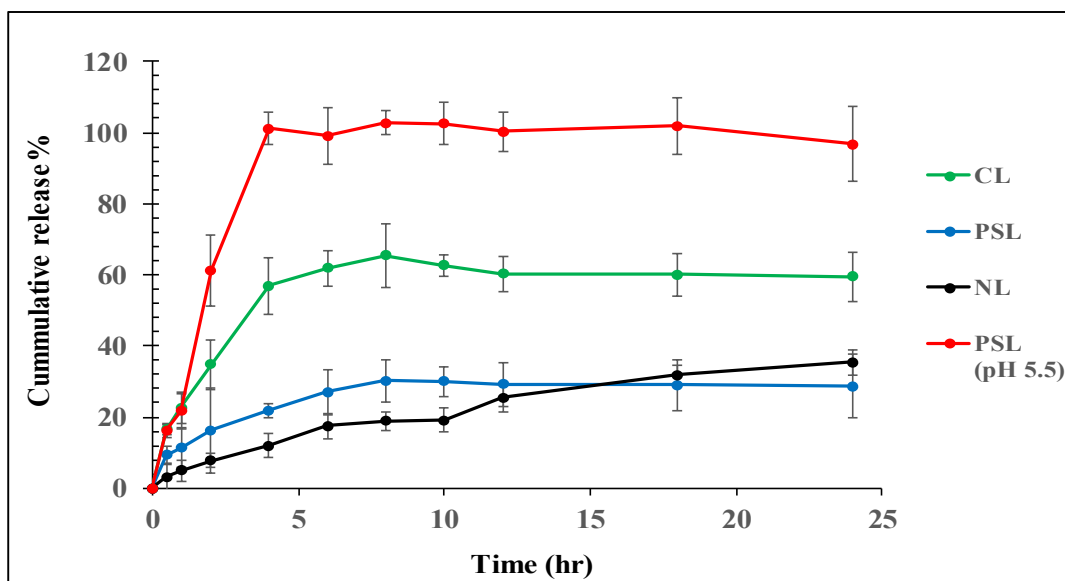
Figure 2- 9: *In vitro* release profiles of NL (nontargeting liposome), PSL (pH sensitive liposome) and CL (cationic liposome) in phosphate-buffered saline containing 0.2% Tween 80 at pH 7.4 and pH 5.5. Values are presented as the mean ± SD.

To fit the release kinetics of AFT from liposomes at pH 5.5 and 7.4, different kinetic models viz. Peppas, Higuchi, zero Order and first order were exploited to predict the dug release profile. The data supported the Korsmeyer-Peppas model at pH 7.4 as it presented the highest value of r^2. Moreover, the values of n were 0.460, 0.681, 0.431 and 0.599 for CL, NL, PSL and PSL (pH 5.5), respectively, indicating a non-Fickian diffusion kinetics (0.5 < n < 1). PSL (n=0.431) followed Fickian diffusion due to slow release at neutral condition. Subsequently, it was concluded that the drug release mechanism was mainly due to the combination of diffusion and erosion of the liposomes containing AFT (Table 2- 4).

Table 2- 4: Modeling of Afatinib release kinetic from different liposomal formulations.

		NL	CL	PSL	PSL
		At pH = 7.4			At pH = 5.5
Zero-Order	r^2	0.928	0.691	0.754	0.647
	k_o (h^{-1})	1.900	4.017	1.776	6.606
First-Order	r^2	0.731	0.559	0.634	0.486
	k_1 (h^{-1})	0.025	0.106	0.022	0.477
Higuchi	r^2	0.988	0.871	0.912	0.835
	k_1 $(h^{-1/2})$	7.676	16.32	7.145	28.05
Korsmeyer-Peppas	r^2	0.994	0.940	0.971	0.889
	k_{KP} (h^{-n})	0.259	0.247	0.280	0.604
	"n" value	0.681	0.460	0.431	0.559

2.4.6. Stability of AFT liposomal dispersions

The short-term stability of selected liposomes, in liquid form, prepared from a AFT: lipid ratio of 0.5:1: was investigated for up to 30 days at $4 \pm 1^{\circ}C$ and $25 \pm 2^{\circ}C$. There was no significant change in the particle size, PDI, zeta potential or EE% of the liposomes compared to the initial preparation over the course of the stability study at $4^{\circ}C$ ($p > 0.05$). However, at $25 ^{\circ}C$, the particle size of the liposomes after storage for 30 days increased from 47.5 ± 2.3 to 75 ± 3.3 nm, 53.8 ± 2.6 to 84 ± 15.9 nm and 55.3 ± 1.2 to 79.5 ± 2.5 for CL, PSL and NL respectively. However, the liposomes were still smaller than 100 nm and there was no appreciable change in PDI. The zeta potential at $4^{\circ}C$ and $25^{\circ}C$ for 30 days

was not significantly different ($p = 0.141$) compared to initial formulation. The EE of AFT

after storage at 4°C and 25°C for 30 days was slightly decreased, but was still higher than

90% and 80%, respectively, of the initial formulations (Figure 2- 10). Therefore,

liposomes formulations were stored at 4°C at all the time.
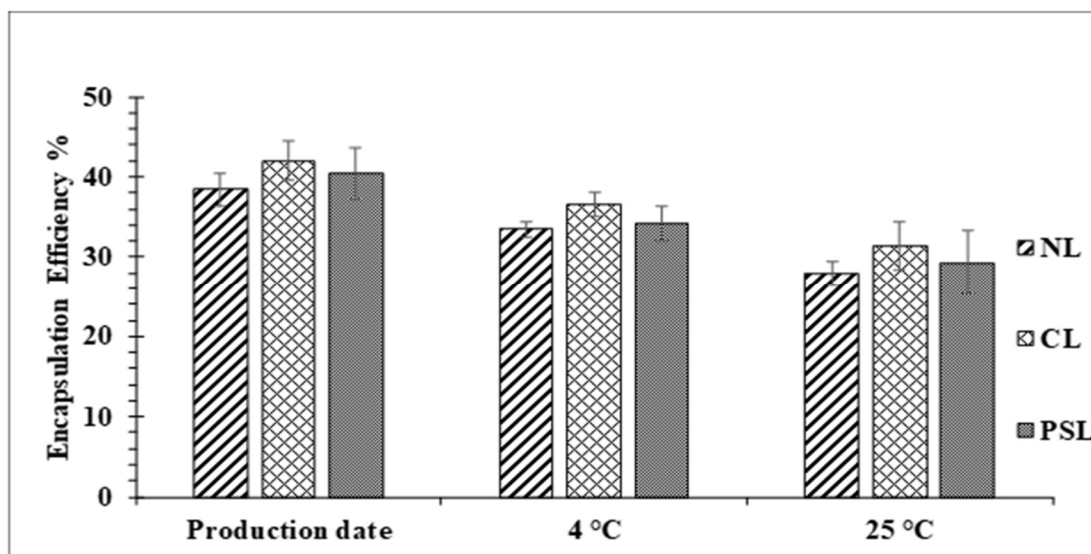
Figure 2- 10: Drug content of afatinb from NL (nontargeting liposome), PSL (pH sensitive liposome) and CL (cationic liposome) at Afatinib: Lipid (0.5:1), following storage for one month at 4 and 25°C, $p = 0.141$.

2.5. Discussion

Liposomes have been reported as potential drug carriers to target cancer cells. Liposomes

less than 100 nm are able to escape the tumor vasculature and accumulate in the cells by

passive targeting [190]. Moreover, targeted liposomes were designed depending on the

type of phospholipids used. In addition, AFT is a potent antitumor drug used in clinical

oncology against a lung tumor. However, AFT had low specificity, systemic toxicity and

indiscriminating of the tumor and healthy tissues [191]. So AFT loaded liposomes NPs

were developed for successful cancer therapy to decrease dose-limiting toxicity. In this

study, two different strategies for AFT loaded liposomes for tumor targeting were selected. Cationic and pH-sensitive phospholipids were used to produce AFT cationic liposome (CL) and AFT pH-sensitive liposome (PSL) to target tumor cells, in addition to the conventional (nontargeting) liposome (NL). The main difference between these two liposomes is the composition of phospholipid used. In general, three lipid components: DSPC, DOPC, and DOPE were used. The rationale for the selection of DSPC was its stability against chemical degradation due to being a saturated lipid, which reduces the drug leakage from liposomes on storage and *in vivo* transit. To increase the fluidity of the liposomal membrane, DOPC was selected due to its high fluidity at room temperature (transition temperature (T_m)= -20°C). While, the T_m of DSPC is +55 °C, which remains in the gel phase [192]. Moreover, DOPE was added to provide fusogenic characters to the liposomes, due to the formation of an inverted hexagonal phase upon destabilization of membranes at a mildly acidic pH [84]. These lipids, with various chain lengths and degrees of saturation, can be used to fine-tune the membrane dynamics and phase properties [84]. The main composition of CL is DOTAP, which is a cationic phospholipid. Whereas PSL is composed of the pH-sensitive phospholipid (CHEMS).

The film hydration method has been used to actively entrap AFT into liposomes with relatively high efficiencies and small vesicle size (<100 nm) [193]. The polydispersity index values of the obtained liposomes are <0.2 indicating narrow size distribution. These findings are in agreement with Mayer et al 1986 who showed that similar procedures can be employed for the production of homogeneously sized liposomes by utilizing filters with pore sizes ranging from 30 to 400 nm [194]. These small sized liposomes have the potential to penetrate tumor cell membranes and be taken up by the cells allowing

efficient drug accumulation at the target site. The TEM of PSL revealed uniform, homogenous and spherical-shaped liposomes with a smooth surface. The higher zeta potential of the obtained liposomes provoked the potential stability of a liposome. Depending on the lipid composition, liposomes and lipid nanoparticles may carry a negative, neutral, or positive net charge. Absence of surface charge (neutral liposomes) increases the aggregation of liposomes, reducing their physical stability. Also, neutral liposomes do not interact sufficiently with cells, and this leads to drug release from the liposomes in the extracellular space [165, 195]. Instead, charged liposomes have several advantages compared with neutral liposomes. Therefore, cationic and pH-sensitive phospholipids were selected for tumor targeting

The zeta potential of the liposomes was influenced by the lipid composition. The cationic lipids DOTAP increased the zeta potential of the liposomes, while CHEMS had a negative effect on the zeta potential.

Kraft et al found that liposomes having a net positive or negative charge accumulated to a greater extent in the lung, compared to uncharged/neutral liposomes [196]. Patil et al investigated the effect of zeta potential of cerium oxide nanoparticles on cellular uptake in adenocarcinoma lung cells (A549) showing preferential cellular uptake for the negatively charged nanoparticles [165]. Thus, the attachment of liposomes to cell membrane appears to be most affected by the surface charge of the liposomes.

Furthermore, to obtain the liposomes with the highest EE%, the best ratio of drug to phospholipid was determined for further studies. Accordingly, the highest EE% of AFT was 43.20%, 50.20%, and 52.01% for NL, PSL, CL, respectively at the 0.5:1 ratio of AFT: lipid and the reproducibility was good. Positively charged liposomes (CL) exhibited

the highest drug content, due to the inclusion of DOTAP in the liposomes, which decreases the rigidity of the liposomes increasing loading capacity. However, increasing the molar ratio of AFT: lipid above 0.5:1, in all formulations, produced a noticeable decline in EE%, since there was not enough lipid to entrap the drug. On the other side, the amount of free drug increased ($P < 0.05$) significantly with increasing the molar ratio of AFT: lipid, thereby decreasing the percent encapsulated drug dramatically. Afatinib is a lipophilic substance, which is easily compatible with the phospholipids used in the preparation of liposomes and forms a part of the bilayer. The incorporation of AFT into liposomes is limited by the availability of encapsulating material as with the three types of liposome prepared. The high EE% also indicated that the lipid bilayer was able to significantly solubilize the hydrophobic drug (AFT), enabling it to be transported through the inner vesicle, which would be an effective solution for the low oral bioavailability of AFT. In this line, Nallamothu et al., found that total liposomal concentration levels increased with increasing lipid concentration in the formulation. As the drug: lipid ratio increased from 1:10 to 2:10, total drug in the liposome formulation increased. When the drug: lipid ratio was further increased to 4:10, the total drug in liposome formulation did not increase, but the amount of free drug increased significantly, thereby decreasing the percent of entrapped drug. Therefore, at higher drug: lipid ratios there are not enough lipids to entrap the drug, so most of the drug is in free, or un-entrapped, form [197].

Thus, the best liposomes were subjected to a stability study, where they exhibited better stability at 4°C or at 25°C after storage for 1 month. In terms of EE%, particle size and zeta potential, CL showed the highest stability.*In vitro* drug release data revealed that PSL and NL demonstrated better sustained release profiles than CL due to the presence

of DSPC (T_m), which led to a decrease in leakage of AFT in the circulation or extracellular environment. But in case of CL, AFT exhibited a high release rate compared with the other liposomes, at pH 7.4. This is due to the complete protonation of DOTAP at pH 7.4 [198]. By contrast, the AFT release was increased significantly when the pH decreased from 7.4 to 5.5 in the case of PSL and showed reasonably good pH-responsiveness, reaching 100% after 4 h. In a physiological environment (pH 7.4), the encapsulated AFT was released at a constant rate. These results indicated that the AFT was well protected inside the liposome bilayers at physiological pH but in acidic condition (pH 5.5) such as a cancer tumor environment, the AFT release would be hastened. Therefore, the release of the PSL containing AFT was controlled by the environmental pH. The PSL underwent destabilization at pH 5.5 and acquired fusogenic properties, thus tending to rupture and quickly release the AFT. This is in line with the results obtained by Düzgünes et al [199] who proved that under acidic conditions, CHEMS becomes partially protonated, consequently losing its negative charge and, therefore, its ability to stabilize the bilayer structure. This results in the destabilization and/or fusion of the liposomes. These liposomes showed that liposomes composed of CHEMS stabilized the entrapment of calcein at pH 7.4 and undergo destabilization and irreversible aggregation under acidic pH [200]. Also, the fusogenic performance of PSL is due to the presence of DOPE in its lipid layer, which forms a hexagonal structure instead of bilayer structure, when dispersed in aqueous media. Doxorubicin was encapsulated in pH-sensitive liposomes, which contained DOPE and CHEMS, leading to high intracellular drug release rates within acidic compartment resulting in further increments in the therapeutic efficacy of targeted anticancer drug containing liposome against B lymphoma [201].

It was reported that the release of the drug from liposomes could be described by three different mechanisms: diffusion, erosion and diffusion-erosion [202]. It was found that the release profiles were supported by the Korsmeyer-Peppas model at pH 7.4, which is presented the highest value of r^2. Moreover, the values of n, the release exponent indicating the drug release mechanism, were 0.460, 0.681, 0.431 and 0.599 for CL, NL, PSL and PSL (pH 5.5), respectively, indicated a non-Fickian diffusion kinetics ($0.5 < n < 1$). While PSL (n=0.431) exposed Fickian diffusion due to slow release at neutral condition [202]. Subsequently, it is concluded that the drug release mechanism was mainly owing to the combination of diffusion and erosion of the liposomes containing AFT (Table 2- 4).

2.6. Conclusion

In this study, a sensitive and selective HPLC method was developed for the quantification of AFT in formulations. Afatinib was successfully incorporated in a variety of different liposomes with different ratios of lipid to AFT, NL, CL and PSL, using a film hydration method. The obtained liposomes were small vesicles less than 100 nm with a low PDI (<0.2) and accepted zeta potential. The highest EE% of AFT obtained was 43%, 50%, and 52% for NL, PSL, CL, respectively at the 0.5:1 ratio of AFT to lipid. The *in vitro* release study confirmed that PSL, CL and NL had sustained release profiles in pH 7.4. However, in acidic pH solutions, PSL exhibited fast release. The stability study, conducted at 4°C and 25°C for 1 month, showed that the characteristics of liposomes in liquid form did not change significantly over this period. This study suggests that NL, PSL, and CL containing AFT should be further investigated for cytotoxicity to NSCLC lung cell line.

Chapter 3

In vitro Cytotoxicity and Molecular Studies of Afatinib- Liposomal Formulations

3.1. Introduction

Cell culture assays have been used widely in different fields such as cancer, and are critical steps in determining the efficacy, pharmacodynamics, and mechanism of action of novel anti-cancer drugs. [203]. Also, they are favoured as preliminary data to predict the performance of drug-loaded NPs systems before moving onto *in vivo* studies [48].

In order to improve the therapeutic efficacy of AFT, AFT-loaded liposomes (NL, CL, and PSL) system were developed as described in chapter 2. Subsequently, the potential toxicity of these vesicles needed to be addressed. Human NSCLC cell lines (H-1975, H1650, and HCC-827) were utilised in the cytotoxicity studies as relevant pulmonary *in vitro* models for liposome DDS (Table 3- 1). The H1975 cell line has L858R/T790M double mutations; and H1650, and HCC827 cells both have an EGFR exon 19 deletion which are the most common EGFR mutations found in patients with NSCLC [204].

Four chemotherapeutic regimens: cisplatin and gemcitabine, cisplatin and docetaxel, carboplatin and paclitaxel, and cisplatin and paclitaxel are used for treatment of NSCLC, affording an average overall survival of 8–10 months [205]. More recently, the identification of lung tumours having mutations in EGFR has led to attention on targeted treatments for EGFR tyrosine kinase inhibitors resulting in an overall survival of more than 2 years for patients with EGFR mutation-positive NSCLC [71]. Therefore, gemcitabine, carboplatin and paclitaxel were used to compare efficacies with AFT (Table 3- 2).

There are many methods that can be used to investigate cytotoxicity, which involve different aspects of cell function, for example cell viability and proliferation, cell morphology, and loss of membrane integrity. [125, 206-208]. WST-1 is a colorimetric

method which provides a tool for studying induction and inhibition of cell proliferation in any *in vitro* cell model [209]. The WST-1 assay is considered to be better than older cell viability assays as it does not have the additional solubilisation step as with 3-(4,5-dimethylthiazol-2-yl)-2,5-diphenyltetrazolium bromide (MTT) and can be measured after 2 - 4 hrs incubation. WST-1 is a stable tetrazolium salt cleaved to a water-soluble orange-coloured salt called formazan by mitochondrial dehydrogenases that are present at viable cell surfaces [210]. The amount of formazan dye formed is directly proportional to the number of metabolically active cells in the culture [211].

Table 3- 1: Non small cell lung cancer lines used in this study.

Cell line name	Gender	ATCC® No.	Histology
H-1975	Female	CRL-5908™	Adenocarcinoma
H-1650	Male	CRL-5883™	Stage 3b, Adenocarcinoma; Bronchoalveolar Carcinoma
HCC-827	Female	CRL-2868™	Adenocarcinoma

Clarifying the mechanism of cytotoxicity of NPs and controling the expression of cytotoxicity should facilitate the development of safe liposomal formulations [212]. Apoptosis has been shown to play a major role in multiple physiologic and pathologic processes, such as oncogenesis, and tumor progression [213]. Unlike necrotic cell death, apoptosis is characterized by cell shrinkage, chromatin condensation, DNA fragmentation, and finally disintegration into apoptotic bodies [214].

To understand the unique response of cells to NP therapeutics, quantitative proteomic technology has been used to study the protein expression profiles of NSCLC cells during treatment with chemotherapeutics [215, 216]. With the development of advanced instruments and maturation in sample preparation approaches, variations in cellular protein abundance as well as phosphorylation events that occur under different treatment regimens can be detected and analysed. Therefore, identification of proteins that are differentially expressed as a result of exposure to drug treatments may provide novel biomarkers for drug targets with improved therapeutic action, and/or predict outcomes during cancer treatment [217-219]. A Synapt G2 HDMS quantitative proteomic approach has been utilized to evaluate cellular protein abundance changes upon AFT treatment.

3.2. Aims

In this study, the aim was to evaluate the efficacy of the novel AFT-loaded liposomal NPs formulations (NL, CL, and PSL) compared to AFT alone.

The main objectives of study were to:

a. Study AFT-loaded liposomal NPs cell toxicity *in vitro* using NSCLC cells.

b. Use flow cytometry to investigate the inhibition of cell proliferation induced by AFT and AFT-loaded liposomal NPs in NSCLC cells.

c. Use proteomic methods to identify differentially expressed proteins in different treated and control NSCLC cells.

3.3. Materials and methods

3.3.1. Materials

Lung cancer cell lines (Table 3- 1) were purchased from the American Type Culture Collection (ATCC), Manassas, USA. RPMI 1640 1x, 0.25% Trypsin-EDTA Solution, Ammonium bicarbonate, Iodoacetamide, and DL-Dithiothritol were purchased from GIBCO®, SIGMA-ALDRICH, Saint Louis, USA. WST-1 Cell Proliferation Assay Kit Reagent were purchased from Roche Diagnostics (Basel, Switzerland). Antibiotic-Antimycotic (100X) and Fetal Bovine Serum (FBS) were purchased from GIBCO®, InvitrogenTM, Carlsbad, USA. Vybrant® Apoptosis Assay Kit were purchased from Molecular Probes^{TM}, Life Technologies^{TM}, Eugene, Oregon, USA. Protein Assay Dye Reagent Concentrate were purchased from Bio-Rad Laboratories, California, USA.RapiGestTM SF Surfactant and Mass PREPTM Alcohol Dehydrogenase Digestion Standard were purchased from Waters Corporation, 34 Marple Street, Manchester, UK. 25 and 75 cm^2/tissue culture flasks with vented cap (IWAKI brand) 96-well flat bottom plates 24-well tissue culture plates were purchased from Fisher Scientific, UK.

3.3.2 Methods

3.3.2.1. Liposomes formulation synthesis and characterisation

Afatinib loaded liposomes (NL, CL, and PSL) and free (unloaded) liposomes were formulated and characterised as described in section 2.3.2 and section 2.3.3 respectively.

3.3.2.2. Cell Culture

Non small cell lung cancer cell line (Table 3- 1) cells were cultured in RPMI-1640 medium supplemented with 10% FBS/1% Antibiotic/Antimycotic solution (complete medium) incubated at 37°C into 5% CO_2 incubator. The medium was changed every four days and cells were passaged weekly using Trypsin.

3.3.2.3. Cytotoxicity study

3.3.2.3.1 Cell proliferation assay, WST-1

The *in vitro* cytotoxicity of AFT compared to different chemotherapeutic agents (carboplatin, gemcitabine and paclitaxel) (Table 3- 2) was determined by WST-1 using NSCLC cells (H-1975 cells) and . In brief, the cells were seeded into 96-well plates at a density of $1x10^4$ cells per well and incubated overnight in complete culture medium. Afterwards, different concentrations of AFT (1, 5, 10, 20, 40 and 80 μM) were added to each well and incubated for an additional 24 h. At the end of the treatment, 10 μl of cell proliferation reagent WST-1 kit was added and incubated for 4 h at 37°C. The intensity of the photometric metabolite (formazan) was measured at 450 nm using an xMark™ Microplate Absorbance Spectrophotometer (Bio-Rad Laboratories, Inc., Hercules, CA, USA). The results were expressed as the IC50, which was obtained graphically using SigmaPlot 10 (SYSTAT Software, Inc., San Diego CA, USA).

Table 3- 2: The selected drugs used to compare their cytotoxicity effects with afatinib.

No.	Name	Manufacture
1	Carboplatin	Actavis
2	Gemcitabine	Ebewe
3	Paclitaxel	Actavis

3.3.2.3.2. Cytotoxicity assessment by flow cytometry

Cell death was assessed using the Vybrant® Apoptosis Assay kit and flow cytometry. This was performed at the Flow Cytometry Core Facility at Research Centre (KFSHRC, Riyadh, KSA). The H-1975 cells were seeded in six-well plates at 7 x 104 cells per well and incubated overnight. Then, the cells were treated with pure free liposomes, as control, and AFT loaded PSL at concentrations of 0.5, 1, 3, 5 and 8 μM for 24 h after dilution with complete culture medium. After treatment, the cells were harvested by trypsinization, centrifuged, and re-suspended in PBS. The cells were stained with Alexa Fluor® 488 Annexin V/propidium iodide (PI) and analyzed using the flow cytometer. The percentage cell death was determined using FACS-CaliburTM apparatus and CellQuest Pro software (Becton-Dikinson Biosciences, Franklin Lakes. NJ, USA). The apoptosis in different cells; H-1975, HCC-827 and H-1650 was tested after application of AFT or AFT loaded liposomes (NL, CL and PSL at 0.25, 0.5, 0.75, 1 and 2 μM) and

using free liposomes as control. The percentage of cell death in the wells containing the free drug and PSL following a 48 and 72h incubation period was subsequently compared with the results of 24 h incubation at 0.25, 0.5, 0.75, 1 and 2 µM.

3.3.2.4. Proteins expression changes induced by afatinib

3.3.2.4.1. Sample Preparation and Protein In-solution Tryptic Digestion

The protein concentration of the whole cell lysates was determined using the Bradford assay. An equal amount (100 µg) of complex protein mixtures was subjected to in-solution tryptic digestion. Protein concentrations of 0.5 to 1 µg/µL were achieved at the end of in-solution tryptic digestion as previously described with minor modification [58]. Briefly, the proteins were denatured in 0.1% RapiGest SF (Waters, Manchester, UK) at 80°C for 15 min, reduced in 10 mM DTT at 60°C for 30 min, centrifuged at 13,000 RPM for 10 seconds to bring together the condensation under the tube cap, allowed to cool to room temperature, and alkylated in 10 mM Iodoacetamide (IAA) for 40 min at room temperature in the dark. The samples were then trypsin-digested at an enzyme: protein ratio (w/w; 1 µg/µL trypsin concentration) of 1:25 overnight at 37°C with gentle shaking. The digestion/ RapiGest was quenched by incubation with 12 M HCl (4 µL/50 µL of sample) at 37°C for 15 min, followed by centrifugation at 13,000 RPM for 10 min. The samples were then diluted with aqueous 0.1% formic acid to allow for a load of approximately 3 µg on the analytical column using the Trizaic Nano tile. All samples were spiked with yeast alcohol dehydrogenase (ADH) as an internal standard at a final concentration of 200 fmol per injection to facilitate absolute quantitation as previously described (Figure 3- 1) [219].
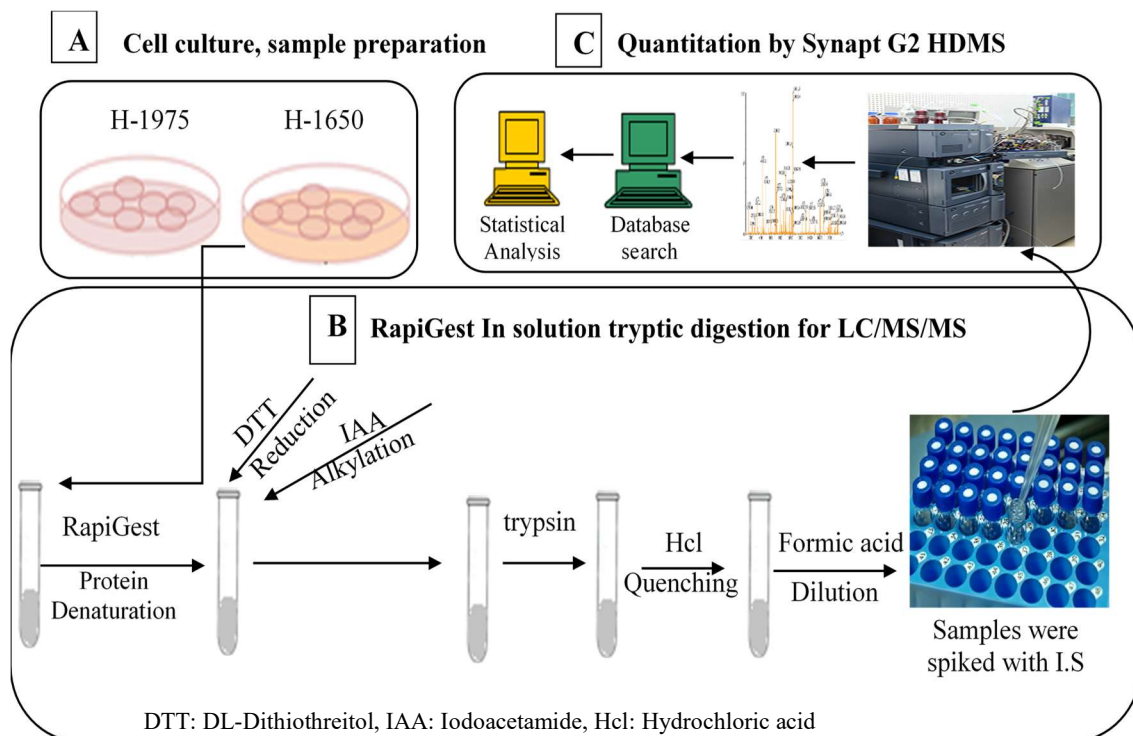
Figure 3- 1: Overview of the protein determination experimental workflow.

3.3.2.4.2. Protein Identification by Synapt G2 Mass Spectrometry

One-dimensional, (1-D) Nano Acquity liquid chromatography coupled with tandem mass spectrometry on a Synapt G2 HDMS (Waters, Manchester, UK) was used to generate expression proteomics data for H-1975 and H-1650 treated and control samples. Prior to analysis, the instrument was optimized as previously described [218, 219]. Briefly, the detector was set using 2-ng/µL-leucine Enkephalin (556.277 Da). Mass/charge (m/z) calibration was achieved with a separate infusion of 500 fmol [Glu] 1-Fibrinopeptide B

(GluFib, 785.843 Da), on a Trizaic Infusion tile using the automated Mass Lynx IntelliStart.

Other parameters were capillary voltage at 3.6 Kv, sample cone at 50 V, extraction cone of 5 V, source temperature at 85°C. All raw data acquisitions were performed on a Trizaic Nano source (Waters, Manchester, UK), using the positive ion mobility mode nano ESI at slow flow rate.

A 3 µl sample containing approximately 3 µg of the digested protein was loaded onto the column, and samples were infused using the Acquity Sample Manager with a mobile phase consisting of A1 (99% water +1% acetonitrile + 0.1% formic acid) and B1 (100% acetonitrile + 0.1% formic acid, with a fast sample flow rate of 1 µl/min). Data-independent acquisition/iron mobility separation experiments (MSEs) were performed, and data were acquired over an m/z range of 50 - 2000 Da, scan time of 1 sec, ramped transfer collision energy of 20 to 50 V, and total acquisition time of 115 min. All samples were run in triplicate and repeated in 2 different experiments to ensure reproducibility of results. The data were accessed via the Mass Lynx program (Version. 4.1, SCN833, Waters, Manchester, UK) using the resolution and positive-polarity modes. The data were background subtracted, smoothed, and de-isotoped at a medium threshold. Progenesis LC/MS QI for proteomics (QIfp was used for all automated data processing and database searches. The generated peptide masses were compared against the Uniprot human proteome database (www.unprot.org) using Progenesis QI for proteomics (Waters, UK, Nonlinear, UK) for protein identification and differential analysis.

3.3.2.4.3. Data Analysis and Informatics

Progenesis QI (Nonlinear Dynamics, Newcastle, UK) software was used for data processing and search. The software generated normalized label-free relative quantification analyses and significantly differentially proteins were subjected to unsupervised principal component analyses (PCA) for all sample groups. Multivariate data analysis Variance (ANOVA) at $p \leq 0.05$ was used to identify significant alterations in regulated proteins and in addition, the expression level of at least ≥ 1.5-fold change between paired of samples being compared.

3.4. Results

3.4.1. *In vitro* cell viability assay of afatinib and other cancer drugs

As shown in Figure 3- 2, the results demonstrated that AFT and paclitaxel on H-1975 cells had a dose-dependent effect on cytotoxicity. On the contrary even up to the highest doses of carboplatin and gemcitabine minor cytotoxicity against H-1975 cells was observed. The IC_{50} values for AFT and paclitaxel were 20 and 25 µM, respectively. By increasing the concentrations of AFT to 40 µM, H-1975 cells exhibited higher sensitivity than with paclitaxel. The cell viability dropped to 2% with 40 µM of AFT and 50% with paclitaxel. Upon further increasing the concentration of AFT up to 80 µM, an insignificant reduction on the cell viability was observed (Figure 3- 2). Thus, demonstrating that AFT has potent cytotoxic effect (IC50 value; 20 µM) compared to other drugs.

The cell toxicity of the optimum liposomes PSL, NL, and CL was also measured by a WST-1 assay on H-1975 cells. Unfortunately, the reduction of cell viability (H-1975 cells) at any AFT concentrations was not recorded. This behavior confirmed that the WST-1 assay unable to detect any reduction in viable cell numbers.
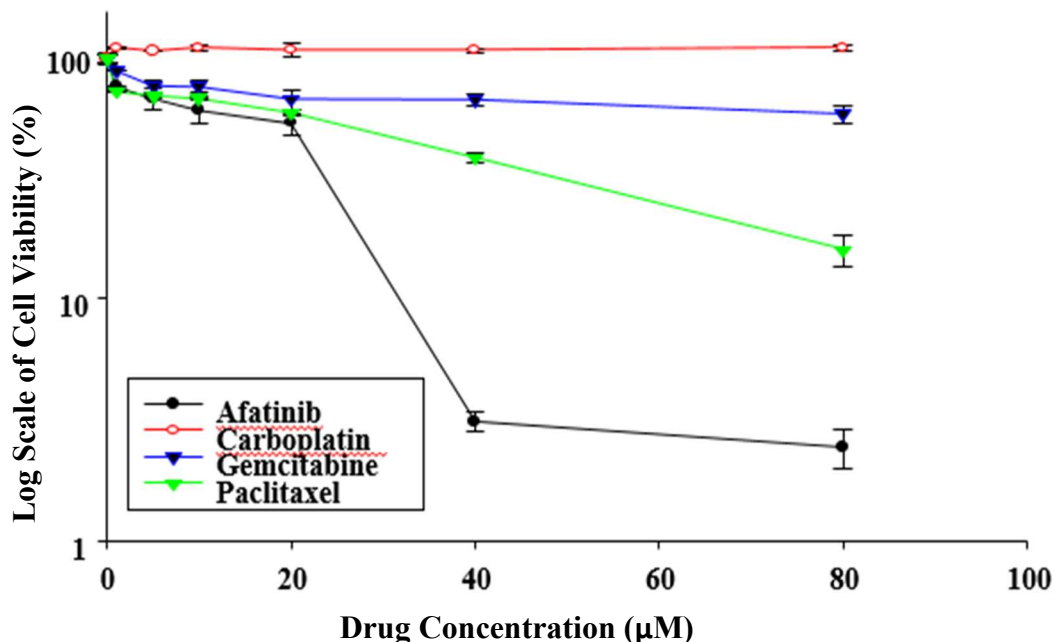
Figure 3- 2: Cytotoxicity of afatinib, carboplatin, gemcitabine and paclitaxel on H-1975 cells, as determined by a WST-1 assay. Cells were treated with varying concentrations of the drugs for 24 h. Results are from three independent experiments and are expressed as the mean ± SD.

In contrast, the cytotoxicity (dose-dependent) was detected by microscopic examination using 1-80 μM of PSL, NL, and CL.Accordingly, intracellular vacuoles and cell aggregates at concentrations from 1 to 5 μM appeared. Further increasing the concentrations from 10 to 80 μM, resulted in observation of indefinite aggregates of damaged and dying cells. The order of liposomes toxicity to H-1975 cell was PSL > NL

> CL. Therefore, AFT-loaded PSL at concentrations less than 10 μM were used for the next study.

3.4.2. Annexin-V apoptosis assay

The quantities of apoptotic cells increased from 55 to 58.9 % after exposure to 0.5 to 1 μM of PSL. However, increasing the concentration to 8 μM resulted in a reduction of the quantities of apoptotic cells from 30% at 3 μM to 9 % at 8 μM. Furthermore, a high cell viability of 87.5 % with unloaded liposomes was observed. When the concentration of PSL was increased from 3 to 8 μM, the proportions of necrotic cells increased as the number of apoptotic cells decreased. The proportion of necrotic cells increased from 3 to 90% depending on the concentrations of PSL at 0.5 and 8 μM (a dose-dependent manner) (Figure 3- 3B).

Consequently, AFT at a concentration of 2.0 μM was selected for further cytotoxicity studies using different lung cancer cell lines due to the high apoptotic activity.

The cell viability of PSL after H-1975 cells were incubated for 24, 48 and 72 h, was also measured (Figure 3- 4). A significant cytotoxic effect in H-1975 cell at a concentration of 2 μM of PSL was observed, with the total cell death proportion exceeding 78, 80 and 84 % after 24, 48 and 72 h, respectively. The cytotoxic effect of the PSL formulation at a concentration of 2 μM was mainly due to induced apoptosis, with slight necrosis. For comparison, the cell viability of unloaded liposomes at 72 h was 90 %. These results revealed no significant difference in the cell death after 24, 48 and 72 h of exposure with H-1975 cells ($p > 0.05$). Therefore, 24 h of exposure was selected for further study. Unloaded liposomes showed insignificant cytotoxicity (apoptosis) after 24 and 48 h of exposure with considerable toxicity (necrosis) after 72 h of exposure.
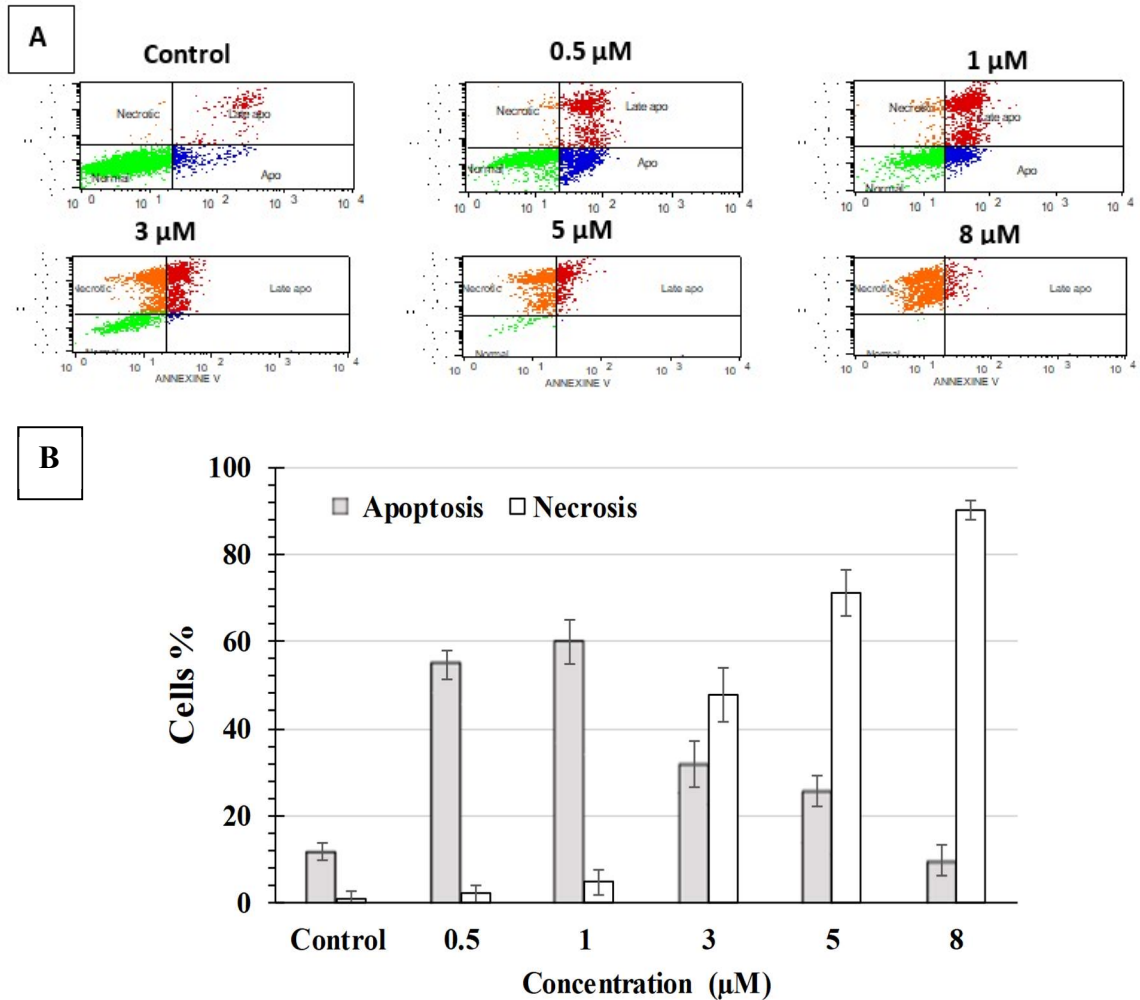
Figure 3- 3: H-1975 lung cancer cells were either treated with free liposomes, as control, or challenged with Afatinib loaded liposomes (PSL) for 24 hr, and then the proportion of apoptosis and necrosis was analyzed by Annexin V/PI flow Cytometry. four groups of cells, viable cells that excluded both Annexin V and PI (Annexin V$^-$/PI$^-$), bottom left; early apoptotic cells that were only stained with Annexin V (Annexin V+/PI$^-$), bottom right; late apoptotic cells that were stained with both Annexin V and PI (Annexin V+/ P+), top right and necrotic cells that were only stained with PI (Annexin V$^-$/PI+), top left. (A) Flow charts. (B) Histogram showing the percentage of induced apoptosis in H-1975cells.
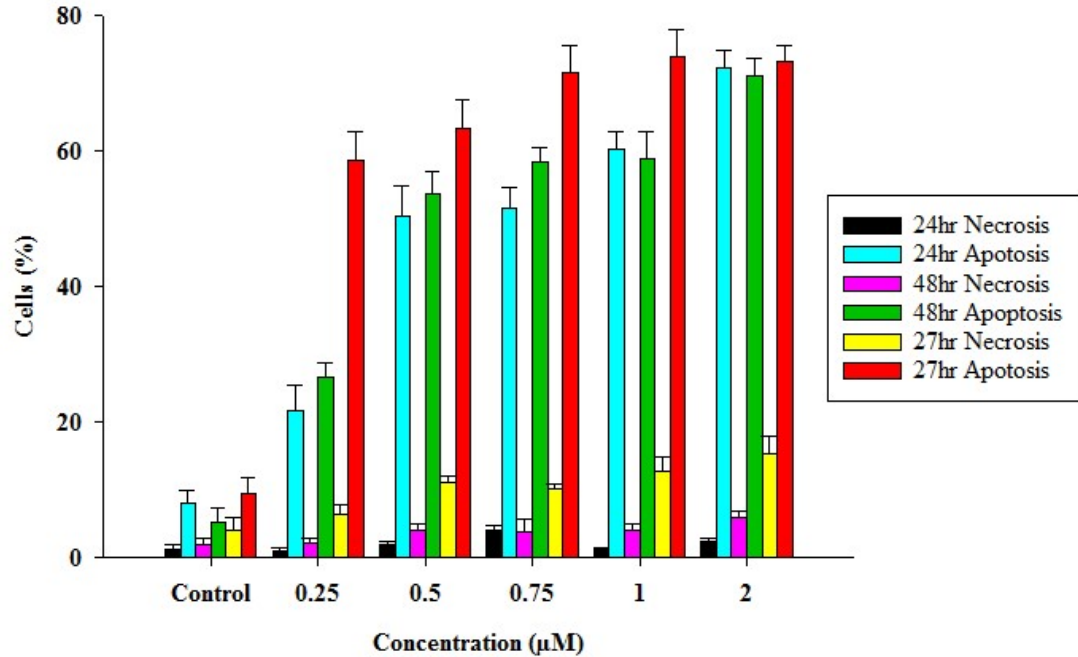
Figure 3- 4: H-1975 cells were challenged with pH-sensitive liposomes (PSL) (0.25-2 μM) for 24, 48 or 72 h, following which apoptosis was analyzed with Annexin V/PI-flow cytometry. Each value represents the mean ± SD of three independent experiments performed in triplicate.

For further cytotoxicity study of PSL, CL and NL using different lung cancer cell lines a period of 24 h was selected. The anticancer activity of these liposomes was analyzed using flow cytometric with three cell lines: H-1975, H-1650, and HCC-827 (Figure 3-5A, B & C). This study was conducted to detect the level of apoptosis induced after incubation with various concentrations of 0.25, 0.5, 0.75, 1, and 2 μM of each liposome formulation for 24 h using dimethyl sulfoxide and unloaded liposomes as the controls. The incubation of the cells with unloaded liposomes did not induce notable cytotoxicity. The viability of H-1975 cells decreased more significantly compared to H-1650 and HCC-827 cells ($p < 0.05$).
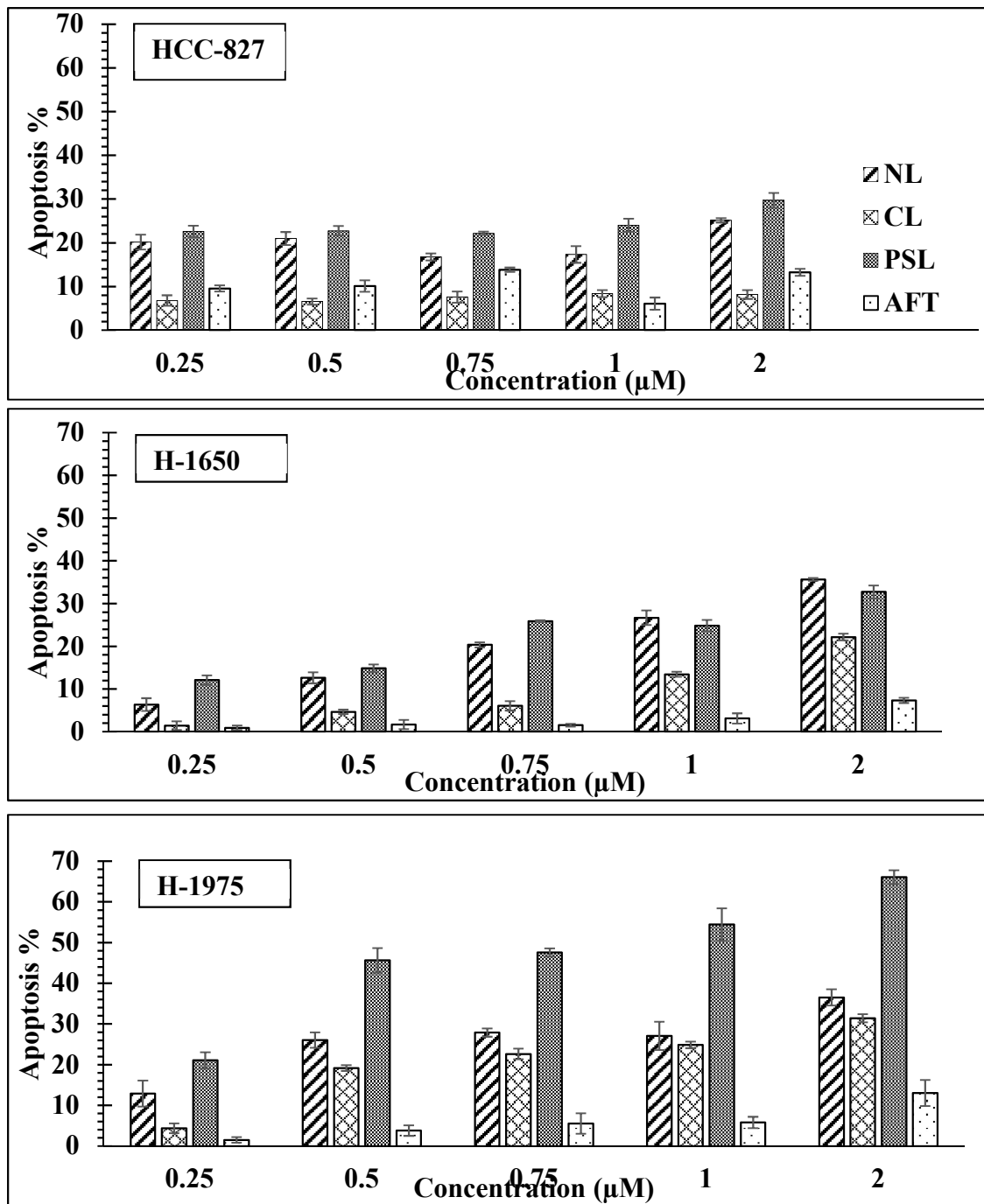
Figure 3- 5: Non-small cell lung cancer cells were either treated with free liposomes, as the control, or challenged with AFT or AFT-loaded liposomes (PSL, NL, and CL) for 24 h, following which the proportion of apoptotic cells was analysed using Annexin V/PI-flow cytometry. Histogram shows the percentage of induced apoptosis in H-1975 cells. Each point represents the mean ± SD of three independent experiments performed in duplicate.

PSL produced highest cytotoxic effect in the different lung cancer cell lines (H-1975 cells and H-1650) compared to NL and CL, when using concentrations 2 µM AFT (Figure 3-5). Overall, the results clearly revealed the superior anticancer activity of PSL.

3.4.3. Differentially expressed proteins in H-1975 and H-1650

A total of 812 proteins were identified across all the sample groups. Among these proteins, 385 were significantly differentially expressed with at least ≥2-fold change ($p < 0.05$) between treated and control samples from the two cell lines (H-1975 and H-1650). The dataset of 385 differentially expressed proteins was subjected to Principal Component Analysis (PCA) and all samples were distinctively clustered into four separate groups (Figure 3- 6). The H-1650, treated (Rx) and control (green and orange respectively) being slightly separated and (not as widely separated as in H1975 pairs). Pair wise comparison of protein expression changes between H-1975 treated (Rx) versus control (Ctrl) was performed resulting in 186 significantly differentially expressed proteins (Figure 3- 7). Similar analysis of pairs of H-1650 Rx versus Ctrl indicated only 27 proteins differed significantly. Only 12 proteins overlapped between the two datasets of significant protein changes between H-1975 Rx/Ctrl and H-1650 Rx/Ctrl (Figure 3- 7). This 12-protein panel might be considered as having similar treatment relatedness between the two different cell lines. The 385 identified differentially expressed protein dataset was subjected to pathway analysis of network signaling in order to further understand the biological processes of some of the identified proteins. Only a fraction of the proteins was represented in the ingenuity pathway analysis database (Ingenuity Systems, Inc., Redwood, CA, USA) and the analysis of some of these proteins was composed of multiple cancer- related networks.

Figure 3- 8 showed the identified proteins that have been associated with NSCLC. The connections and the expression profiles of some of the identified proteins are as indicated. The majority of these molecules are located in the cytoplasm and few of them located in the plasma membrane and another in the nucleus. While many of them act as enzymes, others act in kinase translation and transduction regulation as detailed in Table 3- 3.

Figure 3- 6: Principal Component Analysis (PCA) plot of 385 differentially expressed proteins (ANOVA 0.05 and ≥ 2-fold change) between both H-1975 and H-1650, treated (Rx) and control (Ctrl) cells. Four distinct clusters were observed with samples with H-1975-treated and control (blue and purple respectively). H-1650, treated (Rx) and control (green and orange respectively). The letters in grey scale are the accession numbers of each of the proteins. The PCA plot was generated from Progenesis QI for proteomics (Progenesis QIfp version 2.0.5387) (Nonlinear Dynamics/Waters)].

Figure 3- 7: Comparative analysis of the proteins identified in the study.

Figure 3- 8: Pathway analysis of network signalling of some of the 385 identified proteins as represented in one of the networks signalling in the ingenuity pathway analysis database. The connections and the expression profiles of some of the identified proteins are as indicated. Pink colour is indicative of downregulation. A direct connection is by solid line and broken lines indicate an indirect interaction between different molecules. Network analysis was performed and figure and table partly generated in an ingenuity pathway analysis program (IPA v8.7)].

Table 3- 3: A selection of the identified 385 differentially expressed proteins between H-1975 and H-1650 at treatment and at control that were implicated in Ingenine Pathway Analysis as shown in figure 3- 8.

No	Accession	Peptide count	Unique peptides	ANOVA (p)	Max fold change	Highest mean condition	Lowest mean condition	Protein Symbol	Description	Location	Family
1	Q16543	11	9	0.0087	3.8039	H1975-Ctrl	H1975-Rx	CDC37	Hsp90 co-chaperone Cdc37	Cytoplasm	kinase
2	Q01518	10	7	0.0185	3.0779	H1650-Rx	H1975-Rx	CAP1	Adenylyl cyclase-associated protein 1	Plasma Membrane	other
3	P63167	1	1	0.0264	66.242	H1650-Ctrl	H1975-Ctrl	DYNLL1	Dynein light chain 1, cytoplasmic	Cytoplasm	other
4	Q15056	2	1	0.0200	7.7860	H1975-Ctrl	H1975-Rx	EIF4H	Eukaryotic translation initiation factor 4H	Cytoplasm	translation regulator
5	P41250	11	8	0.0121	2.8167	H1650-Rx	H1975-Rx	GARS	Glycine--tRNA ligase	Cytoplasm	enzyme
6	Q99714	1	1	0.0067	169.19	H1650-Ctrl	H1975-Rx	HSD17B10	3-hydroxyacyl-CoA dehydrogenase type-2	Cytoplasm	enzyme
7	P00338	30	22	0.0001	3.0382	H1975-Ctrl	H1975-Rx	LDHA	L-lactate dehydrogenase A chain	Cytoplasm	enzyme
8	P27816	16	10	0.0057	3.1206	H1975-Ctrl	H1975-Rx	MAP4	Microtubule-associated protein 4	Cytoplasm	enzyme
9	P35749	36	17	0.0101	2.0138	H1975-Ctrl	H1975-Rx	MYH11	Myosin-11	Cytoplasm	other
10	P35579	101	72	0.0001	6.6865	H1975-Ctrl	H1975-Rx	MYH9	Myosin-9	Cytoplasm	enzyme
11	P60660	14	10	0.0008	4.2310	H1975-Ctrl	H1975-Rx	MYL6	Myosin light polypeptide 6	Cytoplasm	other
12	P15531	8	1	0.0001	3.2862	H1650-Ctrl	H1975-Rx	NME1	Nucleoside diphosphate kinase A	Cytoplasm	kinase
13	P13797	12	6	0.0049	4.4763	H1650-Ctrl	H1975-Rx	PLS3	Plastin-3	Cytoplasm	other
14	P17980	6	5	0.0145	3.9959	H1975-Ctrl	H1975-Rx	PSMC3	26S protease regulatory subunit 6A	Nucleus	transcription regulator
15	P09493	14	3	0.0006	4.1765	H1650-Ctrl	H1975-Rx	TPM1	Tropomyosin alpha-1 chain	Cytoplasm	other

3.6. Discussion

In general, it is essential to screen and confirm that antitumor drugs are potent and efficient for cancer therapy. Therefore, the potency of AFT was evaluated in comparison with selected drugs depending on their efficacies against lung cancer in an *in vitro* cell-based assay. Half-maximal inhibitory concentration (IC_{50}) of these drugs was attained from an experimentally derived dose-response curve. In this study the cytotoxicity was evaluated with a WST-1 assay in H-1975 cells. The cells were incubated with AFT, paclitaxel, carboplatin and gemcitabine for 24 h. The WST-1 assay showed that AFT was more effective as a cytotoxic agent compared with other drugs commonly used for lung cancer treatments (Figure 3- 2). These results are comparable to results of two randomized phase III trials, where AFT exhibited significant benefit in progression-free survival compared with standard chemotherapy regimens in NSCLC patients with EGFR mutations [6, 32]. Similarly, in LUX-Lung 6, AFT was compared with cisplatin plus gemcitabine. Afatinib showed a more profound and durable effect and an increased progression free survival of 11 versus 5.6 months compared with standard first-line chemotherapy (cisplatin plus gemcitabine) for Asian patients with NSCLC tumours having EGFR mutations [6]. Since, WST-1 is a colorimetric assay and, by definition the measurement of colour in a solution, whereas liposomes have a whitish colour. It was observed that the phospholipids used in the liposome preparation, interfered with the colour formation and give rise to an opaque milky solution during the reaction with WST-1 which led to unreliable reading results. But under a microscopic examination, it was clear that CL NPs have the highest level of interference in the assay (data not presented) due to the cationic phospholipid DOTAP but a detailed characterization of this interference

was not undertaken. Therefore, cell viability levels were verified for each liposomal formulation using flow cytometry analysis following Annexin V/PI staining.

The apoptosis-inducing influence of AFT loaded-PSL formulation was evidenced by Annexin V/PI protocol. The extent and the nature of the induced cell death were analyzed by flow cytometry. H-1975 cells were incubated with various concentrations of PSL (0.5 - 8 µM) for 24 h, which were selected based on WST-1 assay results. The amounts of the early apoptotic and the late apoptotic cells, with necrotic cells were determined after deduction of the proportion of spontaneous apoptosis. The results clearly reveal that the PSL triggered apoptosis in H-1975 cells (Figure 3- 3A).

The results indicated a marked decline in cell viability following treatment with PSL, compared with AFT solution, indicating that liposomes can improve the therapeutic efficacy of AFT in NSCLC. Liposomes have emerged as an important potential drug delivery vehicle for chemotherapy drugs and small molecule compounds in tumor therapy application [72]. The IC_{50} of PSL was 26 times lower than that of free AFT (Figure 3- 3). The absence of a strong cytotoxic effect of drug solution could be due to a low intracellular drug concentration, which may result from low cellular drug uptake due to poor trans-membrane permeability, or even due to drug efflux. These results are generally in agreement with those obtained by Guan et al. who found that treatment of human colorectal cancer HCT-15 cells with AFT encapsulated micelles showed a higher decrease in the cell viability than treatment with AFT alone. However, micelles alone showed the non-cytotoxicity of the materials in HCT-15. Also, flow cytometric analysis indicated that cell apoptosis was significantly increased in AFT/micelle-treated tumor cells as compared with AFT alone [220].

Of the three cancer cell lines tested, H-1975 cells appeared to be more sensitive to the liposomal formulation as relatively lower drug concentrations effectively induced

cytotoxicity. These results suggest that NSCLC cells with T790M mutant EGFR are relatively more sensitive to AFT than cells carrying wild-type EGFR, which is consistent with the results from earlier studies [221, 222]. Ninomiya1 et al., investigated the *in vitro* efficacy of AFT against tumor cells with activated EGFR mutations with or without the T790M mutation. They found that the presence of AFT significantly increased the cell killing effect in PC-9- GR cells harboring acquired T790M [222]. Moreover, they found that AFT was more potent than gefitinib in the treatment of lung adenocarcinoma with an EGFR exon 19 deletion mutation. Also, Zhang et al reported that NSCLC cells with T790M mutant EGFR are relatively more sensitive to AFT than cells carrying wild-type EGFR [221].

It is possible that PSL released AFT in response to the lower pH environment in the endosome, and thus facilitated diffusion of the released AFT from the endosome to the cytosol. One possible mechanism of such facilitated diffusion could be the destabilization of endosomal membranes generated from the destruction of liposomes. It has been suggested that pH-sensitive liposomes are internalized more efficiently than non-pH-sensitive formulations [223, 224]. In this context, it is noteworthy that studies on the destabilization of liposomes at the endosomal level and investigations involving the incubation of cells with lysosomotropic agents (e.g. ammonium chloride or chloroquine, which prevent endosome acidification) demonstrated that the efficacy of pH-sensitive liposomes depends on the pH decline following endosome maturation [84]. Additionally, various kinetic studies have shown that liposomes composed of DOPE/OA, DOPE/palmitoylhomocysteine, DOPE/dipalmitoylsuccinylglycerol or CHEMS [179] release their contents into the cytoplasm over a period of time that ranges from 5-15 min post incubation with the cells, thus signifying that cytoplasmic delivery occurs from early and late endosomes. These observations suggest that the

fusion or destabilization of liposomes induced by acidification of the endosomal lumen represents the most important stage in the process of intracellular delivery. However, the molecular mechanisms underlying how liposomes can overcome the barriers presented by the cytoplasmic and endosomal membranes to release their contents into the intracellular space remain to be clarified. Carvalho et al developed cisplatin pH-sensitive liposomes (DOPE/CHEMS/DSPE-PEG) to treat SCLC [225]. Compared with free cisplatin, the cytotoxicity of this PSL was significantly enhanced. Furthermore, this approach is effective for cells that are tolerant/resistant to cisplatin [225]. Kim *et al* developed a PSL with an EGFR antibody attached, which was designed and tested using A549 cells and a BALB/c-nu/nu mouse tumour model. They found that PSLs provide an efficient and targeted delivery system for gemcitabine, and may represent a useful, novel treatment approach for tumours that overexpress EGFR [226].

To understand the response of NSCLC cells to PSL NPs therapeutics, a quantitative proteomic approach was used to study the protein expression profiles of NSCLC cells treated with AFT. The results show significantly differentially expressed proteins from both treated and control H1975 and H1650 NSCLC cells demonstrating the ability to discriminate treatment effects between the sample groups.

The strategy of differential gene expression changes provides a unique possibility to identify treatment-related biomarkers from different types of NSCLC thus providing insights into the possibility of translating these findings into humans.

Differential protein expression changes across different types of NSCLC cells were used to accurately classify the samples into different treatment sub groups. Thus, the expression of the 385 protein changes across the four sample groups were further evaluated for their associations with cancer. The analysis of the identified proteins is

composed of cancer- related networks and have been implicated in NSCLC. This means, that it will be challenging that one panel of biomarker proteins will have similar changes across different cell types. Hence a protein dataset might need to be created for each specific treatment cell types.

Interestingly, a review of literature indicated that 15 molecules that were implicated in the IPA analysis in one of the networks as shown in Figure 3- 8 have been associated with NSCLC. The analysis of the identified proteins is composed of cancer- related networks some of the associated molecules in pink color have been implicated in NSCLC. This demonstrates the power of proteomics in the identification of 15 potential biomarkers in one study that have previously been described in different individual studies using different analysis platforms [227, 228].

Even though some of these potential biomarkers have been singly described, these findings indicate that rather than the use of a single marker, analyses of a panel of protein markers has the potential to provide better insights and understanding of a particular treatment response on NSCLC cells. There is still a limitation in translating the findings of this *in vitro* study into humans, as markers of treatment responses. However, these molecules could be validated using other methods such as immunohistochemistry and possibly using an animal model prior to translation into humans.

Targeting the tumor metabolism via anti-glycolytic treatments can be a therapeutic option as it considers an important converging step for multiple deregulated signaling pathways in cancer cells. Lactate dehydrogenase-A (LDHA) catalysis the interconversion of pyruvate and L-lactate and also regenerates NAD^+, which is essential for the continued high glycolysis rate in cancer cells [229]. LDHA plays an important role in the development, invasion and metastasis of malignancies, including

lung cancer [230]. LDHA is overexpressed in NSCLC tissues which is linked to tumor hypoxia, angiogenic factor production and poor prognosis [231]. Fantin et al. proved that tumor cells depend on LDHA activity, while nonmalignant cells depend on the oxidative phosphorylation system, by showing that growth of LDHA-deficient tumor cells was reduced in mouse Neu4145 mammary gland tumor cells even under hypoxic conditions (0.5% oxygen) [232].

Adenylate cyclase-associated protein 1 (CAP1) is one of the major actin-regulating proteins in cancers [233] and the role of CAP1 in the proliferation and differentiation of cancer cells has been paid much consideration [234]. A study by Tan et al assessed the diagnostic and prognostic value of CAP1 for lung cancer using real-time PCR and Western blot analysis and/or immunostaining in biopsy specimens of lung cancer and in cultured lung cancer cells. They found that overexpression of CAP1 in lung cancer cells, mainly at the metastatic stage, may have important medical implications as a diagnostic/prognostic factor for lung cancer [235]. It has been found that expression of CAP1 was significantly higher in NSCLC tissues as compared to the corresponding normal lung tissues and there is connection between the tissue protein CAP1 level and the stage of NSCLC [228, 233].

One of the most important proteins is TGFβ1 (Figure 3- 8), a multifunctional cytokine that widely involved in the adjustment of life activities, such as proliferation, differentiation, migration, and apoptosis [236]. At present, an increasing number of researchers have showed that the TGF-β signaling pathway is related to tumor progression [237-239]. The TGFB1 expression may be a predictive biomarker for the risk of developing metastasis in non-small cell. Importantly, increased TGFb1 expression and increased serum levels are linked with progression of lung cancer in patients with NSCLC [187, 188, 240-242]. Interestingly, Sang et al demonstrated that

polymorphism of the TGFB1 gene was linked with clinical progression of NSCLC patients and might be a predictive marker for NSCLC prognosis [154]. These data indicate that TGFb1 (Figure 3- 8) is at the center of the network interacting with all these molecules. Therefore, expression of these molecules may be predictive biomarkers for the risk of developing metastasis in non-small cells.

3.7. Conclusion

The obtained results revealed the efficiency of AFT as potent cytotoxic drug (IC50 value; 20 µM) compared to other drugs commonly used for lung cancer treatments. Also, AFT-loaded liposomes showed enhanced cytotoxicity on cancer cells (NSCLC). The PSL inhibited the cell growth of lung cancer cells more efficiently than CL, NL and free AFT based on using Annexin V assay. The PSL produced the highest cytotoxic effect in the different lung cancer cell lines. Also, the identified protein signatures have been capable of prediction of treatment response and choice of therapy for two different types of human NSCLC cells (H1975 and H1650) using expression proteomics as biomarker discovery for treatment options. These findings lend further support to the efficacy of PSL NPs in treatment of NSCLC harboring EGFR mutations, and the identification of a new biomarker in lung cancer will provide a theoretical basis for clinicians and researchers to develop a new therapeutic approach for NSCLC.

All together, these data indicate that PSL NPs is a promising targeted drug delivery for NSCLC and should be further investigated for incorporation of PSL NPs into micron-scale structures NCMPs via spray drying.

Chapter 4

Formulation of Afatinib Loaded Nanoparticles as Aerosolizable Microcarriers

4.1. Introduction

Local administration of nanoparticulate chemotherapeutic agents to the respiratory tract of patients with NSCLC is a promising therapeutic technique [243]. Inhalation therapy can play an important role in the fight against cancer by delivering chemotherapeutic drugs locally to the lung tumor cell and thus; reduce systemic exposure to the drugs, enhance exposure of tumor tissue to the drug, and reduce systemic side effects [61]. One approach for delivering chemotherapeutic drugs to the lung is the use of DPIs, owing to their advantages over pressurized metered dose Inhalers (pMDIs), such as being breath-activated and having no requirement for propellant [16, 244].

Several studies have demonstrated the applicability of liposomes for the pulmonary delivery of a large variety of drugs such as; anti-asthmatic drugs, cytotoxic agents, and drugs for systemic action [245]. However, there are some drawbacks with liposomal formulations that can restrict their commercial use such as high manufacturing cost and instability during storage, even at low temperatures [246].

One strategy to increase the stability of liposomes is spray drying (SD). The SD process is an attractive solidification technique in the field of drug delivery, due to its relative simplicity, the ability to produce a homogenous particle size distribution, the availability of large-scale equipment, and the capability to control several parameters to optimize the particle characteristics such as shape, morphology, size, size distribution, and density [247]. Accordingly, it can be used to produce dry powders for inhalation.

The pulmonary delivery of NPs requires incorporation into microcarriers, of between 1 to 5 μm, consisting of NPs and inert pharmaceutical excipients, such as sugars, amino acids, or phospholipids. Delivering NPs within nanocomposite microparticles

(NCMPs), directly to the lungs via DPI, offers many advantages. These include; the elimination of potential drug degradation in the low pH environment of the stomach, reduced exposure to proteolytic enzymes, and the improved physical and chemical stability as a dry formulations [248].

Biocompatible excipients (carbohydrates, amino acids, and lipids) are generally added to the formulation feed to produce dry powders of a desirable aerodynamic particle size that will rapidly release the NPs upon contact with the lung fluid lining [255]. Additionally, the excipients will impart some level of protection to both the NPs and encapsulated drug during SD, against the high shear forces and the elevated temperatures used, and offer stability during storage [249].

L-leucine (LEU) is an example of an amino acid excipient that is commonly used in the pharmaceutical industry due to its potential to improve the bioavailability and dispersibility of aerosols. Spray drying of a LEU solution produces corrugated particles with low density which improves the aerosolization of the incorporated species [250].

Chitosan (CH) is a cationic mucoadhesive polymer derived from the natural polymer chitin, one of the most abundant polysaccharides in nature [251]. Chitosan has been widely used in drug delivery research because of its biocompatibility, biodegradability, very low toxicity and its potential to be chemically modified [252]. Recently, particulate carriers based on CH and its derivatives have been extensively investigated for pulmonary delivery of various therapeutic drugs and proteins [253-255]. Due to its mucoadhesive properties, permeation-enhancing effect, controlled release properties, and capability to open tight junctions between epithelial cell, CH is a promising material for countless DDS [255-257]. Chitosan can significantly enhance the adsorption of therapeutic agents to mucosal surfaces [258, 259] and

improves the dispersion characteristics of dry powders [251], offering several important advantages for the pulmonary delivery of macromolecules locally in the lung or systemically upon absorption through the alveolar region [260, 261].

Chitosan can be formulated as powders or well-structured micro and nanocarriers that can be engineered to have optimal aerodynamic particle diameters for deep lung deposition and prolonged retention [262]. The mucoadhesive properties of CH are due to the molecular attractive forces formed by the electrostatic interaction between the positively charged CH molecules and the negatively charged mucosal surfaces [263, 264].There are several examples in the literature of the successful spray-drying of liposomes using different carriers. Cationic liposomes spray dried with and without paclitaxel using trehalose as carrier indicated that liposomes were well retained after SD under different drying conditions and the protective effect of trehalose was very important at high inlet temperatures [206]. Charnvanich et al. studied the effect of cholesterol on the encapsulation efficiency and physical characteristics of spray dried liposomes [265]. Cholesterol enhanced the encapsulation and reduced the diameter of the reconstituted liposomes. A stable, spray dried preparation of CH coated liposomes was also prepared using maltodextrin as an excipient [266]. Liposomes composed of soybean PC (SPC) were spray dried in the presence of lactose at an inlet temperature of 110 °C and an outlet temperature of 75 – 80 °C and dispersed in water to rehydrate liposomes without major changes in the vesicle size distribution. Moreover, the chemical stability (hydrolysis and oxidation) of the phospholipids was not significantly affected by this process [264]. A study by Hauser and Strauss, reported that 90% of the entrapped hydrophilic model compounds (raffinose and KFe(CN)) remained encapsulated in small unilamellar palmitoyloleoylphosphatidylcholine (POPC) / dioleoylphosphatidylserine (DOPS) vesicles after SD and rehydration, by

applying sucrose as a stabilizer at an inlet temperature of 140°C and an outlet temperature of 67°C [266]. Lo et al, showed that the use of Dipalmitoylphosphatidylcholine (DPPC), a natural lung surfactant, with sucrose showed good results for the liposomal preparation of superoxide dismutase enzyme, efficiently protecting the enzyme from degradation and loss of activity [267]. Moreover, the formulation demonstrated good powder aerosolization with mean particle sizes of 3 μm [267]. Chougule et al. evaluated liposomal encapsulated Dapsone in a dry powder inhaler, reporting *in vitro* prolonged drug release up to 16 h [268]. Liposomal tacrolimus was reported to have a prolonged residence time of up to 24 h within the lungs. Also, the stability of liposomal tacrolimus embedded in a trehalose matrix, for six months at 40 °C / 75 % RH, showed an increase in liposome size, a decrease in Fine Particle Fraction (FPF) and prolonged retention at the lung [268].

4.2. The aim of the Study

The aim of this study was to develop a suitable formulation for the dry powder delivery of AFT-liposomes to the deep lung.

In this study, pH sensitive liposome (PSL) NPs (optimized in chapters 2 and 3) encapsulating AFT were incorporated into microparticle carriers via SD to produce PSL NPs/NCMPs as DPIs suitable for pulmonary delivery.

The aim of the study was achieved by the following objectives to:

1. Incorporate optimum PSL NPs into NCMPs via spray drying with L-leucine as a dispersibility enhancer.

    a. Optimize NCMPs formulations in term of size and yield%.

2. Formulate NCMPs using CH containing the optimum ratio of LEU to generate highly respirable powders.

   a. Evaluate the effect of different ratios of CH on the morphology, particle size, yield %, and drug content of NCMPs.

   b. Investigate NPs size recovery from NCMPs and the release of AFT from NCMPs vs NPs.

   c. Study the *in vitro* aerosolization behavior and cell toxicity of the optimal coated NCMPs.

   d. Determine the stability of the coated NCMPs.

4.3. Materials and Methods

4.3.1. Materials

AFT (99.8% purity) was purchased from Green Stone Swiss Co., Limited. Triton X-100, Triethylamine, Sodium hydroxide pellets, L-leucine, Chitosan poly (D-glucosamine) Deacetylated chitin low molecular weight, and Acetic acid glacial were purchased from Sigma-Aldrich, Saint Louis, USA. All other reagents and chemicals were of analytical grade.

4.3.2. Methods

4.3.2.1. Synthesis and characterization of pH sensitive liposome nanoparticles

The pH sensitive liposomes (PSL NPs) was synthesized and characterized as described earlier in sections 2.3.2. and 2.3.3, respectively.

4.3.2.2. Preparation of nanocomposite microparticles

4.3.2.2.1. Preparation of nanocomposite microparticles using L-leucine
(LNCMPs). Nanocomposite microparticles (NCMPs) of PSL NPs were prepared by SD using LEU as a carrier at different lipid: carrier ratios (w/w). A quantity of PSL NPs was dispersed in LEU solution (10 mL) at lipid: LEU ratios of 1:0.5, 1:1, and 1:1.5 w/w, and spray dried using a Büchi B-290 mini spray-dryer (Büchi Labortechnik, Flawil, Switzerland) with a nozzle atomizer, and nozzle orifice diameter of 0.7 mm. The spray drying was performed at a feed rate of 10%, an atomizing air flow of 400 L/h, aspirator capacity of 100% and an inlet temperature of 100°C (outlet temperature approximately 30–35°C). The dry NCMPs were separated from the air stream via a high-performance cyclone (Büchi Labortechnik), collected and stored in desiccator room temperature until further use.

4.3.2.2.2. Preparation of coated nanocomposite microparticles using L-leucine and chitosan (CNCMPs)

Appropriate amounts of LEU and CH were dissolved under stirring in distilled water or acetic acid (0.1%) aqueous solution, respectively. A quantity of PSL NPs was dispersed in the LEU solution (lipid: LEU ratio of 1:1.5 w/w) with stirring at 25∘C for 1 min and then the CH solution was added at different CH ratios (CNCMPs). The lipid: LEU: CH ratios are; 1:1.5:0.5 (C1NCMP), 1: 1.5:1 (C2NCMP), 1: 1.5:1.5 (C3NCMP) and 1: 1.5:2 (C4NCMP) (w/w)) and stirred for 5 min at 25∘C to maintain homogeneity. The dispersions were spray dried as stated in section 4.3.2.2.

4.3.3. Characterization of nanocomposite microparticles

4.3.3.1. Particle size and zeta potential of the reconstituted liposomes

The reconstituted liposomes were characterized for particle size, polydispersability (PDI), and zeta potential as described previously in section 2.3.3.1. Before measurements, 5 mg of spray dried powders was dispersed in 10 mL distilled water with vortexing for 5 minutes.

4.3.3.2. Morphology and size of nanocomposite microparticles

The surface morphology of NCMPs was determined using a Field Emission Scanning Electron Microscope (JSM-6060LV, JEOL Scaning Electron Microscope, Japan). A thin layer of NCMPs was fixed on carbon adhesive tape on an aluminium stub. The sample was sputter coated with platinum under argon atmosphere at 180 mA for 1 min using the autofine coater (JEC-3000FC, JEOL Japan). Photographs of the spray dried powders were taken by random scanning of the stub.

Five milligrams of the spray dried powders were suspended in 2 ml deionized water and immediately measured by laser diffraction [269], using a Zetasizer Nano ZS (Malvern Instruments, UK) at 25°C (n=3), to determine the geometric particle size by laser diffraction using a Zetasizer Nano ZS (Malvern Instruments, UK).

For scanning electron microscopy (SEM) the spray-dried powders were coated with gold in a sputter coater and their surface morphology was observed using a scanning electron microscope (JEOL 6500F field emission scanning electron microscope; Tokyo, Japan).

4.3.3.3. Nanocomposite microparticle yield

The yield of spray dried NCMPs powders were computed as the percentage mass of expected total powder yield according to the following equation [270]:

$$Yield\ \% \ = \ \frac{Weig\quad of\ dry\ powde\quad collected\ after\ spray\ drying}{Weight\ of\ total\ dry\ mass\ used\ for\ the\ preparation} \times 100 \qquad \text{Equation 4-1}$$

4.3.3.4. Flow Properties and primary aerodynamic diameter

4.3.3.4.1. Angle of repose

The fixed funnel method was used for calculating the angle of repose for different powder formulations. The angle of repose (θ) was measured to determine the powder flowability and determined by the method described by Huang et al [271, 272].

4.3.3.4.2. Powder density

The powder density was evaluated using the tapped density measurement. The tapped density was determined from the volume occupied by a known mass of powder in a 5 ml measuring cylinder after tapping the measuring cylinder from a constant height until no further change in powder volume was observed [276]. Measurements were performed in triplicate (n= 3).

4.3.3.4.3. Aerodynamic diameter

The theoretical primary aerodynamic diameter (d_{ae}) was calculated using data acquired from geometric particle size (d) and tapped density(ρ) according to the

following equation [273]: $d_{ae} = d \sqrt{\frac{\rho}{\rho 1}}$ \qquad Equation 4-2

$\rho 1 = 1$ g/cm3

4.3.4. Drug content

The spray dried samples (10 mg) were dispersed into 5mL PBS at pH 5.5 and sonicated for 5 min before adding 5mL methanol, vortexing for 1 min, and then filtering through a 0.22 μm membrane filter. The AFT content was determined by HPLC as previously described in section 2.3.4.

4.3.5. *In vitro* aerosolization studies

The aerodynamic particle size of the CNCMPs was assessed using a Next Generation Impactor (NGI) (Copley Scientific, UK) (Figure 4- 1). The NGI has a range of cut off diameters at 60 L/min, with particles captured on any specific stage having an aerodynamic diameter less than the previous stage, assuming ideal collection behavior on each stage, using a low resistance DPI Cyclohaler® (Teva pharma) inhaler.

The DPI flow resistance is a fixed property that determines the air flow rate through the inhaler in response to the inspiratory effort of the patient. Each inhaler has a unique resistance and current inhalers have a wide range of resistance values. The maximum flow rate generated by the patient is affected by the resistance of the device, which is closely linked to the structure and mechanism of deaggregation. The higher the resistance of the DPI, the higher is the force needed to ensure a sufficient pressure drop within the device and the lower the maximum flow rate [274].

The CNCMPs samples were weighed (4 triplicates, each corresponding to 10-15 mg spray-dried powder) and manually loaded into hydroxypropyl methylcellulose capsules (size 3) and aerosolised via a low resistance DPI Cyclohaler® (Teva pharma) into NGI. The capsule was punctured using the actuator of the Cyclohaler® prior to inhalation and a pump (Copley HCP5, Copley Scientific, UK) was used to simulate inspiration (the flow rate was 60L/min for 4-5s). Prior to testing, the preseparator was filled with 15ml of mobile phase solution A (0.1% triethanolamine and 1% acetonitrile

in HPLC water (pH=6)) and the NGI stages were coated with 1% tween 80: methanol solution to eliminate particle bounce [275]. One capsule was emptied in each of the 4 runs.

Following aerosolization, the samples were collected from each stage of the NGI, pre-separator, throat, mouth piece, inhaler, and capsule by washing with a PBS/methanol mixture (50%) to dissolve the polymer and the encapsulated AFT, which was determined by HPLC as described in section 2.3.4.

The emitted dose (ED) was determined as the sum of powder deposited in the mouthpiece, throat, pre-separator, NGI stages and micro-orifice collector of the NGI (MOC). The fine particle dose (FPD was determined as the sum of powder deposited in NGI stages and MOC with aerodynamic diameters less than 4.6 μm. The FPF% was determined as the fraction of ED deposited in the NGI and MOC with aerodynamic diameters less than 4.6 μm. The mass median aerodynamic diameter (MMAD) and geometric standard deviation (GSD) were determined using online software (MMAD calculator.com).

4.3.6. *In vitro* release

The CNCMPs samples (10 - 15 mg) were placed in micro tubes, dispersed in 1 ml of PBS (pH 5.5) containing 0.2% tween 80, incubated at 37 °C and rotated at 20 rpm in a sample mixer (HulaMixer, Invitrogen Dynal AS, Life Technologies). At programmed time intervals, up to 24 h, the samples were centrifuged (Sigma 3-30k, Fixed-angle rotor 12110, SIGMA Laborzentrifugen GmbH, Germany) at 20,000 rpm for 30 min) and 0.5 ml of the supernatant removed and replaced with fresh buffer contained 0.2% tween 80 and vortexed for 1 min. The supernatant was analyzed by HPLC as described in section 2.6 (n=3).

4.3.6.1. Kinetic modelling

Kinetic modeling was carried out as described in section 2.3.5.1.

4.3.7. Cytotoxicity assessment using flow cytometry
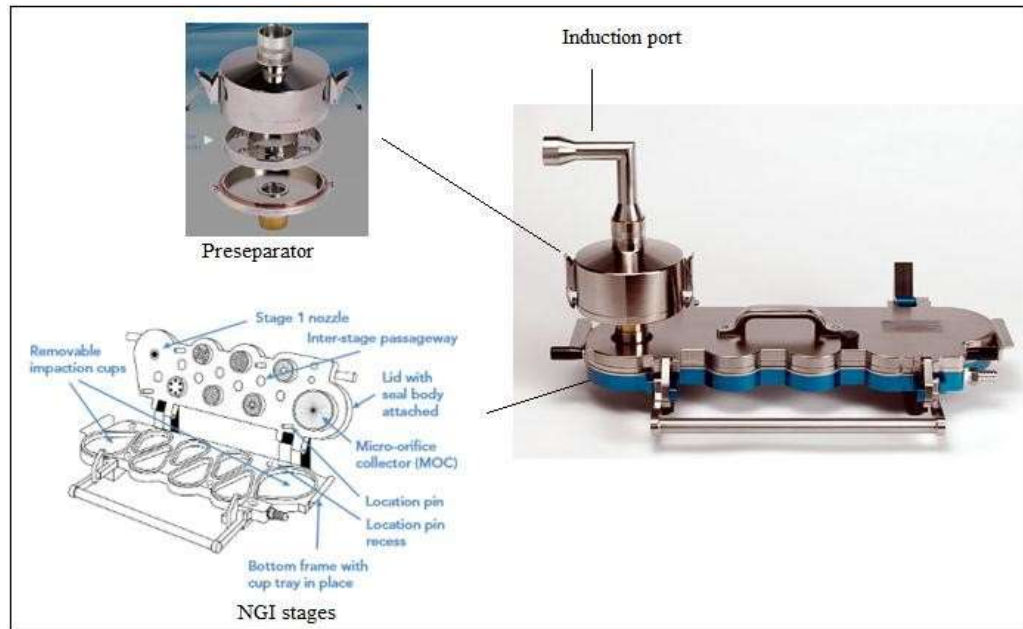
Figure 4- 1: NGI with induction port and preseparator (Source: Copley Scientific Limited, UK).

The cytotoxicity of NCMPs was determined as described in section 3.3.2.3.2.

4.3.8. Stability of dry powder

The CNCMPs powders were stored for 3 months. Freshly prepared spray dried samples were filled into glass vials and placed in a desiccator and stored at accelerated conditions (40 °C ± 2 °C, 75% ± 5% RH) as stated by ICH guidelines [276]. The spray dried samples were retested after 0, 2, 4, 8, and 12 weeks with respect to liposome size, PDI, zeta potential and drug content as described in 4.3.3.1. and 4.3.4. The samples were also examined visually for any evidence of caking or discoloration.

4.3.9. Statistical analysis

Quantitative data were expressed as the mean ± SD of at least three replicates. The Student's t-test and one-way analysis of variance (ANOVA) using IBMSPSS Statistics 21 was used to assess multiple comparisons between different methods and times. The level of confidence was set as 95%.

4.4. Results

4.4.1. Characterization of spray dried NCMPs using L-leucine.

Spray-drying was used to incorporate the selected PSL NPs into NCMPs using LEU as a carrier and to improve powder dispersion. The geometric particle size of the LNCMPs was in the range of 2.60 - 4.85 μm. The yield of LNCMPs (dry powder) was between 50 and 60 % (Table 4- 1). Photomicrographs of the L3NCMPs (at lipid: LEU ratio of 1:1.5) showed an irregular and corrugated surface (Figure 4- 2). It was noticed that a mass ratio of 1:1.5 produced the highest yield. Therefore, this ratio was selected for further SD studies using CH. The liposomal size increased after reconstitution to 60.77 nm with minimal change in zeta potential.

Table 4- 1: The mean particle size and yield % of the NCMP using L-leucine alone. (mean ± S.D., n=3).

Code	Lipid:L-leucine ratio	Geometric Particle size (μm) ± SD	Yield (%) ± SD
L1NCMPs	1: 0.5	2.60 ± 5.3	50.1 ± 2.2
L2NCMPs	1: 1	3.20 ± 2.7	54.6 ± 3.5
L3NCMPs	1: 1.5	3.57 ± 3.7	60.2 ± 2.8
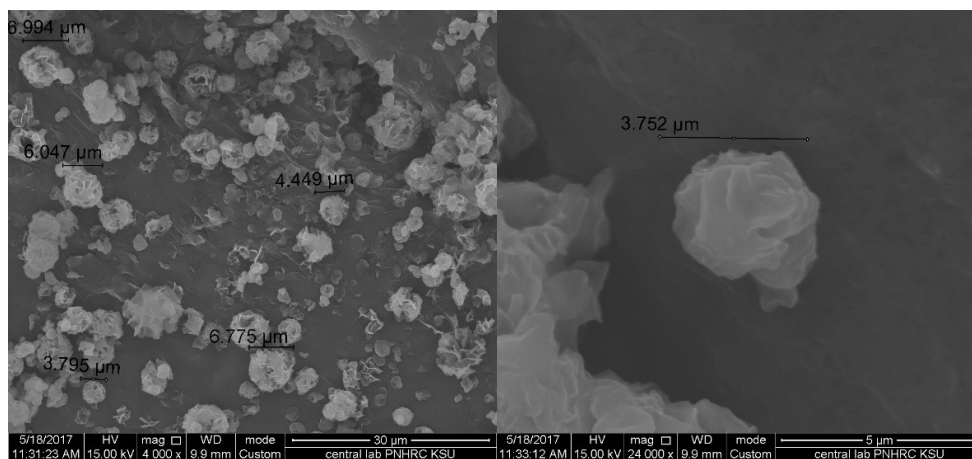
Figure 4- 2: SEM images of spray drying of PSL NPs using L-Leucine at lipid: leucine ratio of 1:1.5.

4.4.2. Characterization of spray dried NCMPs using L-leucine and chitosan

4.4.2.1. Production yield

The dry powder yield ranged from 62.1 to 71.8 %. Table 4- 2 shows the values of the yield obtained after SD. The lowest mean yield was obtained for C4NCMPs, at lipid: LEU:CH 1:1.5:2 w/w, (63.8 ± 4.3 %) and the highest was obtained for C1NCMPs (at lipid: LEU:CH 1:1.5:0.5 w/w) formulation (71.8 ± 3.5 %). As seen in Table 4- 2, there was a gradual decrease in the production yield, with increasing the CH ratio.

4.4.2.2. Powder Properties and primary aerodynamic diameter

The CNCMPs had a geometric particle size in the range of 3.61 –5.39 μm (Table 4- 2). The tapped density was found to be in the range of 0.3 – 0.6 g/cm^3 and this was used together with the geometric particle size to calculate the theoretical aerodynamic diameter within the respirable range (2.8 – 3.23 μm). The angle of repose for the formulations fell in the range of 28 to 29 degrees.

4.4.2.3. Morphology

The morphology of the coated NCMPs was evaluated by SEM and a selection of microphotographs is presented in Figure 4- 3. The microparticles had wrinkled surface, which look like raisins but by increasing the ratio of CH, more homogenous and smooth particles with some small indentations were obtained.

Table 4- 2: The geometric particle size, yield %, tapped density, angle of repose, and theoretical aerodynamic diameter of NCMPs prepared by spray drying of PSL NPs using L-leucine at lipid: LEU ratio of 1:1.5 w/w and different ratios of chitosan. Mean ± S.D, (n=3).

	C1NCMPs	C2NCMPs	C3NCMPs	C4NCMPs
Ratio (Lipid: LEU:CH)	1:1.5:0.5	1: 1.5:1	1: 1.5:1.5	1:1.5:2
Geometric particle size (µm)	3.61±0.19	4.17±0.14	4.93±0.73	3.40±0.35
Yield (%) ± SD	71.8±3.5	67.2±5.3	64.8±4.9	63.8±7.9
Tapped density (g/cm³)	0.35±0.013	0.40±0.018	0.43±0.019	0.27±0.021
Angle of repose	28.8±0.2	29.1±0.5	29.1±0.4	27.5±0.7
Flow propertied	Excellent flow			
d_{ae} **(µm)**	2.14±0.1	2.64±0.1	3.23±0.3	2.80±0.2
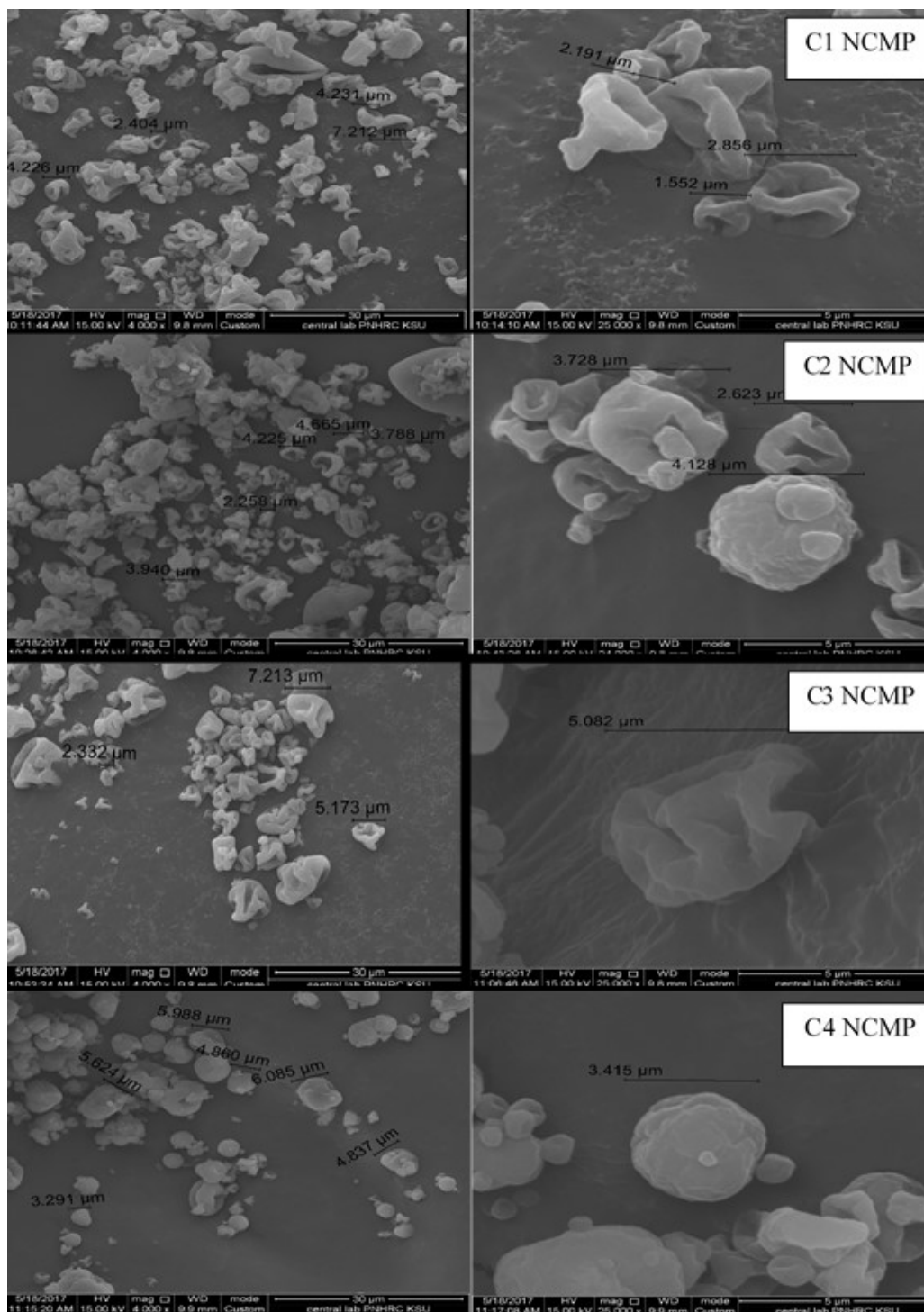
Figure 4- 3: SEM photographs of liposomes spray dried in the presence of L-Leucine and different ratios of chitosan (at lipid: Leu:CH ratio of 1:1.5:0.5 (C1NCMP), 1: 1.5:1 (C2NCMP), 1: 1.5:1.5 (C3NCMP) and 1: 1.5:2 (C4NCMP) (w/w)). Pictures were taken at 4000× and 25000× magnifications.

4.4.2.4. Particle size and zeta potential of reconstituted NCMPs

The size of PSL NPs after recovery from spray dried CNCMPs powders increased significantly (P < 0.05) compared to the size of pre-spray dried liposomes. Spray drying of CNCMPs with CH induced a substantial increase in average particle size and zeta potential of the developed microparticles (Table 4- 3). The average size of liposomes was between 62.4 - 89.4 nm, which is larger than the original liposomes, with low poly dispersibility index. The lower the ratio of the CH, the smaller the size of liposomal vesicle. The difference in mean particle size (approximately 20 nm ± 7.23) was not significant for the ratios of 1:0.5 and 1:1 but was significant (by > 40 nm ± 11.45) for ratio of 1:2 (P < 0.05). The surface charge of reconstituted liposomes changed when CH used toward positive values (Table 4- 3). The zeta potential of CNCMPs was dependent on CH ratio; at low CH ratio (C1NCMPs), the zeta potential increased (-14 mV). When CH ratio was increased to the highest ratio (C4NCMPs) zeta potential changed to -8.46.

Table 4- 3: The mean particle size, polydispersity index, and drug content of the reconstituted CNCMPs using chitosan. (Mean ± S.D., n=3).

	Ratio (Lipid:LEU:CH)	Particle size (nm) ± SD	PDI ± SD	Zeta Potential (mV) ± SD	Drug content %
C1NCMPs	1:1.5:0.5	60.4±3.2	0.240±0.01	-14±0.2	92.5±3.9
C2NCMPs	1:1.5:1	70.2±2.4	0.227±0.01	-11.6±0.1	89.7±4.8
C3NCMPs	1:1.5:1.5	84.6±3.1	0.237±0.06	-9.8±0.1	89.4±5.1
C4NCMPs	1:1.5:2	89.4±2.8	0.164±0.06	-8.5±0.2	87.2±2.3

4.4.3. Aerosolisation

The FPF and FPD values show the fraction and the amount of AFT particles reach to the lower respiratory tract. Among the formulations prepared, increasing the ratio of lipid: CH made a significant change on FPF values ($P < 0.05$). C1NCMPs produced higher FPD and FPF %, 40 µg 51.2 % respectively, and this was attributed to the more porous structure of the NCMPs. In contrast, C4NCMP powders have the lowest FPF% of 33.7 % and MMAD with smaller MMAD (3.2 µm). All prepared formulations have MMAD values in the optimal size range of 3.2–5.9 µm. Also, more than 50% (FPF) deposition in respirable airways (1-5 um) delivered 40 µg dose (FPD), i.e. 40 µg deliver from the delivery system, which contain 100 µg dose was, and deposited in the target site.

Table 4- 4: The Fine particle dose (FPD), percentage fine particle fraction (FPF), and mass median aerodynamic diameter (MMAD) of NCMPs. (mean ± S.D., n=3).

	Ratio (Lipid:LEU:CH)	FPD[a](µg)	FPF[b](%)	MMAD[c] (µm)
C1NCMPs	1:1.5:0.5	40.0 ± 4.2	51.2 ± 2.2	4.8 ± 0.1
C2NCMPs	1:1.5:1	33.7 ± 5.2	45.9 ± 5.7	4.2 ± 0.8
C3NCMPs	1:1.5:1.5	31.7 ± 2.8	40.9 ± 2.4	5.9 ± 0.7
C4NCMPs	1:1.5:2	28.4 ± 4.6	33.7 ± 4.9	3.2 ± 0.7

[a]Fine particle dose (FPD)
[b]Fine particle fraction (FPF)
[c]Mass median aerodynamic diameter (MMAD)

4.4.4. *In Vitro* Release Studies

The % cumulative AFT released *in vitro* from NCMPs is presented in Figure 4- 4. The release, of the reconstituted NCMPs, in a PBS (pH 5.5) showed a delayed drug release compared to PSL NPs. The drug release was 15 % and 4.3 % within 2h and 72.2% and 46.3% after 12 h, and 89.4 % and 67.4 % over 24 h for C1 NCMP and C4 NCMP, respectively. All systems show the best correlation with the Higuchi and anomalous (non-Fickian) diffusion models (n > 0.5) (Table 4– 4).
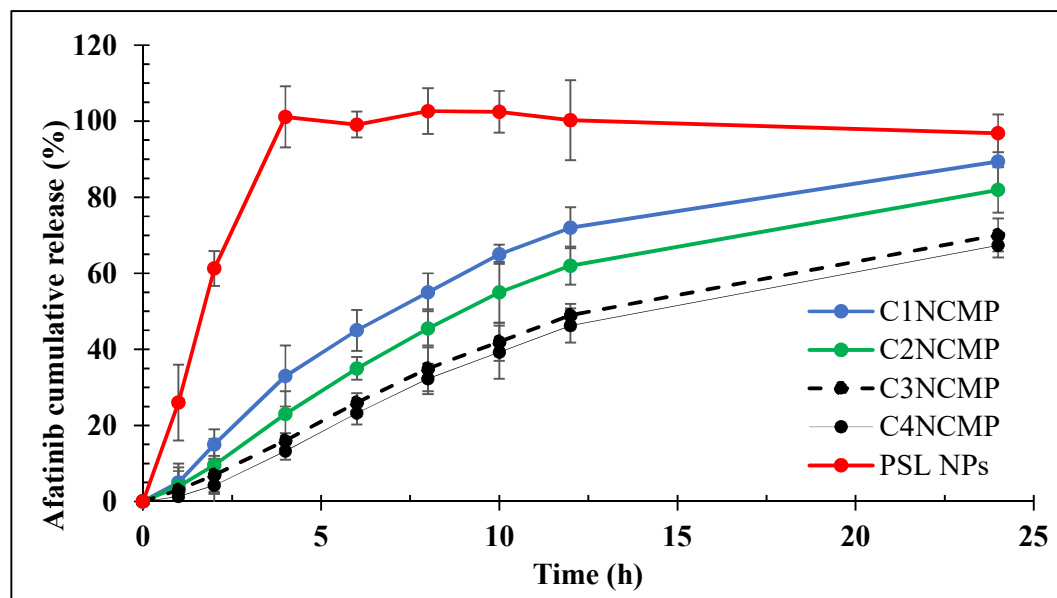
Figure 4- 4: *In-vitro* release of afatinib from NCMPs and pH sensitive liposomes (PSL) in PBS buffer (pH 5.5) at 37°C. (Mean ± S.D., n=3).

Table 4- 5: The kinetic parameters of afatinib from CNCMPs prepared by spray drying of PSL NPs using L-leucine at lipid: LEU ratio of 1:1.5 w/w and different ratios of chitosan.

		C1 NCMP	C2 NCMP	C3 NCMP	C4 NCMP
Zero- Order	r^2	0.932	0.935	0.894	0.862
	k_o (h^{-1})	1.872	1.859	2.467	2.251
First- Order	r^2	0.953	0.977	0.933	0.875
	k_1 (h^{-1})	4.560	4.565	4.531	4.546
Higuchi	r^2	**0.978**	**0.983**	**0.966**	**0.922**
	k_1 (h$^{-1/2}$)	10.170	9.957	13.891	12.285
Korsmeyer-Peppas	r^2	0.957	0.982	0.954	0.925
	N value	0.790	0.679	0.675	0.682
	k_{KP} (h^{-n})	0.0450	0.0559	0.0829	0.0554

4.4.5. Stability study

The stability of CNCMPs was studied to monitor the influence of storage conditions on their physiochemical characteristics and percent drug content. Figure 4- 5 represents the liposome size after the rehydration of spray dried powders. At the beginning, the liposome size was between 62.43 and 89.54 nm for C1NCMP and C4NCMP, respectively and the PDI > 0.327. All measurements revealed a liposome size in the range of 97.85 – 108 nm after 4 weeks of storage. Aside from minor fluctuations, after 8 weeks there were no significant increase in the sizes of all powders. After 12 weeks, only one powder showed size > 121 nm and almost all reconstituted powders were cloudy, the liposome PDI was > 0.44. Zeta potentials of the reconstituted liposomes dispersions at different times are displayed in Figure 4- 6. The measured zeta potentials were between - 14 and -4.9 mV. Zeta potentials were constant regardless of the size measured. When exposed to high temperature and

humidity, AFT content was reduced in all powders. After 12 weeks AFT contents were reduced from 92.5% to 2% in C1NCMP and 87.2% to 0.93% in C4NCMP (Figure 4- 7). A discoloration in all powders was noticed upon storage, ranging from a light-yellow to dark-yellow coloration depending on CH ratio, yellowing was not seen in the control specimens.
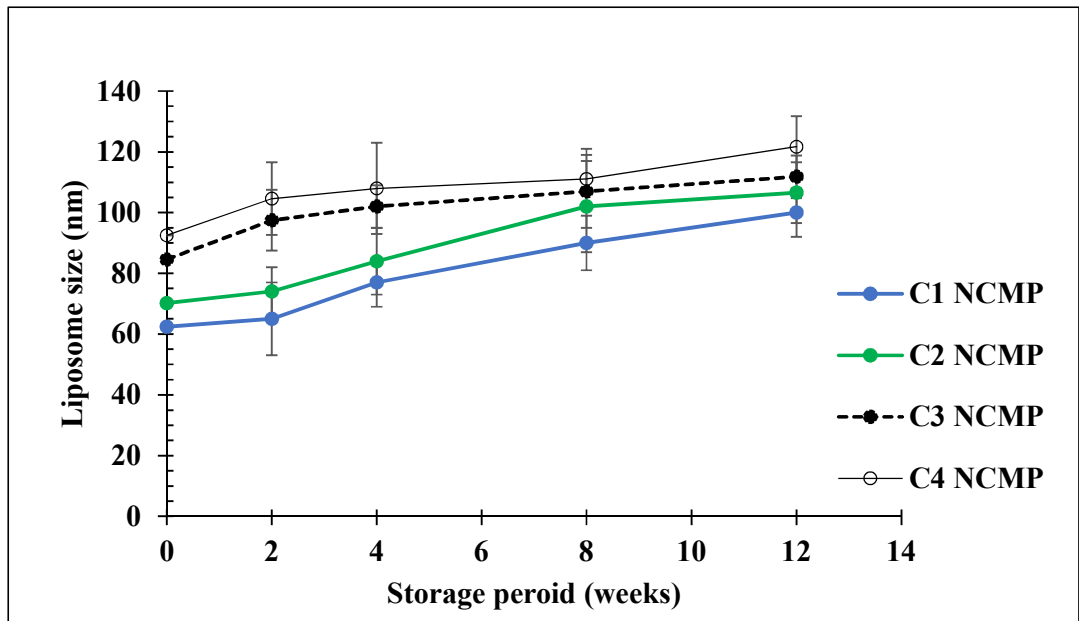
Figure 4- 5: The effect of time on the reconstituted mean liposomes size stored at 40°C. (Mean ± S.D., n=3).
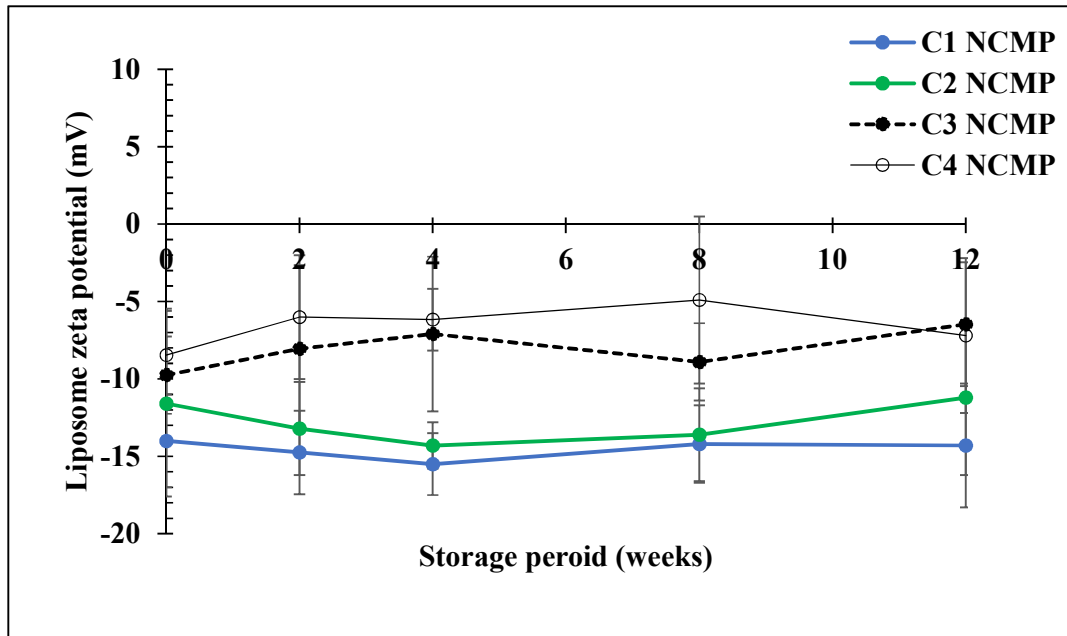
Figure 4- 6: Reconstituted Liposome mean zeta potential at different time stored at 40°C. (Mean ± S.D., n=3).
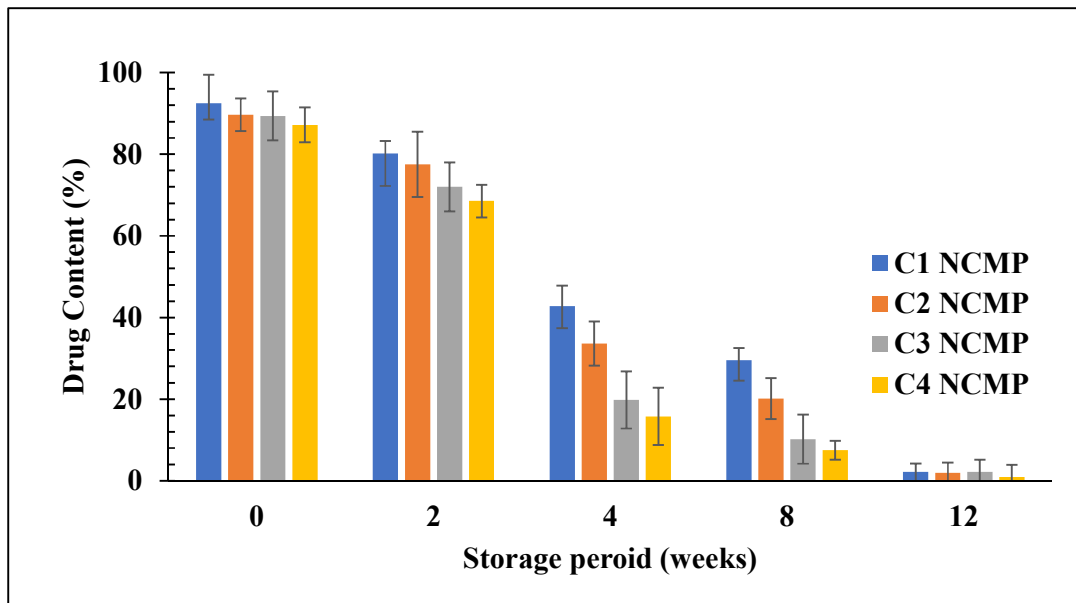
Figure 4- 7: Drug content % of NCMPs, following storage for different periods at 40°C, 75% ± 5% RH. (mean ± S.D., n=3).

4.4.6. Cytotoxicity assessment using flow cytometry

The levels of cytotoxicity of C1NCMPs were measured via flow cytometry analysis after Annexin V/PI staining. Of the three cancer cell lines tested, H-1975 cells appeared more sensitive to the liposomes formulations as relatively lower drug concentrations effectively induced cytotoxicity. In this cell line, C1NCMPs treatment at a concentration of 0.75 μM resulted in 38.9% death, after 24 h of exposure which is mainly due to induced apoptosis with slight necrosis (< 2%), indicating a good efficacy of the developed C1NCMPs (Figure 4- 8). Further, the experiments showed no significant difference ($P<0.05$) between PSL NPs and C1NCMPs in the cytotoxic effect after 24 h of exposure with H-1975 cells.
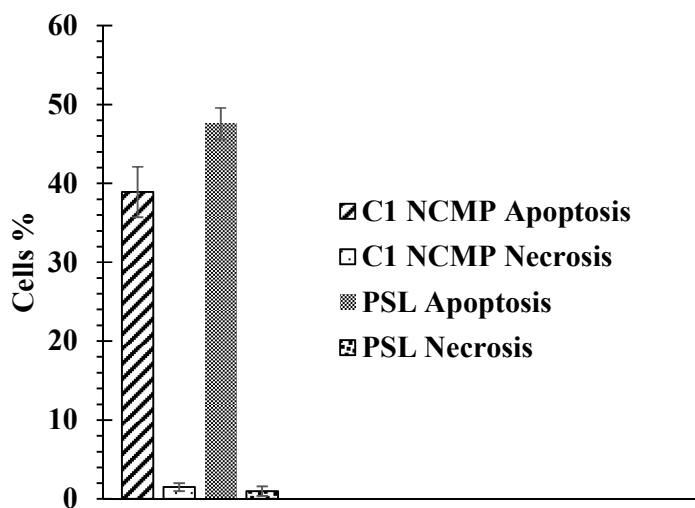
Figure 4- 8: The cytotoxicity effect of PSL NPs and C1NCMP (at lipid: Leu:CH ratio 1:1:0.5 w/w) at concentration 0.75 μM, on H-1975 cells for 24h, following which the proportion of apoptosis and necrosis was analysed with Annexin V/PI-flow cytometry. (Mean ± S.D., n=3).

4.5. Discussion

The size change of any liposomes before and after spray drying is a critical parameter in the assessment of liposomal stability so this was used as an initial screening parameter when choosing formulations to take forward to the next step of formulation optimization. Initially the optimum concentration of either sucrose or trehalose as protectants during the SD process was determined. The results obtained for PSL NPs in chapter 2 and 3 were promising so these NPs were selected for formulation into dry powders for inhalation. Since PSL NPs have an average size of 46±8.5 nm, they cannot directly be used for inhalation as most of the inhaled dose will be exhaled with a minimal amount of the dose deposited in the lung [277]. In addition, there are some stability issues with using liposome dispersion alone [246]. Therefore, PSL NPs were formulated into NCMPs for administration by dry powder inhalation.

NCMPs were produced by SD using LEU as a carrier and a dispersibility enhancer. The geometric particle size of the resultant NCMPs was in the respirable range (2.60 - 4.85 μm). SEM pictures show irregular or wrinkled surface (Figure 4- 2) which is due to an excessive build-up of vapor pressure through water evaporation during the SD process and usually occurs with hydrophobic amino acids, such as LEU [241, 278, 279]. Kunda et al observed the same irregular surface for NCMP containing LEU [269]. It is also worth noting that increasing Leu ratio correlated with increased yield value. Therefore, L3NCMP (lipid: LEU ratio of 1:1.5 w/w) was selected for further studies as it exhibited the highest yield %. This is inconsistent with the results obtained by Tawfeek et al., who found that yield increases with increasing Leu ratio in spray drying of PGA-co-PDL, 1.5% Leu had the highest value of 54.7 % ±2.6 [241].

The size of the CNCMPs was acceptable for respirable particles (3.61-5.39 μm) suitable for pulmonary delivery, with a high production yield (63.8-71.8) obtained for

all formulations (Table 4- 2). The CH ratio affected the production yield, with an increasing ratio of CH resulting in a decreased yield, which can be attributed to some of the liquid droplets attaching to the inside wall of the drying chamber and cyclone of the spray dryer. This was reported previously by Learoyd et al., with powders spray-dried from 30% v/v aqueous ethanol formulations containing terbutaline sulfate as a model drug, chitosan as a drug release modifier and leucine as an aerosolisation enhancer[280]. Also, Cevher et al prepared biodegradable chitosan microspheres containing vancomycin hydrochloride by spray drying with different CH: drug ratios. The production yield was relatively low due to powder adherence to the chamber wall and reduced cyclone efficiency in collecting the fine powder particles[281]. The SEM photographs (Figure 4- 3) demonstrate that the morphology of the CNCMPs is a wrinkled (collapsed) surface, which look like raisins and is classified as type III (adopting the classification suggested by Prinn K. et al. [37]. At a high CH ratio (C4NCMPs), CH effectively imparted a spherical shape and surface smoothness to the microparticles. This is due to the rapid internal evaporation of droplets. Wrinkles and dents on the surface of spray dried powders have been previously described by Tonon et al., when carbohydrates excipients had been used [282]. They found that due to the faster water evaporation from droplets during the drying process and subsequently when the water fully evaporates, the surface layer collapses resulting in the observed wrinkled structure. Increasing CH ratio increases the viscosity of the fed solution resulting in slower evaporation. This is in line with He et al, who found that chitosan microspheres prepared by a spray drying using a low viscosity solution of chitosan had a depressed surface morphology (slightly wrinkled) but those prepared from a high viscosity solution of chitosan had a smooth surface [283]. The advantage of wrinkled particle surfaces within the spray dried powder is decreasing aggregation

from a reduction in cohesiveness and an increase in dispersibility thereby resulting in a better lung deposition [284, 285].

The drug content of CNCMPs was relatively high and the HPLC peaks of AFT appears at the same retention time which indicate that AFT is stable during SD. The size change of liposomes before and after spray drying is a critical parameter in the assessment of liposomal stability. The sizes of the reconstituted liposomes with various CH ratios increased when compared to those of the extruded liposomes before spray drying (P<0.05). Chitosan was found to have notable effect on increasing the size and zeta potentials of reconstituted liposomes. This can be explained by the fact that the conventional spray drying and rehydration process may result in liposome disruption or aggregation [286]. The higher the ratio of chitosan in formulations, the zeta potential changed to less negative values (Table 4- 3). This can be explained by the presence of areas uncoated by CH at low CH ratios, since there are not enough CH amino groups to complex with LEU. Manca et al, developed rifampicin microparticles for delivery to the lungs by coating negative liposomes (∼−46 mV) with chitosan (CH)–xanthan gum (XG) to obtain chitosomes [287]. They found that the zeta potential of the prepared chitosomes was dependent on CH–XG ratio. When XG concentration increased, zeta potential changed to more negative values due to the free amino groups complexed with the XG. These results confirmed the effective surface coating of liposomes by the CH–XG complexes [287].

The CNCMPs formulations showed a slower cumulative release of AFT. It can be emphasized that the cumulative amount of AFT release was influenced by the ratio of CH. The release rate of AFT decreased with an increase of the ratio of the CH in the formulation. The C1NCMPs released 33% AFT after 4 hr, but 24 h dissolution time was necessary for the C1NCMPs powder to release more than 89%. The C4NCMPs

powder displayed a slower release profile, with 13.25 and 67% drug release after 4 and 24hr. In contrast, PSL NPs underwent very rapid dissolution, with 100% AFT released after approximately 4 hr (Figure 4- 4). This indicates that CH controls the drug release of AFT. A DPI formulation containing hydrophobic (beclomethasone dipropionate) and hydrophilic (terbutaline sulfate) drugs, leucine (aerosolization enhancer) and CH (as a drug release modifier) showed promising sustained release delivery of both drugs from a single formulation [287]. Earlier investigators have suggested that when microspheres containing hydrophilic polymers such as chitosan are immersed in water, diffusion of the drug through a gel diffusion layer produced by polymer swelling, results in a sustained drug release effect. Increasing the amount of chitosan in the microsphere increases the thickness of this diffusion layer, resulting in greater retention of drug release [288-290]. The *in vitro* release kinetics were studied to determine the AFT release mechanism. Afatinib was released from CNCMPs formulations according to Higuchi diffusion model. This is because AFT is entrapped inside the phospholipid bilayer of the liposomes and must diffuse through the bilayer and the CH layer to be released. Therefore, the addition of CH in the formulations could successfully prolong the drug release time. Furthermore, a potential change in drug release profiles could be achieved depending on the amount of CH in the NCMPs. These data were in agreement with a previous study where, terbutaline sulfate CH spray-dried powders for inhalation exhibited a sustained release profile[280].

All the CNCMPs powders tested had Lower angles of repose corresponding to freely flowing powders [291], low tapped densities, and aerodynamic diameters <5 μm, indicating that the powders were suitable for deposition in the lungs. The CNCMPs powders, when subjected to aerosol performance using the NGI, had MMAD values

that were a little higher than the d_{ae} values. Higher MMAD values could be the result of the aggregation of particles, friction, or interlocking between the particles, which might not disaggregate upon aspiration. These MMAD values are in the optimal size range of 3.2–5.9 μm indicating the suitability of the NCMPs for targeting deep lung airways as reported by different groups of researchers [292, 293]. The % FPF characterizes the efficiency of drug deposition in the lower respiratory tract. Comparing all formulations, C1NCMPs (at lipid: LEU: CH ratio of 1:1.5:0.5) had the highest % FPF and FPD values, 51.2% and 40.0 μg of AFT, respectively, suggesting that it was efficient at delivering the most AFT to the lower respiratory tract. This is because of the correlation that is seen between FPF and FPD; that is to say, when FPF increases, the expected amount of AFT that is delivered to the lower respiratory tract also increases, while no clear relationship between MMAD and FPF could be found. Also, it is important to note that the MMAD and FPF will also depend on the inhaler device. The use of microparticulate Leu as a carrier, in this case, improved the aerosolization dispersibility of the PSL NPs powder; but the % FPF was low. It might be a result from the agglomeration of microparticulate Leu coated with CH.

Leucine has previously been shown to enhance a spray dried formulation's aerosolization [294]. Learoyd and coworkers reported that the decrease in FPF across a series with increased CH molecular weight could be due to the decreased effect of LEU surface modification [280]. Two groups of liposomes were prepared, using soy phosphatidylcholine and hydrogenated soy phosphatidylcholine, to encapsulate rifampicin [287]. The obtained vesicles were then coated with different CH–XG weight ratios. The nebulization and rheological properties of powders were affected by the CH–XG weight ratio in the formulation. It was concluded that the CS–XG weight ratio of 1:0.5 (w/w) coating was able to greatly improve drug deposition (FPF

= 37.8%) in comparison with the corresponding uncoated liposomes (FPF = 13%). It was suggested that the coating of liposomes with a polyelectrolyte complex at an appropriate ratio improved liposome resistance to aerosolization, which suggests that CH has an impact on drug dispersion from DPI formulations[287].

Liposomal formulation being a carrier for different drug, there are chances that formulation may get destabilized over time on exposure to humidity and temperature. Liposome systems have been reported to show various physicochemical changes on storage, such as liposomal aggregation, fusion, loss of drug, etc. which will affect the in vivo performance of the formulation [295] Additionally, phospholipids may undergo hydrolysis reaction forming fatty acids and lysophospholipids [296]. However, under dried state, there is least possibility for such degradation, but, there are still chances of hydrolysis due to residual water content remaining in dried powders and also under humid conditions and temperature. Another aspect of stability of liposomes is oxidation of lipids. These changes may lead to structural integrity problems in liposomes and this might cause release of entrapped drug [297]. Thus, these effects induce time dependent changes in desired properties of formulation during storage, therefore accelerated and stress stability studies at 40 °C ± 2 °C, 75% ± 5% RH are potential tools to get an idea of any such possibility. The stability of CNCMPs powders showed that there were physical changes during the study period and drastic changes in the drug content for all powders. This might be due to the heat sensitivity of AFT when exposed to high temperatures for longer times. The stress studies showed that the finished product of AFT is sensitive to excessive heat and humidity and is sensitive to light exposure therefore needs to be kept in special packaging material[298]. Also, both moisture level and thermal processing are recognized as crucial parameters affecting the stability of CH-based formulations

[299].]. Long-term storage at high relative humidity might not only accelerate the hydrolytic damage of CH, but also change the polymer's physicochemical and biological properties. Viljoen et al. showed that after six-month storage of CH tablets at 70% relative humidity, markedly lower mechanical properties were observed compared to those kept at 60% relative humidity [299]. Similar results were observed for CH /amylose corn starch composite films that became mechanically weaker after three-month storage at the same storage conditions [300]. Furthermore, the studies conducted by Lim et al., revealed that both dry heat (160 °C for 2 h) and autoclave sterilization (under 100 kPa, at 105–125 °C for 30 min) produced darkening of CH dried powder to a yellow color [301].

Since C1NCMPs had a higher drug content, yield % and good FPF value indicating reasonable probability of deep lung deposition, it was used for cell viability studies on H-1975 cell line. The outcome revealed a good cytotoxicity of C1NCMPs as compared to drug solution. The cytotoxicity of C1NCMPs was slightly lower than that of PSL NPs but the difference was not significant. This may be attributed to the retarded release of AFT from the CNCMPs with CH. Singh et al., studied the lung delivery of CH coated cisplatin and higher cytotoxic effects on A549 human lung cancer cells and a higher IC50 value were recorded compared with the free drug[302].

4.6. Conclusion

The selected PSL NPs formulations were incorporated into NCMPs using LEU to enhance powder dispersion. The highest yield % of NCMPs powder (60.2 %) was obtained using lipid to LEU 1:1.5 w/w. This NCMPs at lipd: LEU ratio 1:1.5 was coated with different ratios of CH. The morphology of coated NCMPs showed a corrugated surface but at high CH ratios, more homogenous and smooth particles with some small indentations were obtained. Also, the results showed reproducible size

and good AFT content. The *in vitro* release studies showed a delayed drug release compared to PSL NPs. Stability studies showed physical changes and substantial changes in the drug content for all coated NCMPs powders during the study period. Furthermore, a direct relationship between CH ratio and FPF was observed, C1NCMPs (lipid: LEU:CH ratio of 1:1.5:0.5) exhibited the highest FPF (51.2%) and FPD (40.0 μg of AFT) indicates deep lung deposition. The cytotoxic study revealed that C1NCMPs, at a concentration of 0.75 μM showed a good cytotoxicity effect on H-1975 cells, these *in vitro* results suggest that C1NCMPs could provide a novel method of delivering targeted nano-therapy to the lungs in a safe and effective manner.

Chapter 5

General Discussion

5.1. Overview

Lung cancer has the highest mortality rate amongst all cancers [303]. The complicated genetic and phenotypic levels in cancer cells cause clinical diversity and therapeutic resistance in cancer cells. Generally, chemotherapy is the most commonly used treatment, but has numerous limitations and side effects [13]. To overcome the restrictions of conventional chemotherapy, a number of nanocarrier delivery systems have been developed to improve drug delivery to cancer cells [304]. Currently, several nanocarriers such as liposomes, are now on the market, or under research for cancer treatment [122]. Liposomes have many advantages for pulmonary delivery, over other vehicles as they are prepared from phospholipids endogenous to the lung as surfactants [54]. Liposomes can be spray-dried to be formulated as liposomal dry powders for inhalation which is a useful technology for pulmonary delivery. The aim of this project was to formulate and characterize nanocomposite microparticles of AFT-loaded liposomes NPs as a treatment for NSCLC by dry powder pulmonary delivery.

5.2. Optimization of Liposome Nanoparticles

Precise modification of various formulation and processing parameters is important to obtain NPs of a desired size and drug content. In this study, the film hydration method was successfully used to actively entrap AFT into liposomes of small vesicle size (<100 nm) with relatively high efficiencies [36]. The PDI values of the obtained liposomes were less than 0.27 indicating a narrow size distribution. Afatinib is used as a potent antitumor drug against NSCLC tumors. However, AFT alone has low specificity and indiscrimination of tumor and healthy tissues [209]. Therefore, AFT loaded-liposomes were developed as a new cancer cell therapy with decreased dose-limiting toxicity.

Two different strategies for tumor targeting were selected using cationic and pH-sensitive phospholipids to produce CL and PSL. The main difference between these two liposomes is the composition of phospholipid used. In general, three lipid components: DSPC, DOPC, and DOPE were used. The rational for the selection of DSPC was its stability against chemical degradation due to being a saturated lipid, which reduces drug leakage from liposomes on storage and *in vivo* transit. To increase the fluidity of liposomal membrane, DOPC was selected due to its high fluidity at room temperature (transition temperature (T_m) = $-20°C$). While, the T_m of DSPC is $+55 °C$, which remains in the gel phase [192]. Moreover, DOPE was combined to provide fusogenic characters to the liposomes, due to the formation of an inverted hexagonal phase upon destabilization of membranes at a mildly acidic pH [84]. Theses lipids possess various chain lengths and degrees of saturation, which can fine-tune the membrane dynamics and phase properties [193]. The main composition of CL is DOTAP, which is a cationic phospholipid and PSL contains the pH-sensitive phospholipid, CHEMS. As expected, the zeta potential depends on the lipids used and the higher zeta potential of the liposomes obtained produced the stable liposomes.

In general, a successful drug delivery system should achieve efficient drug encapsulation resulting in significant anticancer activity with reduced toxicity [305, 306]. In order to obtain liposomes with the highest EE%, the optimal ratio of drug to phospholipid was determined. It was found that the highest EE% of AFT was 43.20%, 50.20%, and 52.01% for NL, PSL, CL, respectively at the 1:0.5 ratio of lipid to AFT. These results suggest that AFT loading into the liposomes increases only up to a certain level with increasing lipid to the drug ratio in the formulation. At higher lipid to drug ratios, free drug in the formulation increases which is not a desired feature. A similar observation was reported by Mahmud et al. and Myer et al, who found that EE

increases only up to a certain level with increasing lipid to drug ratio in the formulation [307, 308]. Also, the liposomes incorporated up to 88% paclitaxel when the drug to phospholipid molar ratio was 3%. However, a higher drug-to-lipid molar ratio would lead to the occurrence of needle-like crystals precipitating during preparation [309].

In vitro drug release data revealed that PSL and NL exhibited sustained release profiles due to the presence of DSPC (T_m), which led to a decrease in leakage of AFT in the circulation or extracellular environment. But in case of CL, AFT exhibited a higher release rate compared with the other liposomes, at pH 7.4. This is due to the complete protonation of DOTAP at pH 7.4 [198]. By contrast, the fast drug release profile of AFT was found with PSL in acidic media, which reached 100% after 4 h. The PSL undergoes destabilization at pH 5.5 and acquires fusogenic properties, thus tending to rupture and quickly release AFT. The fusogenic performance of PSL is due to the presence of DOPE in the lipid layer, which forms a hexagonal structure instead of a bilayer structure after dispersion in aqueous media. These results were consistent with results reported by Chen et al. who found that pH-sensitive liposomes of calcein had superior pH sensitivity. The rate of release of calcein was less than 10% at pH 7.0, but gradually increased with decreasing pH. When the pH was decreased from 6.0 to 5.5, the rate of calcein release increased noticeably while at pH 4.5, the rate was nearly 90% [310]. The Reddy group designed novel PSL to co-deliver Paclitaxel and Bcl-2 siRNA into the tumor cells and mice models. They observed the highest release of siRNA and Paclitaxel (>90% at 6 h time interval) from liposomes at pH 6.5 and pH 5.5 respectively while in physiological pH (pH 7.4) the release was only 10% [311]. According to the kinetic models, the release of AFT at pH 7.4 displayed release with Korsmeyer-Peppas model. This effect is due to early rapid release followed by slow

release of the liposomes [312]. In case of the release pattern of AFT at pH 5.5 was quite faster with a first order model. This behavior because AFT exists liposomal membrane, which leaks out at a faster rate in acidic condition [313].

5.3. Antitumor activity and Molecular studies

The potency of free AFT was compared with other common drugs used to treat lung cancer. Cell toxicity was evaluated by WST-1 using H-1975 cells. The WST-1 assay showed that AFT was more effective as a cytotoxic agent compared to the other compounds (H-1975 cells). Furthermore, the anti-proliferative effect of AFT on H-1975 cells was investigated at various concentrations for 24 h. The results indicated that the inhibition of cell viability by AFT was concentration-dependent.

In two large phase III studies (LUX-Lung 3, and LUX-Lung 6), AFT significantly enhanced progression free survival rates, objective response rates compared with platinum-based chemotherapy (pemetrexed/cisplatin in LUX-Lung 3 and gemcitabine/cisplatin in LUX-Lung 6) as first-line treatment of NSCLC patients [6, 24, 32]. Additionally, both studies presented AFT to be the only TKI to improved overall survival versus standard platinum doublet chemotherapy in patients having EGFR mutations [314].

Anticancer activity of the AFT-loaded liposomes was also investigated with the WST-1 assay using H-1975 cells. Unfortunately, WST-1 gave unreliable results, therefore, the cell viability of each liposome formulation was measured with flow cytometry analysis after Annexin V/PI staining. The flow cytometry data for the treatment of cells with different concentrations of PSL exhibited a comparable level of cell intensity to free AFT. It was clear that the uptake of AFT loaded PSL by H-1975 cells was higher than free AFT. The results revealed a marked decline in cell viability with AFT loaded-PSL up to 60.4% of cell apoptosis at 1 μM after 24 h. The free AFT

resulted in apoptosis in only 11.88% of the cells after 24 h. The low cytotoxic effect of free AFT could be attributed to the low cellular uptake and poor trans-membrane permeability. Of the three cancer cell lines tested, H-1975 cells appeared more sensitive to the liposomes. Particularly, the cytotoxicity of PSL is high compared with that of CL and NL.

PSL released AFT in response to the lowered pH in the endosome, and thus facilitated diffusion of the released AFT from the endosome to the cytosol. It has been suggested that pH-sensitive liposomes are internalized more efficiently than non-pH-sensitive formulations [43]. It is notable that the destabilization of PSL at the endosomal demonstrated that the efficacy of PSL depends on the pH of the tumor tissues [34]. Additionally, the liposomes containing CHEMS released their contents into the cytoplasm from 5 to 15 min upon their incubation with the cells [44]. The destabilization of PSL induced by acidification of the endosomal lumen represents the most important stage in the process of intracellular delivery. Kim *et al* developed a PSL with an efficient and targeted delivery system for gemcitabine, and potentially a useful, novel treatment approach for tumors that overexpress EGFR [45].

Quantitative proteomic analysis was used to evaluate the cellular protein changes upon AFT treatment. The proteomic analysis revealed a total of 385 proteins were differentially expressed from at least one of the four groups; treated and control H1975 and H1650 NSCLC cells, which help to differentiate treatment effects between the sample groups. Correspondingly, the expression of the 385 protein changes across the four sample groups were further assessed for their relations with cancer. Analysis using IPA software revealed 15 proteins in one of the networks which found in multiple categories of functions related to cancer development including cell-to-cell signaling and interaction, cell signaling, cell death, cellular growth and proliferation.

These findings indicate that rather than the use of a single marker, analyses of a panel of protein markers have the potential to provide better insights and understanding of a particular treatment response on NSCLC cells.

5.4. Spray drying of the selected afatinib loaded liposome nanoparticles

The PSL NPs were dispersed into a L-leucine solution and spray dried to produce NCMPs carriers suitable for pulmonary delivery via DPI. The particle size of the LNCMPs were $3.57 \pm 3.7 \mu m$ and LNCMPs with a lipid: LEU ratio of 1:1.5 producing the highest yield. Photomicrographs of L3NCMPs showed irregular microparticles. Therefore, this ratio was selected for further SD studies using different ratios of CH. Photomicrographs of CNCMPs powders showed wrinkled particles but at high chitosan ratio, more spherical particles were observed with good yield% (63.8 to 71.8 %). There was a gradual decrease in the production yield, upon increasing the chitosan ratio due to adherence of powders to the wall of the chamber. A few materials used as excipients in the spray drying solution have been proved to generate crinkly surfaces to some extent for spray dried microspheres such as amino acids, poly-saccharides, specifically leucine, chitosan and albumin [278, 283, 315-320]. Sheu and coworkers found that the structure of spray dried microcapsules was affected by the type of carbohydrate and by the protein to carbohydrate ratio whereas, the extent of surface indentation was inversely related to the proportion of protein in the powder [321].

Spray drying of CNCMPs with chitosan induced a substantial increase in average particle size and zeta potential of the developed microparticles. The size of reconstituted liposomes from the powders was 60.4 - 89.4 nm depending on the ratio of the chitosan and were larger than those of the pre-dried liposomes. The lower the

ratio of the chitosan, the smaller the NPs. The difference in mean particle size was not significant in the lower ratios but was significant for higher ratio of CH (P < 0.05). The size of the prepared particles was greatly dependent on chitosan ratio [322]. The size modifications of the vesicles due to chitosan coating are in line with the results obtained by Zaru et al [323]. It is clear that using chitosan in the spray drying has shifted the zeta potential toward more positive values. The zeta potential of reconstituted liposomes was dependent on the chitosan ratio, at low chitosan ratio (C1NCMPs at lipid: LEU: CH ratio of 1:1.5: 0.5), the zeta potential shifted to positive values (-14 mV). When the chitosan ratio was increased (C4NCMPs at lipid: LEU: CH ratio of 1:1.5: 2), the zeta potential changed to -8.5. This was due to the electrostatic interactions which are implicated in the vesicle coating procedure which is provided by the fact that the zeta-potential of the vesicles that initially have negative charge is drastically changed as the vesicles become coated with polymer [323].

The *in vitro* release profile of AFT from microparticles showed a similar pattern in all formulations, slow and steady and the drug release time was prolonged as the chitosan content was increased in the formulations. This is in agreement with results reported in previous work of Dubey et al [324]. The spray dried powders had good flow properties, aerodynamic diameter and drug content. The MMAD values were within the optimal size range of 3.2–5.9 μm indicated the suitability of the microparticles for targeting deep lung airways as reported by meenach et al [159, 325]. The *in vitro* release profile of AFT from microparticles showed, similar pattern in all formulations, slow and steady and the drug release time was prolongated as chitosan content is increased in the formulations. The release mechanism from CNCMPs formulations was according to Higuchi diffusion model. Significant decrease in AFT content and discoloration in all CNCMPs after storage at 40°C/75% relative humidity for 3

months. Yang et al., showed that high temperature produced changes in chitosan dried powder to [326]. Furthermore, the studies conducted by Lim et al., revealed that both dry heat (160 °C for 2 h) and autoclave sterilization (under 100 kPa, at 105–125 °C for 30 min) produced darkening of CH dried powder to a yellow color [301].

As C1NCMPs has a higher drug content, a sustained release profile and FPF value with acceptable powder properties, indicative of deep lung deposition. Therefore, the cell viability studies were performed on H-1975 cell line. C1 NCMPs appear to have a good toxicity profile in comparison with AFT solution.

5.5. Conclusions

In this work, a novel PSL NPs for targeted therapy of NSCLC were developed. For comparison purpose, NL, CL and PSL NPs were successfully designed. The obtained liposomes were small spherical particles of less than 100 nm with a low PDI (<0.27) and an acceptable zeta potential. The highest EE% values of the liposomes were achieved according the following order: CL>PSL>NL. The selected liposomes were stable at 4 and 25°C for 1 month. The PSL, CL and NL showed slow release profiles in pH 7.4. However, in acidic pH values, PSL exhibited fast release, which improved its tumor targetability. The selected liposomes revealed efficiency on NSCL cells. Moreover, PSL NPs inhibited the cell growth of lung cancer cells more efficiently than free AFT, CL and NL based on using Annexin V assay. Therefore, the selected PSL NPs were incorporated into NCMPs using LEU to enhance powder dispersion. The resulted LNCMPs was in the respirable range and the highest yield % obtained in lipid: LEU 1:1.5 w/w (60.2 % ±2.8). This LNCMPs at lipid: LEU ratio 1:1.5 was coated with different ratios of CH. The morphology of CNCMPs showed a corrugated surface and more smooth particles were obtained at high CH ratios. Also, the results showed reproducible size. The *in vitro* release profiles showed a delayed AFT release

compared to PSL NPs. Stability studies showed physical changes and substantial changes in the drug content for all CNCMPs powders during the study period. Furthermore, C1NCMPs (lipid: LEU:CH ratio of 1:1.5:0.5) exhibited the highest FPF (51.2%) and the lowest FPD (28.4 μg of AFT) indicates deep lung deposition. The cytotoxic study revealed that C1NCMPs, at a concentration of 0.75 μM showed a relatively similar good cytotoxicity effect on H-1975 cells as PSL NPs, these *in vitro* results suggest that C1NCMPs is a promising a targeted drug delivery for NSCLC therapy in a safe and effective manner.

Chapter 6

Future Work

6.1. Future work

Moving forward from the achievements of this project, some additional studies could be performed to further develop this DDS.

6.1.1. Optimization of the current formulation

There is a need for additional investigation and optimization studies to reach the goal of a formulation suitable for further *in vivo* studies. It would thus be of great interest to continue developing the current selected formulations with high encapsulation efficiency using new elements, such as polymers, in the formulations to achieve an improved incorporation of afatinib. Liposome components are not exclusively lipids as a new generation liposome, called the polymersomes, can also be prepared from polymers. With better stability and versatility than liposomes, polymersomes are found many applications in nanomedicine. Hydrophobic, hydrophilic, or amphiphilic compounds can be encapsulated in polymersoms, which makes them very attractive vesicles for many applications in drug delivery. Thus, highly lipophilic anticancer drugs [327, 328]. Studies done by Wang et al has reported that the cationic PLGA/folate coated PEGlated polymeric liposome core shell nanoparticles were successfully developed for co-delivery of anticancer drug and gene. The nanoparticles have core shell structure with nano size, sustained drug release profile and good efficacy. which indicated that the drugs and genes carried by the nanoparticles were co-delivered into the tumor cells [329]. Rifampicin, first line anti-Tuberculosis drug was successfully encapsulated within nanopolymersomes. The polymeric vesicles represent a potential platform for inhalable rifampicin therapy. Furthermore, rifampicin -loaded nano-sized polymersomes promoted drug accumulation in macrophages versus a drug solution representing promising results for a potential TB

inhaled therapy [330]. These properties make them more applicable than liposomes and other vesicle structures.

6.1.2. Validation of proteomics data

Validation of the data obtained by quantitative proteomics, using biological &/or biochemical techniques prior to testing in an animal model for future translation into humans, is recommended to guarantee significance and reliability of novel information. Those techniques do not only validate the quantitative proteomics findings but they may also enable information on a protein of interest, as its specific activity or cellular location to be obtained. Western blotting, a commonly used biochemical method to detect changes in protein abundance, is sensitive, specific, and convenient. In order to obtain quantitative data from western blots, a rigorous methodology must be used. Briefly, the validation of antibodies is critical both to assure that the Ab/antigen interaction is specific and correct and to determine the dilution factor of samples that is required for protein loading in the quantitative linear dynamic range for each antibody. Furthermore, the appropriate selection of normalization method (based on reference signals obtained either by housekeeping proteins (HKPs) after immunochemical staining or total protein (TP) intensity on blotting membranes after total protein staining) must be considered to assure that the reported fold changes of the target protein are not an artifact of reference signal. Thus, data normalization is crucial to identify and correct experimental errors where reference instability becomes increasingly important with the measurement of smaller differences in target protein expression between samples [215, 331].

Further refinement in animal models for pulmonary drug products is also anticipated but also urgently required. To appropriately test inhalation drug products, improved animal models are needed since the use of animal models is a prerequisite to

substantiate the marketing authorization dossier. These models should be able to discriminate between different drug products in terms of aerosol behavior and subsequent pharmacokinetics and –dynamics. In addition, the deposition characteristics would need to be analyzed. Improvements in methods to determine the deposition characteristics in laboratory animals are possible, for example by *in vivo* bioluminescence or fluorescence.

6.1.3. Stability studies

Stability studies of any formulation on storage are essential as it reflects whether the required properties of the drug and its liposomal formulation are retained on storage. investigate the physical stability of liposomes containing AFT under different conditions. The chemical stability of AFT and bilayer components was determined as well

These desirable properties include integrity of lipid vesicles and size distribution of particles in addition to the stability of the encapsulated drug. Upon storage, liposomes are susceptible to many physical changes i.e. lipid particles may undergo fusion and aggregation leading to increase in particle size of liposomes. Also, loss of structural integrity of liposomes and subsequent leakage of encapsulated drug may take place [295]. Liposomal formulations are not stable in an aqueous media. Hence, to increase their stability the liposomal formulations are spray dried. However, during spray drying the drug and liposomal formulation may undergo aforementioned physical changes. The physical testing of such a product should be performed to check whether any changes have taken place in the liposomal product in terms of its particle size and entrapment efficiency. Thus, following storage, the liposomal formulation, on rehydration, should retain the same characteristics it possessed before spray drying. For liposomal products, attention has focused on two processes affecting the quality

and therefore acceptability of liposomes. First leakage of entrapped molecules from the vesicles may occur into the extra liposomal compartment. Secondly, there is a possibility of liposomal aggregation and/or fusion, which leads to formation of larger particles. Hydrolysis of phospholipids is one of the parameters likely to cause the formation of fatty acids and lysophopholipids. Although under dehydrated storage this is limited. Another aspect to be considered is liposome oxidation [297].

As per the ICH stability study guideline, accelerated stability studies should be performed on a drug and drug product at accelerated stability testing (25 ± 2 °C/60% RH $\pm$ 5% RH and at refrigerated conditions (2 - 8 °C) up to 3 months [276]. The samples at different temperatures should be withdrawn periodically and analyzed for chemical and physical stability as in section (4.3.8.). The stability of the drug within the liposomal carrier will be compared to the stability of the drug alone to determine if the use of these carriers affords additional stability to the drug.

References

References

1. **Bahader, Y., Jazieh, AR.** Epidemiology of lung cancer. Ann. Thoracic Med. 2008, 3(6): p. 65-67.

2. **Alamoudi, O.S.** Prevalence of respiratory diseases in hospitalized patients in Saudi Arabia: A 5 years study 1996-2000. Ann. Thoracic Med. 2006, 1(2): p. 76-80.

3. Saudi Cancer Registry. (2016). Cancer incidence report Saudi Arabia 2013. http://www.chs.gov.sa/Ar/HealthCenters/NCC/CancerRegistry/CancerRegistryRports/2013.pdf. Accessed at 21st March 2017.

4. **Al-Ahmadi, K., Al-Zahrani, A., Al-Ahmadi, S.** Spatial Accessibility to Cancer Care Facilitiesin Saudi Arabia. http://proceedings.esri.com/library/userconf/health13/papers/health_11.pdf/ ccessed at 21st April 2017.

5. **Alamoudi, O.S.** Lung cancer at a University Hospital in Saudi Arabia: A four-year prospective study of clinical, pathological, radiological, bronchoscopic, and biochemical parameters. Ann. Thoracic Med. 2010. 5(1): p. 30.

6. Lung cancer and smoking. UK. Cancer Stats. Cancer Research UK. 2008. http://www.info.cancerresearchuk.org/cancerstats/types/lung/html. [cited in 2008].

7. **Thun, M.J., Hannan, L.M., Adams-Campbell, L.L., Boffetta, P., Buring, J.E., Feskanich, D., Flanders, W.D., Jee, S.H., Katanoda, K., Kolonel, L.N. and Lee, I.M.** Lung cancer occurrence in never-smokers: An analysis of 13 cohorts and 22 cancer registry studies. PLoS Med. 2008, 5(9): p. e185.

8. **Abdel-Rahman, M., Stockton, D., Rachet, B., Hakulinen, T., & Coleman, M. P.** What if cancer survival in Britain were the same as in Europe: how many deaths are avoidable? Br. J. Cancer. 2009, 101(Suppl 2): p. S115.

9. **Travis, W.D., Brambilla, E., Muller-Hermelink, H.K. and Harris, C.C.** World Health Organization classification of tumours. Pathology and genetics of tumours of the lung, pleura, thymus and heart. 2004, 10: p.179-84.

10. **Sihoe, A.D., Yim, A.P.,** Lung cancer staging. J. Surg. Res. 2004. 117(1): p. 92-106.

11. **Pirker, R., Filipits, M.** Personalized treatment of advanced non-small-cell lung cancer in routine clinical practice. Cancer Metastasis Rev. 2016, 35(1): p. 141-150.

12. **Rao, R.D., Markovic, S.N., Anderson, P.** Aerosol therapy for malignancy involving the lungs. Curr. Cancer Drug Targets. 2003, 3(4): p. 239-250.

13. **Ezendam, N.P., Pijlman, B., Bhugwandass, C., Pruijt, J.F., Mols, F., Vos, M.C., Pijnenborg, J.M., van de Poll-Franse L.V.** Chemotherapy-induced peripheral neuropathy and its impact on health-related quality of life among ovarian cancer survivors: results from the population-based profiles registry. Gynecol. Oncol. 2014, 135(3): p. 510-517.

14. **Barreto, J.N., McCullough, K.B., Ice, L.L., Smith, J.A.** Antineoplastic agents and the associated myelosuppressive effects: a review. J. Pharm. Pract. 2014, 27(5): p. 440-446.

15. **Li, H., Qian, Z.M.** Transferrin/transferrin receptor-mediated drug delivery. Med. Res. Rev. 2002, 22(3): p. 225-250.

16. **Novello, S., Barlesi, F., Califano, R., Cufer, T., Ekman, S., Giaj Levra, M., Kerr, K., Popat, S., Reck, M., Senan, S., Simo, G. V., Vansteenkiste, J,. Peters, S.** Metastatic non-small-cell lung cancer: ESMO Clinical Practice Guidelines for diagnosis, treatment and follow-up. Ann. Oncol. 2016, 27(suppl 5): p. v1-v27.

17. **Hynes, N.E., Lane, H.A.** ERBB receptors and cancer: the complexity of targeted inhibitors. Nat. Rev. Cancer. 2005. 5(5): p. 341-354.

18. **Herbst, R.S., Bunn, P.A.** Targeting the epidermal growth factor receptor in non-small cell lung cancer. Clin. Cancer Res. 2003, 9(16): p. 5813-5824.

19. **Schlessinger, J.** Cell signaling by receptor tyrosine kinases. Cell. 103(2): p. 211-225.

20. **Mukohara, T.** Mechanisms of resistance to anti-human epidermal growth factor receptor 2 agents in breast cancer. Cancer Sci. 2011, 102(1): p. 1-8.

21. **Hurwitz, J.L., Scullin, P., Campbell, L.** Afatinib treatment in advanced non-small cell lung cancer. Lung Cancer: Targets and Therapy. 2011, 2: p. 47-57.

22. **Giaccone, G., Wang, Y.** Strategies for overcoming resistance to EGFR family tyrosine kinase inhibitors. Cancer Treat. Rev. 2011, 37(6): p. 456-464.

23. **Metro, G., Crinò, L.** The LUX-Lung clinical trial program of afatinib for non-small-cell lung cancer. Expert Rev. Anticancer Ther. 2011, 11(5): 673-682.

24. **Dungo, R.T., Keating, G.M.** Afatinib: first global approval. Drugs. 2013, 73(13): p. 1503-1515.

25. European Medicines Agency. Giotrif: summary of product characteristics, version 24 May 2016. http://www.ema.europa.eu/docs/en_GB/document_library/EPAR_-_Product_Information/human/002280/WC500152392.pdf. Accessed 7Jun 2016.

26. **Wind, S., Wind, S., Schnell, D., Ebner, T., Freiwald, M., Stopfer, P.**Clinical Pharmacokinetics and Pharmacodynamics of Afatinib. Clin. Pharmacokinet. 2017, 56(3): p. 235-250.

27. **Hirsh, V.** Afatinib (BIBW 2992) development in non-small-cell lung cancer. Future Oncol. 2011, 7(7): p. 817-825.

28. **Reid, A., Vidal, L., Shaw, H., de Bono J.** Dual inhibition of ErbB1 (EGFR/HER1) and ErbB2 (HER2/neu). Eur. J. Cancer. 2007, 43(3): p. 481-489.

29. **Wind, S., Schmid, M., Erhardt, J., Goeldner, R.G., Stopfer, P.** Pharmacokinetics of afatinib, a selective irreversible ErbB family blocker, in patients with advanced solid tumours. Clin. Pharmacokinet. 2013, 52(12): p. 1101-1109.

30. **Freiwald, M., Schmid, U., Fleury, A., Wind, S., Stopfer, P., Staab, A.** Population pharmacokinetics of afatinib, an irreversible ErbB family blocker, in patients with various solid tumors. Cancer Chemother. Pharmacol. 2014, 73(4): p. 759-770.

31. **Yap, T.A., Yap, T.A., Vidal, L., Adam, J., Stephens, P., Spicer, J., Shaw, H., Ang, J., Temple, G., Bell, S., Shahidi, M., Uttenreuther-Fischer, M., Stopfer, P., Futreal, A., Calvert, H., de Bono, J.S., Plummer, R.** Phase I trial of the irreversible EGFR and HER2 kinase inhibitor BIBW 2992 in patients with advanced solid tumors. J. Clin. Oncol. 2010, 28(25): p. 3965-3972.

32. **Sequist, L.V., Yang, J.C., Yamamoto, N., O'Byrne, K., Hirsh, V., Mok, T., Geater, S.L., Orlov, S., Tsai, C.M., Boyer, M., Su W.C., Bennouna, J., Kato, T., Gorbunova, V., Lee, K.H., Shah, R., Massey, D., Zazulina, V., Shahidi, M., Schuler, M.** Phase III study of afatinib or cisplatin plus pemetrexed in patients with metastatic lung adenocarcinoma with EGFR mutations. J. Clin. Oncol. 2013, 31(27): p. 3327-3334.

33. **Solca, F., Dahl, G., Zoephel, A., Bader, G., Sanderson, M., Klein, C., Kraemer, O., Himmelsbach, F., Haaksma, E., Adolf, G.R.** Target binding properties and cellular activity of afatinib (BIBW 2992), an irreversible ErbB family blocker. J. Pharmacol. Exp. Ther. 2012, 343(2): p. 342-350.

34. **Modjtahedi, H., Cho, B.C., Michel, M.C., Solca, F.** comprehensive review of the preclinical efficacy profile of the ErbB family blocker afatinib in cancer. Naunyn-Schmiedeberg's Arch. Pharmacol. 2014, 387(6): p. 505-521.

35. **Kwak, E.L., Sordella, R., Bell, D.W., Godin-Heymann, N., Okimoto, R.A., Brannigan, B.W., Harris, P.L., Driscoll, D.R., Fidias, P., Lynch, T.J., Rabindran, S.K., McGinnis, J.P., Wissner, A., Sharma, S.V., Isselbacher, K.J., Settleman, J., Haber, D.A.** Irreversible inhibitors of the EGF receptor may circumvent acquired resistance to gefitinib. Proc Natl Acad Sci U S A. 2005, 102(21): p. 7665-7670.

36. **Chan, B.A., Hughes, B.G.** Targeted therapy for non-small cell lung cancer: current standards and the promise of the future. Transl. Lung Cancer Res. 2015, 4(1): p. 36-54.

37. **Peer, D., Karp, J.M., Hong, S., Farokhzad, O.C., Margalit, R., Langer, R.** Nanocarriers as an emerging platform for cancer therapy. Nat. Nanotechnol. 2007, 2(12): p. 751-760.

146

38. **Sanna, V., Pala, N., Sechi, M.** Targeted therapy using nanotechnology: focus on cancer. Int. J. Nanomedicine. 2014, 9: p. 467-483.

39. **Frank, D., Tyagi, C., Tomar, L., Choonara, Y.E., du Toit, L.C., Kumar, P., Penny, C., Pillay, V.** Overview of the role of nanotechnological innovations in the detection and treatment of solid tumors. Int. J. Nanomedicine. 2014, 9: p. 589-613.

40. **Conde, J., Bao, C., Cui, D., Baptista, P.V., Tian, F.** Antibody–drug gold nanoantennas with Raman spectroscopic fingerprints for in vivo tumour theranostics. J. Control. Release. 2014, 183: p. 87-93.

41. **Conde, J., Oliva, N., Artzi, N**. Implantable hydrogel embedded dark-gold nanoswitch as a theranostic probe to sense and overcome cancer multidrug resistance. Proc. Natl. Acad. Sci. U.S.A. 2015, 112(11): p. E1278-E1287.

42. **Ferrari, M.,** Cancer nanotechnology: opportunities and challenges. Nat Rev Cancer. 2005. 5(3): p. 161-171.

43. **Barratt, G.M.** Therapeutic applications of colloidal drug carriers. Pharm. Sci. Technolo. Today. 2000, 3(5): p. 163-171.

44. **Emeje, M.O., Obidike, I.C., Akpabio, E.I., Ofoefule, S.I.** Nanotechnology in drug delivery. In: Recent advances in novel drug carrier systems. 2012, Sezer, A.D. (Ed.). Chapter 4, InTech Publisher, p: 69-106.

45. **Byron, P.R., Patton, J.S.** Drug delivery via the respiratory tract. J. Aerosol Med. 1994, 7(1): p. 49-75.

46. **Garbuzenko, O.B., Saad, M., Pozharov, V.P., Reuhl, K.R., Mainelis, G., Minko, T.** Inhibition of lung tumor growth by complex pulmonary delivery of drugs with oligonucleotides as suppressors of cellular resistance. Proc. Natl. Acad. Sci. U S A. 2010, 107(23): p. 10737-10742.

47. **Valle, M.J., F.L. González, F.L., A.N. Sánchez, A.N.** Pulmonary versus systemic delivery of levofloxacin. The isolated lung of the rat as experimental approach for assessing pulmonary inhalation. Pulm. Pharmacol. Ther. 2008, 21(2): p. 298-303.

48. **Garbuzenko, O. B., Saad, M., Pozharov, V. P., Reuhl, K. R., Mainelis, G., Minko, T.** Inhibition of lung tumor growth by complex pulmonary delivery of drugs with oligonucleotides as suppressors of cellular resistance. Proceedings of the National Academy of Sciences of the United States of America. (2010), 107(23): p. 10737–10742.

49. **Liang, X.-J., Chen, C., Zhao, Y., Wang, P.C.** Circumventing tumor resistance to chemotherapy by nanotechnology. Methods Mol. Biol. 2010, 596: p. 467-88.

50. **Mozafari, M.R., Pardakhty, A. Azarmi, S., Jazayeri, J.A. Nokhodchi, A., Omri, A.** Role of nanocarrier systems in cancer nanotherapy. Journal of liposome research. 2009, 19(4): p. 310-321.

51. **Wang, Y. Kohane, D.S**. External triggering and triggered targeting strategies for drug delivery. Nature Reviews Materials. 2017, 2(6): 17020.

52. **Vega-Villa, K.R., Takemoto, J.K., Yáñez, J.A.** Clinical toxicities of nanocarrier systems. Advanced Drug Delivery Reviews. 2008, 60(8): p. 929-938.

53. **Malam, Y., Loizidou, M., Seifalian, A.M.** Liposomes and nanoparticles: nanosized vehicles for drug delivery in cancer. Trends in pharmacological sciences. 2009, 30(11): p. 592-599.

54. **Bozzuto, G., Molinari, A.** Liposomes as nanomedical devices. International journal of nanomedicine. (2015), 10: 975-999.

55. **Bae, Y.H., Park, K.** Targeted drug delivery to tumors: myths, reality and possibility. Journal of Controlled Release. 2011, 153(3): p. 198-205.

56. **Sinha, R., Kim, G.J., Nie, S., Shin, D.M.** Nanotechnology in cancer therapeutics: bioconjugated nanoparticles for drug delivery. Molecular Cancer Therapeutics. 2006, 5(8): p. 1909-1917.

57. **Alexis, F., Pridgen, E., Molnar, L.K., Farokhzad, O.C.** Factors affecting the clearance and biodistribution of polymeric nanoparticles. Molecular pharmaceutics, 2008. 5(4): p. 505-515.
58. **Byrne, J.D., Betancourt, T., Brannon-Peppas, L.** Active targeting schemes for nanoparticle systems in cancer therapeutics. Advanced drug delivery reviews. 2008, 60(15): p. 1615-1626.
59. **Pilcer, G., Amighi, K.** Formulation strategy and use of excipients in pulmonary drug delivery. Int J Pharm. 2010, 392(1-2): p. 1-19.
60. **Goel, A., Baboota, S., Sahni, J.K. Ali, J.** Exploring targeted pulmonary delivery for treatment of lung cancer. International journal of pharmaceutical investigation. 2013, 3(1), p.8-14.
61. **Alipour, S., Montaseri, H., Tafaghodi, M.** Preparation and characterization of biodegradable paclitaxel loaded alginate microparticles for pulmonary delivery. Colloids and Surfaces B: Biointerfaces. 2010, 81(2): p. 521-529.
62. **Patil, J.S., Sarasija, S.** Pulmonary drug delivery strategies: A concise, systematic review. Lung India. 2012, 29(1): p. 44-49.
63. **van Swaay, D., deMello, A.** Microfluidic methods for forming liposomes. Lab on a Chip. 2013, 13(5): p. 752-767.
64. **Wauthoz, N., Amighi, K.** Phospholipids in pulmonary drug delivery. European journal of lipid science and technology. 2014, 116(9): p. 1114-1128.
65. **Schiffelers, R.M., Metselaar, J.M., Fens, M.H., Janssen, A.P., Molema, G., Storm, G.** Liposome-encapsulated prednisolone phosphate inhibits growth of established tumors in mice. Neoplasia. 2005, 7(2): p. 118-127.
66. **Batzri, S., Korn, E.D.** Single bilayer liposomes prepared without sonication. Biochimica et Biophysica Acta (BBA) – Biomembranes. 1973, 298(4): p. 1015-1019.
67. **Szoka, F., Papahadjopoulos, D.** Procedure for preparation of liposomes with large internal aqueous space and high capture by reverse-phase evaporation. Proceedings of the National Academy of Sciences U S A. 1978, 75(9): p. 4194-4198.
68. **Kirby, C., Gregoriadis,** G. Dehydration-rehydration vesicles: A simple method for high yield drug entrapment in liposomes. Nature Biotechnology. 1984, 2(11): p. 979-984.
69. **Perrett, S., Golding, M., Williams, W.P.** A simple method for the preparation of liposomes for pharmaceutical applications: characterization of the liposomes. Journal of pharmacy and pharmacology, 1991. 43(3): p. 154-161.
70. **Hope, M.J., Bally, M.B., Webb, G., Cullis, P.R.** Production of large unilamellar vesicles by a rapid extrusion procedure: characterization of size distribution, trapped volume and ability to maintain a membrane potential. Biochimica et Biophysica Acta (BBA)-Biomembranes, 1985. 812(1): p. 55-65.
71. **Lynch, T.J., Bell, D.W., Sordella, R., Gurubhagavatula, S., Okimoto, R.A., Brannigan, B.W., Harris, P.L., Haserlat, S.M., Supko, J.G., Haluska, F.G. Louis, D.N.** Activating mutations in the epidermal growth factor receptor underlying responsiveness of non–small-cell lung cancer to gefitinib. New England Journal of Medicine. 2004, 350(21), pp.2129-2139.
72. **Ait-Oudhia, S., Mager, D.E., Straubinger, R.M.** Application of pharmacokinetic and pharmacodynamic analysis to the development of liposomal formulations for oncology. Pharmaceutics, 2014. 6(1): p. 137-174.
73. **Bulbake, U., Doppalapudi, S., Kommineni, N., Khan, W.** Liposomal Formulations in Clinical Use: An Updated Review. Pharmaceutics, 2017. 9(2): p. 12.
74. **Liu, D., He, C., Wang, A.Z., Lin, W.** Application of liposomal technologies for delivery of platinum analogs in oncology. International journal of nanomedicine. 2013, 8: p. 3309-3319.

75. **Hang, Z., Cooper, M.A., Ziora, Z.M.** Platinum-based anticancer drugs encapsulated liposome and polymeric micelle formulation in clinical trials. Biochemical Compounds. 2016, 4(1): p. 2.
76. **Boulikas, T.,** Low toxicity and anticancer activity of a novel liposomal cisplatin (Lipoplatin) in mouse xenografts. Oncology reports. 2004, 12(1): p. 3-12.
77. **Newman, M.S., Colbern, G.T., Working, P.K., Engbers, C., Amantea, M.A**. Comparative pharmacokinetics, tissue distribution, and therapeutic effectiveness of cisplatin encapsulated in long-circulating, pegylated liposomes (SPI-077) in tumor-bearing mice. Cancer chemotherapy and pharmacology, 1999. 43(1): p. 1-7.
78. **Ishida, T., Kirchmeiera, M.J., Moase, E.H., Zalipsky, S., Allen, T.M.** Targeted delivery and triggered release of liposomal doxorubicin enhances cytotoxicity against human B lymphoma cells. Biochimica et Biophysica Acta (BBA)-Biomembranes. 2001, 1515(2): p. 144-158.
79. **Cheng, Y.S.** Mechanisms of pharmaceutical aerosol deposition in the respiratory tract. AAPS PharmSciTech. 2014, 15(3), pp.630-640.
80. **Puri, A., Loomis, K., Smith, B., Lee, J.-H. Yavlvoich, A., Heldman, E., Blumenthal, R.** Lipid-based nanoparticles as pharmaceutical drug carriers: from concepts to clinic. Critical Reviews™ in Therapeutic Drug Carrier Systems. 2009, 26(6): p. 523-580.
81. **Moghimi, S.M. Szebeni, J.** Stealth liposomes and long circulating nanoparticles: critical issues in pharmacokinetics, opsonization and protein-binding properties. Progress in lipid research. 2003, 42(6): p. 463-478.
82. **Ulrich, A.S.** Biophysical aspects of using liposomes as delivery vehicles. Bioscience reports. 2002, 22(2): p. 129-150.
83. **Torchilin, V.P., Zhou, F. Huang, L.** pH-sensitive liposomes. Journal of liposome research, 1993. 3(2): p. 201-255.
84. **Karanth, H. Murthy, R.S.** pH-Sensitive liposomes-principle and application in cancer therapy. Journal of pharmacy and pharmacology. 2007, 59(4): p. 469-483.
85. **Simões, S., Moreira, J.N., Fonseca, C., Düzgüneş, N., de Lima, M.C.** On the formulation of pH-sensitive liposomes with long circulation times. Advanced drug delivery reviews. 2004, 56(7): p. 947-965.
86. **Torchilin, V.P.** Recent advances with liposomes as pharmaceutical carriers. Nature reviews Drug discovery. 2005, 4(2): p. 145-160.
87. **Provoda, C.J., Stier, E.M., Lee, K.-D.** Tumor cell killing enabled by listeriolysin O-liposome-mediated delivery of the protein toxin gelonin. Journal of Biological Chemistry, 2003. 278(37): p. 35102-35108.
88. **Mastrobattista, E., Koning, G.A., van Bloois, L., Filipe, A.C., Jiskoot, W., Storm, G.** Functional characterization of an endosome-disruptive peptide and its application in cytosolic delivery of immunoliposome-entrapped proteins. Journal of Biological Chemistry. 2002, 277(30): p. 27135-27143.
89. **Deshpande, P.P., S. Biswas, S., Torchilin, V.P.** Current trends in the use of liposomes for tumor targeting. Nanomedicine. 2013, 8(9): p. 1509-1528.
90. **Zalipsky, S.,** Chemistry of polyethylene glycol conjugates with biologically active molecules. Advanced Drug Delivery Reviews. 1995, 16(2-3): p. 157-182.
91. **Hafez, I.M., Cullis, P.R.** Roles of lipid polymorphism in intracellular delivery. Advanced drug delivery reviews. 2001, 47(2-3): p. 139-148.
92. **Saari, M., Vidgren, M.T., Koskinen, M.O., Turjanmaa, V.M., Nieminen, M.M.** Pulmonary distribution and clearance of two beclomethasone liposome formulations in healthy volunteers. International journal of pharmaceutics. 1999, 181(1): p. 1-9.
93. **Goyal, P., Goyal, K., Vijaya Kumar, S.G., Singh, A., Katare, O.P., Mishra, D.N.** Liposomal drug delivery systems--clinical applications. Acta Pharmaceutica. 2005, 55(1): p. 1-25.

94. **Paul, S., Rao, S., Kohan, R., McMichael, J., French, N., Zhang, G., Simmer, K.** Poractant alfa versus beractant for respiratory distress syndrome in preterm infants: A retrospective cohort study. Journal of paediatrics and child health. 2013, 49(10): p. 839-844.

95. **Myers, M.A, Thomas, D.A., Straub, L., Soucy, D.W., Niven, R.W., Kaltenbach, M., Hood, C.I., Schreier, H., Gonzalez-Rothi R.J.** Pulmonary effects of chronic exposure to liposome aerosols in mice. Experimental lung research. 1993, 19(1): p. 1-19.

96. **Schreier, H., McNicol, K.J., Ausborn, M., Soucy, D.M., Derendorf, H., Stecenko, A.A., Gonzalez-Rothi, R.J.** Pulmonary delivery of amikacin liposomes and acute liposome toxicity in the sheep. International journal of pharmaceutics. 1992, 87(1-3): p. 183-193.

97. **Clancy, J.P., Dupont, L., Konstan, M.W., Billings, J., Fustik, S., Goss, C.H., Lymp, J., Minic, P., Quittner, A.L., Rubenstein, R.C., Young, K.R., Saiman, L., Burns, J.L., Govan, J.R., Ramsey, B., Gupta, R.** Phase II studies of nebulised Arikace in CF patients with Pseudomonas aeruginosa infection. Thorax. 2013, 68(9): p. 818-825.

98. **Anabousi, S., Bakowsky, U., Schneider, M., Huwer, H., Lehr, C.M., Ehrhardt, C.** In vitro assessment of transferrin-conjugated liposomes as drug delivery systems for inhalation therapy of lung cancer. European journal of pharmaceutical sciences. 2006, 29(5): p. 367-374.

99. **Wittgen, B.P., Kunst, P.W., van der Born, K., van Wijk, A.W., Perkins, W., Pilkiewicz, F.G., Perez-Soler, R., Nicholson, S., Peters, G.J., Postmus, P.E.** Phase I study of aerosolized SLIT cisplatin in the treatment of patients with carcinoma of the lung. Clinical Cancer Research. 2007, 13(8): p. 2414-2421.

100. **Verschraegen, C.F., Gilbert, B.E., Loyer, E., Huaringa, A., Walsh, G., Newman, R.A., Knight, V.** Clinical evaluation of the delivery and safety of aerosolized liposomal 9-nitro-20(s)-camptothecin in patients with advanced pulmonary malignancies. Clinical Cancer Research. 2004, 10(7): p. 2319-2326.

101. **Verschraegen, C.F., Gilbert, B.E., Huaringa, A.J., Newman, R., Harris, N., Leyva, F.J., Keus, L., Campbell, K., Nelson-Taylor, T., Knight V.** Feasibility, Phase I, and Pharmacological Study of Aerosolized Liposomal 9-Nitro-20(S)-Camptothecin in Patients with Advanced Malignancies in the Lungs. Annals of the New York Academy of Sciences. 2000, 922(1): p. 352-354.

102. **Gautam, A., Waldrep, J.C., Densmore, C.L., Koshkina, N., Melton, S., Roberts, L., Gilbert, B., Knight, V.** Growth inhibition of established B16-F10 lung metastases by sequential aerosol delivery of p53 gene and 9-nitrocamptothecin. Gene therapy. 2002, 9(5): p. 353-357.

103. **Knight, V., Kleinerman, E.S., Waldrep, J.C., Giovanella, B.C., Gilbert, B.E., Koshkina, N. V.** 9-Nitrocamptothecin liposome aerosol treatment of human cancer subcutaneous xenografts and pulmonary cancer metastases in mice. Annals of the New York Academy of Sciences. 2000, 922(1): p. 151-163.

104. **Koshkina, N.V., Kleinerman, E.S., Waidrep, C., Jia, S.-F., Worth, L.L., Gilbert, B.E., Knight, V.** 9-Nitrocamptothecin liposome aerosol treatment of melanoma and osteosarcoma lung metastases in mice. Clinical Cancer Research. 2000, 6(7): p. 2876-2880.

105. **Skubitz, K.M., Anderson, P.M.,** Inhalational interleukin-2 liposomes for pulmonary metastases: a phase I clinical trial. AntiCancer Drugs. 2000, 11(7): p. 555-563.

106. **Khanna, C., Hasz, D.E., Klausner, J.S., Anderson, P.M.** Aerosol delivery of interleukin 2 liposomes is nontoxic and biologically effective: canine studies. Clinical cancer research. 1996, 2(4): p. 721-734.

107. **Koshkina, N.V., Waldrep, J.C., Roberts, L.E., Golunski, E., Melton, S., Knight, V.** Paclitaxel liposome aerosol treatment induces inhibition of pulmonary metastases in murine renal carcinoma model. Clinical cancer research. 2001, 7(10): p. 3258-3262.

150

108. **Koshkina, N.V., Golunski, E., Roberts, L.E., Gilbert, B.E., Knight, V.** Cyclosporin A aerosol improves the anticancer effect of paclitaxel aerosol in mice. Journal of aerosol medicine. 2004, 17(1): p. 7-14.

109. **Garbuzenko, O.B., Mainelis, G., Taratula, O., Minko, T.** Inhalation treatment of lung cancer: the influence of composition, size and shape of nanocarriers on their lung accumulation and retention. Cancer biology & medicine. 2014, 11(1): p. 44-55.

110. **Koshkina, N.V., Gilbert, B.E., Waldrep, J.C., Seryshev, A., Knight, V**. Distribution of camptothecin after delivery as a liposome aerosol or following intramuscular injection in mice. Cancer chemotherapy and pharmacology. 1999, 44(3): p. 187-192.

111. **Zhang, L.J., Xing, B., Wu, J., Xu, B. and Fang, X.L.** Biodistribution in mice and severity of damage in rat lungs following pulmonary delivery of 9-nitrocamptothecin liposomes. Pulmonary pharmacology & therapeutics. 2008, 21(1), pp.239-246.

112. **Canonico, A.E., Plitman, J.D., Conary, J.T., Meyrick, B.O., Brigham, K.L.** No lung toxicity after repeated aerosol or intravenous delivery of plasmid-cationic liposome complexes. Journal of Applied Physiology. 1994, 77(1): p. 415-419.

113. **Waldrep, J.C., Scherer, P.W., Hess, D., Black, M., Knight, V.** Nebulized glucocorticoids in liposomes: aerosol characteristics and human dose estimates. Journal of aerosol medicine. 2009, 7(2): p. 135-145.

114. **Cipolla, D., Huiying, W., Gonda, I., Chan, H.-K.** Aerosol performance and stability of liposomes containing ciprofloxacin nanocrystals. Journal of aerosol medicine and pulmonary drug delivery. 2015, 28(6): p. 411-422.

115. **Niven, R.W., Carvajal, T.M., Schreier, H.** Nebulization of liposomes. III. The effects of operating conditions and local environment. Pharmaceutical research. 1992, 9(4): p. 515-520.

116. **Taylor, K.M.G., Taylor, G., Kellaway, I.W., Stevens, J.** The stability of liposomes to nebulisation. International journal of pharmaceutics. 1990, 58(1): p. 57-61.

117. **Bridges, P.A. Taylor, K.M.G.** Nebulisers for the generation of liposomal aerosols. International journal of pharmaceutics. 1998, 173(1-2): p. 117-125.

118. **Sung, J.C., Pulliam, B.L. Edwards, D.A.** Nanoparticles for drug delivery to the lungs. Trends in biotechnology. 2007, 25(12): p. 563-570.

119. **Jensen, D.M., Cun, D., Maltesen, M.J., Frokjaer, S., Nielsen, H.M., Foged, C.** Spray drying of siRNA-containing PLGA nanoparticles intended for inhalation. Journal of Controlled Release. 2010, 142(1): p. 138-145.

120. **Ungaro, F., d'Angelo, I., Miro, A., La Rotonda, M.I., Quaglia, F.** Engineered PLGA nano-and micro-carriers for pulmonary delivery: challenges and promises. Journal of Pharmacy and Pharmacology. 2012, 64(9): p. 1217-1235.

121. **Seville, P.C., Li, H.-y., Learoyd, T.P.** Spray-dried powders for pulmonary drug delivery. Critical Reviews™ in Therapeutic Drug Carrier Systems. 2007, 24(4): p. 307-360.

122. **Darquenne, C.** Aerosol deposition in health and disease. Journal of aerosol medicine and pulmonary drug delivery. 2012, 25(3), pp.140-147.

123. **Gonda I.** Targeting by deposition. In: Pharmaceutical Inhalation Aerosol Technology. Hickey AJ, editor. New York, NY: Marcel Dekker; 2003. p. 65–88.

124. **Dickinson, P.A., Seville, P.C., Taylor, G.** Further evidence of extensive pulmonary first-pass ester hydrolysis after airways administration in rats. Pharmacy and Pharmacology Communications. 2000, 6: p. 441–445.

125. **Labiris, N. Dolovich, M.** Pulmonary drug delivery. Part I: physiological factors affecting therapeutic effectiveness of aerosolized medications. British journal of clinical pharmacology. 2003, 56(6): p. 588-599.

126. **Siow, L.F., Rades, T. Lim, M.H.** Characterizing the freezing behavior of liposomes as a tool to understand the cryopreservation procedures. Cryobiology. 2007, 55(3): p. 210-221.

127.   **Solis, C., Forsberg, F. Wheatley, M.A.** Preserving enhancement in freeze-dried contrast agent ST68: Examination of excipients. International journal of pharmaceutics. 2010, 396(0): p. 30-38.

128.   **Peukert, W. Wadenpohl, C.** Industrial separation of fine particles with difficult dust properties. Powder Technology. 2001, 118(1-2): p. 136-148.

129.   **Malcolmson, R.J. Embleton, J.K.** Dry powder formulations for pulmonary delivery. Pharmaceutical Science & Technology Today. 1998, 1(9): p. 394-398.

130.   **Goldbach, P., Brochart, H. Stamm, A.** Spray-drying of liposomes for a pulmonary administration. I. Chemical stability of phospholipids. Drug development and industrial pharmacy. 1993, 19(19): p. 2611-2622.

131.   **Sweeney, L.G., Wang, Z., Loebenberg, R., Wong, J.P., Lange, C.F., Finlay, W.H.** Spray-freeze-dried liposomal ciprofloxacin powder for inhaled aerosol drug delivery. International journal of pharmaceutics. 2005, 305(1-2): p. 180-185.

132.   **Pilcer, G., Amighi, K.** Formulation strategy and use of excipients in pulmonary drug delivery. International journal of pharmaceutics. 2010, 392(1-2): p. 1-19.

133.   **Kawashima, Y. York, P.** Drug delivery applications of supercritical fluid technology. Preface. Advanced Drug Delivery Reviews. 2008, 60(3): p. 297-298.

134.   **Karn, P.R., Cho, W., Hwang, S.J.** Liposomal drug products and recent advances in the synthesis of supercritical fluid-mediated liposomes. Nanomedicine. 2013, 8(9): p. 1529-1548.

135.   **Meure, L.A., Foster, N.R., Dehghani, F.** Conventional and dense gas techniques for the production of liposomes: a review. AAPS PharmSciTech. 2008, 9(3): p. 798-809.

136.   **Varona, S., Martín, A., Cocero, M.J.** Liposomal incorporation of lavandin essential oil by a thin-film hydration method and by particles from gas-saturated solutions. Industrial & Engineering Chemistry Research. 2011, 50(4): p. 2088-2097.

137.   **Frederiksen L, Anton, K., Barratt, B.J., van Hoogevest, P., Keller, H.R., Leuenberger, H.** Use of supercritical carbon dioxide for preparation of pharmaceutical formulations. Proceedings of the 3rd International Symposium on Supercritical Fluids; October 17–19, 1994; Strasbourg, France. 1994. p. 235–240.

138.   **Otake, K., Shimomura, T., Goto, T., Imura, T., Furuya, T., Yoda, S., Takebayashi, Y., Sakai, H., Abe, M.** Preparation of liposomes using an improved supercritical reverse phase evaporation method. Langmuir. 2006, 22(6): p. 2543-2550.

139.   **O'callaghan, C. Barry, P.W.** The science of nebulised drug delivery. Thorax. 1997, 52(Suppl 2): p. S31-S44.

140.   **Taylor, K.M.G., McCallion, O.N.** Ultrasonic nebulisers for pulmonary drug delivery. International journal of pharmaceutics. 1997, 153(1): p. 93-104.

141.   **Waldrep, J.C., Dhand, R.** Advanced nebulizer designs employing vibrating mesh/aperture plate technologies for aerosol generation. Current Drug Delivery. 2008, 5(2): p. 114-119.

142.   **Dolovich, M.B., Dhand, R.** Aerosol drug delivery: developments in device design and clinical use. Lancet. 2011, 377(9770): p. 1032-1045.

143.   **Ari, A., Areabi, H., Fink, J.B.** Evaluation of aerosol generator devices at 3 locations in humidified and non-humidified circuits during adult mechanical ventilation. Respiratory Care. 2010, 55(7): p. 837-844.

144.   **Dhand, R.** Nebulizers that use a vibrating mesh or plate with multiple apertures to generate aerosol. Respiratory care. 2002, 47(12): p. 1406-1416; discussion 1416-8.

145.   **Waldrep, J.C., Gilbert, B.E., Knight, C.M., Black, M.B., Scherer, P.W., Knight, V., Eschenbacher, W.** Pulmonary delivery of beclomethasone liposome aerosol in volunteers: tolerance and safety. Chest. 1997, 111(2): p. 316-323.

146.   **Elhissi, A., Faizi, M., Naji, W.F., Gill, H.S., Taylor, K.M.** Physical stability and aerosol properties of liposomes delivered using an air-jet nebulizer and a novel micropump

device with large mesh apertures. International journal of pharmaceutics. 2007, 334(1-2): p. 62-70.

147.   **Ghazanfari, T., Elhissi, A.M., Ding, Z., Taylor, K. M.** The influence of fluid physicochemical properties on vibrating-mesh nebulization. International journal of pharmaceutics. 2007, 339(1-2): p. 103-111.

148.   **Yadav, A.V., Murthy M.S., Shete A.S., and Sfurti Sakhare.** Stability aspects of liposomes. Indian Journal Of Pharmaceutical Education And Research. 2011, 45(4): p. 402-413.

149.   **Steckel, H., Eskandar, F.** Factors affecting aerosol performance during nebulization with jet and ultrasonic nebulizers. European journal of pharmaceutical sciences. 2003, 19(5): p. 443-455.

150.   **Ari, A., Atalay, O.T., Harwood, R., Sheard, M.M., Aljamhan, E.A., Fink, J.B.** Influence of nebulizer type, position, and bias flow on aerosol drug delivery in simulated pediatric and adult lung models during mechanical ventilation. Respiratory care. 2010, 55(7): p. 845-851.

151.   **Vecellio, L., De Gersem. R., Le Guellec, S., Reychler, G., Pitance, L., Le Pennec, D., Diot, P., Chantrel, G., Bonfils, P., Jamar, F.** Deposition of aerosols delivered by nasal route with jet and mesh nebulizers. International journal of pharmaceutics. 2011, 407(1-2): p. 87-94.

152.   **Elhlssl, A.M., Brar, J., Najlah, M., Roberts, S.A., Faheem, A., Taylor, K.M.G.** An Ethanol-Based Proliposome Technology for Enhanced Delivery and Improved Respirability of Antiasthma Aerosols Generated Using a Micropump Vibrating-Mesh Nebulizer. Journal of Pharmaceutical Technology, Research and Management. 2013, 1(2): p. 171-180.

153.   **Vyas, S.P., Sakthivel, T.** Pressurized pack-based liposomes for pulmonary targeting of isoprenaline—development and characterization. Journal of microencapsulation. 1994, 11(4): p. 373-380.

154.   **Alouache, A.I., Kellaway, I.W., Taylor, K.M.G. Rogueda, P.** Stability kinetics of HFA suspensions prepared with a fluoroalcohol and PEG-phospholipids. J Aerosol Med. 2006, 20, p.373.

155.   **Al-Hallak, M.H., Sarfraz, M.K., Azarmi, S., Roa, W.H., Finlay, W.H., Löbenberg, R**. Pulmonary delivery of inhalable nanoparticles: dry powder inhalers. Therapeutic Delivery. 2011, 2(10): p. 1313-1324.

156.   **Ashurst, I.I., Malton, A., Prime, D., Sumby, B.** Latest advances in the development of dry powder inhalers. Pharmaceutical science & technology today. 2000, 3(7): p. 246-256.

157.   **Lange, C.F., Hancock, R.E.W., Samuel, J., Finlay, W.H.** In vitro aerosol delivery and regional airway surface liquid concentration of a liposomal cationic peptide. Journal of pharmaceutical sciences. 2001, 90(10): p. 1647-1657.

158.   **Patel, G., Chougule, M., Singh, M., Misra, A.** Nanoliposomal Dry Powder Formulations. Methods in enzymology. 2009, 464: p. 167-191.

159.   **Rojanarat, W., Changsan, N., Tawithong, E., Pinsuwan, S., Chan, H.K., Srichana, T.** Isoniazid proliposome powders for inhalation—preparation, characterization and cell culture studies. International journal of molecular sciences. 2011, 12(7): p. 4414-4434.

160.   **Joshi, M.R., Misra, A.** Liposomal budesonide for dry powder inhaler: preparation and stabilization. AAPS PharmSciTech. 2001, 2(4): p. 44-53.

161.   **Joshi, M., Misra, A.** Dry powder inhalation of liposomal Ketotifen fumarate: formulation and characterization. International journal of pharmaceutics. 2001, 223(1): p. 15-27.

162.   **Ourique, A.F., Chaves Pdos S., Souto, G.D., Pohlmann, A.R., Guterres, S.S**., **Beck, R.C.** Redispersible liposomal-N-acetylcysteine powder for pulmonary administration:

development, in vitro characterization and antioxidant activity. European Journal of Pharmaceutical Sciences. 2014, 65: p. 174-182.

163. **Sawant, R.R., Torchilin, V.P.** Challenges in development of targeted liposomal therapeutics. The AAPS journal. 2012, 14(2): p. 303-315.

164. **Bareford, L.M., Swaan, P.W.** Endocytic mechanisms for targeted drug delivery. Advanced drug delivery reviews. 2007, 59(8): p. 748-758.

165. **Zhao, W., Zhuang, S., Qi, X.-R.** Comparative study of the in vitro and in vivo characteristics of cationic and neutral liposomes. International journal of nanomedicine. 2011, 6: p. 3087-3098.

166. **Soenen, S.J., Brisson, A.R., De Cuyper, M.** Addressing the problem of cationic lipid-mediated toxicity: the magnetoliposome model. Biomaterials. 2009, 30(22): p. 3691-3701.

167. **Knudsen, K.B., Northeved, H., Kumar, P.E., Permin, A., Gjetting, T., Andresen, T.L., Larsen, S., Wegener, K.M., Lykkesfeldt, J., Jantzen, K., Loft, S., Møller, P., Roursgaard, M**. In vivo toxicity of cationic micelles and liposomes. Nanomedicine. 2015, 11(2): p. 467-477.

168. **Bibi, S., Lattmann , E., Mohammed , A. R., and Perrie , Y.** Trigger release liposome systems: local and remote controlled delivery? Journal of microencapsulation. 2012, 29(3): p. 262-276.

169. **Lai, M.Z., Duzgunes, N. Szoka, F.C.** Effects of replacement of the hydroxyl group of cholesterol and tocopherol on the thermotropic behavior of phospholipid membranes. Biochemistry. 1985, 24(7): p. 1646-1653.

170. **Nayar, R. Schroit, A.J.** Generation of pH-sensitive liposomes: use of large unilamellar vesicles containing N-succinyldioleoylphosphatidylethanolamine. Biochemistry. 1985, 24(21): p. 5967-5971.

171. **Webb, M.S., Wheeler, J.J., Bally, M.B., Mayer, L.D.**The cationic lipid stearylamine reduces the permeability of the cationic drugs verapamil and prochlorperazine to lipid bilayers: implications for drug delivery. Biochimica et Biophysica Acta (BBA)-Biomembranes. 1995, 1238(2): p. 147-155.

172. **Venugopalan, P., Jain, S., Sankar, S., Singh, P., Rawat, A., Vyas, S.P.** pH-sensitive liposomes: mechanism of triggered release to drug and gene delivery prospects. Pharmazie. 2002, 57(10): p. 659-671.

173. **Paliwal, S.R., Paliwal, R. Vyas, S.P.** A review of mechanistic insight and application of pH-sensitive liposomes in drug delivery. Drug delivery. 2015, 22(3): p. 231-242.

174. **Júnior, Á.D., Mota, L.G., Nunan, E.A., Wainstein, A.J., Wainstein A.P.D., Leal, A.S., Cardoso, V.N., De Oliveira, M.C.,** Tissue distribution evaluation of stealth pH-sensitive liposomal cisplatin versus free cisplatin in Ehrlich tumor-bearing mice. Life sciences. 2007, 80(7): p. 659-664.

175. **Lesoin, L., Crampon, C., Boutin,O., Badens**, E. Preparation of liposomes using the supercritical anti-solvent (SAS) process and comparison with a conventional method. The Journal of Supercritical Fluids. 2011, 57(2): p. 162-174.

176. **Gregoriadis, G.** Engineering liposomes for drug delivery: progress and problems. Trends in biotechnology. 1995, 13(12): p. 527-537.

177. **Drummond, D.C., Meyer, O., Hong, K., Kirpotin, D.B., Papahadjopoulos, D.** Optimizing liposomes for delivery of chemotherapeutic agents to solid tumors. Pharmacological reviews. 1999, 51(4): p. 691-743.

178. **Hamilton, R.L., Goerke, J., Guo, L.S., Williams, M.C., Havel, R.J.** Unilamellar liposomes made with the French pressure cell: a simple preparative and semiquantitative technique. Journal of lipid research. 1980, 21(8): p. 981-992.

179. **Woodbury, D.J., Richardson, E.S., Grigg, A.W., Welling, R.D., Knudson, B.H.** Reducing liposome size with ultrasound: bimodal size distributions. Journal of liposome research. 2006, 16(1): p. 57-80.

180. **Brandl, M., Bachmann, D., Drechsler, M., Bauer, K.H.** Liposome preparation by a new high pressure homogenizer Gaulin Micron Lab 40. Drug Development and Industrial Pharmacy. 1990, 16(14): p. 2167-2191.

181. **Berger, N., Sachse, A., Bender, J., Schubert, R., Brandl, M.** Filter extrusion of liposomes using different devices: comparison of liposome size, encapsulation efficiency, and process characteristics. International journal of pharmaceutics. 2001, 223(1-2): p. 55-68.

182. **Ong, S.G.M., Chitneni, ., Lee, K.S., Ming, L.C., Yuen, K.H.** Evaluation of extrusion technique for nanosizing liposomes. Pharmaceutics, 2016. **8**(4): p. 36-48.

183. **Bangham, A.D., Standish,M.M., Watkins, J.C.** Diffusion of univalent ions across the lamellae of swollen phospholipids. Journal of molecular biology. 1965, 13(1): p. 238-252.

184. **Guideline, I.H.T.,** Validation of analytical procedures: text and methodology. Q2 (R1), In International Conference on Harmonization, Geneva, Switzerland (p. 11-12). 2005. 1.

185. **Moghaddam, B., Ali, M.H., Wilkhu, J., Kirby, D.J., Mohammed, A.R., Zheng, Q. and Perrie, Y.** The application of monolayer studies in the understanding of liposomal formulations. International journal of pharmaceutics. 2011, 417(1-2), pp.235-244.

186. **Zhong-li, H., Gui-zhou, H. Xiao-wei, C.** Determination of Afatinib Tablets by HPLC. Qilu Pharmaceutical Affairs. 2014,(6): p. 337-338.

187. **Vejendla, R., Subramanyam, C. Veerabhadram, G.** New RP-HPLC method for the determination of afatinib dimaleate in bulk and pharmaceutical dosage forms. Indo-American Journal Pharmaceutical Research. 2015,(5): p. 2098-2111.

188. **Xiang, S.X., Wu, H.L., Kang, C., Xie, L.X., Yin, X.L., Gu, H.W. Yu, R.Q.** Fast quantitative analysis of four tyrosine kinase inhibitors in different human plasma samples using three-way calibration-assisted liquid chromatography with diode array detection. Journal of separation science. 2015, 38(16): p. 2781-2788.

189. **Meng, F., Cheng, R., Deng, C., Zhong, Z.** Intracellular drug release nanosystems. Materials Today. 2012, 15(10): p. 436-442.

190. **Brandl, M.** *Liposomes as drug carriers: a technological approach.* Biotechnology annual review. 2001, **7**: p. 59-85.

191. **Coelho, S.C., Almeida, G.M., Pereira, M.C., Santos-Silva, F., Coelho, M.A.** Functionalized gold nanoparticles improve afatinib delivery into cancer cells. Expert opinion on drug delivery. 2016, 13(1): p.133-141.

192. **Fahr, A., Van Hoogevest, P., May, S., Bergstrand, N., Leigh, M.L.** Transfer of lipophilic drugs between liposomal membranes and biological interfaces: consequences for drug delivery. European Journal of Pharmaceutical Sciences. 2005, 26(3-4): p. 251-265.

193. **Michaelis, U., Haas, H.** Targeting of cationic liposomes to endothelial tissue. In Liposome Technology. 2006, 3: p. 151-170.

194. **Mayer, L.D., Hope, M.J., Cullis, P.R.** Vesicles of variable sizes produced by a rapid extrusion procedure. Biochimica et Biophysica Acta (BBA)-Biomembranes. 1986, 858(1): p. 161-168.

195. **Senior, J.H., Trimble, K.R. Maskiewicz, R.** Interaction of positively-charged liposomes with blood: implications for their application in vivo. Biochimica et Biophysica Acta (BBA)-Biomembranes. 1991, 1070(1): p. 173-179.

196. **Kraft, J.C., Freeling, J.P., Wang, Z., Ho, R.J.** Emerging research and clinical development trends of liposome and lipid nanoparticle drug delivery systems. Journal of pharmaceutical sciences. 2014, 103(1): p. 29-52.

197. **Nallamothu, R., Wood, G.C., Kiani, M.F., Moore, B.M., Horton, F.P., Thoma, L.A.** A targeted liposome delivery system for combretastatin A4: formulation optimization through drug loading and in vitro release studies. PDA Journal of Pharmaceutical Science and Technology. 2006, 60(3): p. 144-155.

198. **Zuidam, N.J. Barenholz, Y.** Electrostatic and structural properties of complexes involving plasmid DNA and cationic lipids commonly used for gene delivery. Biochimica et Biophysica Acta (BBA)-Biomembranes. 1998, 1368(1): p. 115-128.

199. **Düzgünes, N., Simóes, S., Lopez-Mesas, M., Pedroso de Lima, M.C.** Intracellular delivery of therapeutic oligonucleotides in pH-sensitive and cationic liposomes. Liposome Technology,, 3, pp.253-275.Intracellular delivery of therapeutic oligonucleotides in pH-sensitive and cationic liposomes. Liposome Technology. 2006, **3**: p. 253-275.

200. **Sudimack, J.J., Guo, W., Tjarks, W., Lee, R.J.** A novel pH-sensitive liposome formulation containing oleyl alcohol. Biochimica et Biophysica Acta (BBA)-Biomembranes. 2002, 1564(1): p. 31-37.

201. **Ishida, T., Okada, Y., Kobayashi, T., Kiwada, H.** Development of pH-sensitive liposomes that efficiently retain encapsulated doxorubicin (DXR) in blood. International journal of pharmaceutics. 2005, 309(1): p. 94-100.

202. **Peppas, N.A., J.J. Sahlin,** *A simple equation for the description of solute release. III. Coupling of diffusion and relaxation.* International journal of pharmaceutics, 1989. **57**(2): p. 169-172.

203. **Alley, M.C., Scudiero, D.A., Monks, A., Hursey, M.L., Czerwinski, M.J., Fine, D.L., Abbott, B.J., Mayo, J.G., Shoemaker, R.H., Boyd, M.R.** Feasibility of drug screening with panels of human tumor cell lines using a microculture tetrazolium assay. Cancer research. 1988, 48(3): p. 589-601.

204. **Yang, C.-H., Chou, H.C., Fu, Y.N., Yeh, C.L., Cheng, H.W., Chang, I.C., Liu, K.J., Chang, G.C., Tsai, T.F., Tsai, S.F., Liu, H.P., Wu, Y.C., Chen, Y.T., Huang, S.F., Chen, Y.R.** EGFR over-expression in non-small cell lung cancers harboring EGFR mutations is associated with marked down-regulation of CD82. Biochimica et Biophysica Acta (BBA)-Molecular Basis of Disease. 2015, 1852(7): p. 1540-1549.

205. **Schiller, J.H., Harrington, D., Belani, C.P., Langer, C., Sandler, A., Krook. J., Zhu, J., Johnson, D.H.** Comparison of four chemotherapy regimens for advanced non–small-cell lung cancer. New England Journal of Medicine. 2002, 346(2): p. 92-98.

206. **Wiggenhorn, M.** Scale-Up of Liposome Manufacturing (Doctoral dissertation, lmu) 2007.

207. **Goldbach, P., Brochart, H. and Stamm, A.** Spray-drying of liposomes for a pulmonary administration. II. Retention of encapsulated materials. Drug development and industrial pharmacy. 1993, 19(19): pp.2623-2636.

208. **Sakagami, M.** In vivo, in vitro and ex vivo models to assess pulmonary absorption and disposition of inhaled therapeutics for systemic delivery. Advanced drug delivery reviews. 2006, 58(9-10): pp.1030-1060.

209. **Coelho, S.C., Almeida, G.M., Pereira, M.C., Santos-Silva, F. Coelho, M.A.** Functionalized gold nanoparticles improve afatinib delivery into cancer cells. Expert opinion on drug delivery. 2016, 13(1): pp.133-141.

210. **Lunova, M., Prokhorov, A., Jirsa, M., Hof, M., Olżyńska, A., Jurkiewicz, P., Kubinová, Š., Lunov, O. Dejneka, A.** Nanoparticle core stability and surface functionalization drive the mTOR signaling pathway in hepatocellular cell lines. Scientific reports. 2017, 7(1): p.16049.

211. **Quent, V., Loessner, D., Friis, T., Reichert, J.C., Hutmacher, D.W.** Discrepancies between metabolic activity and DNA content as tool to assess cell proliferation in cancer research. Journal of cellular and molecular medicine. 2010, 14(4): p. 1003-1013.

212.   **Iwaoka, S., Nakamura, T., Takano, S., Tsuchiya, S., Aramaki, Y.** Cationic liposomes induce apoptosis through p38 MAP kinase–caspase-8–Bid pathway in macrophage-like RAW264. 7 cells. Journal of leukocyte biology. 2006, 79(1): p. 184-191.

213.   **Steller, H.** Mechanisms and genes of cellular suicide. Science-AAAS-Weekly Paper Edition. 1995, 267(5203): p. 1445-1449.

214.   **Raff, M.** Cell suicide for beginners. Nature. 1998, 396(6707): p. 119-122.

215.   **Ocak, S., Chaurand, P. Massion, P.P.** Mass Spectrometry–based Proteomic Profiling of Lung Cancer. Proceedings of the American Thoracic Society. 2009, 6(2): p. 159-170.

216.   **Chanin, T.D., Merrick, D.T., Franklin, W.A., Hirsch, F.R.** Recent developments in biomarkers for the early detection of lung cancer: perspectives based on publications 2003 to present. Current opinion in pulmonary medicine. 2004, 10(4): p. 242-247.

217.   **Yap, T.A., Vidal, L., Adam, J., Stephens, P., Spicer, J., Shaw, H., Ang, J., Temple, G., Bell, S., Shahidi, M. Uttenreuther-Fischer, M.** Phase I trial of the irreversible EGFR and HER2 kinase inhibitor BIBW 2992 in patients with advanced solid tumors. Journal of clinical oncology. 2010, 28(25): pp.3965-3972.

218.   **Alaiya, A., Fox, J., Bobis, S., Matic, G., Shinwari, Z., Barhouse, E., MÁRQUEZ, M., Nilsson, S., Holmberg, A.R.** Proteomic analysis of soft tissue tumor implants treated with a novel polybisphosphonate. Cancer Genomics and Proteomics. 2014, 11(1): p. 39-49.

219.   **Wu, Y.-L., Zhou, C., Hu, C.P., Feng, J., Lu, S., Huang, Y., Li, W., Hou, M., Shi, J.H., Lee, K.Y., Xu, C.R., Massey, D., Kim, M., Shi, Y., Geater, S.L.** Afatinib versus cisplatin plus gemcitabine for first-line treatment of Asian patients with advanced non-small-cell lung cancer harbouring EGFR mutations (LUX-Lung 6): an open-label, randomised phase 3 trial. The lancet oncology. 2014, 15(2): p. 213-222.

220.   **Guan, S.-S., Chang, J., Cheng, C.C., Luo, T.Y., Ho, A.S., Wang, C.C., Wu, C.T., Liu, S.H.** Afatinib and its encapsulated polymeric micelles inhibits HER2-overexpressed colorectal tumor cell growth in vitro and in vivo. Oncotarget. 2014, 5(13): p. 4868-4880.

221.   **Zhang, S., Zheng, X., Huang, H., Wu, K., Wang, B., Chen, X. Ma, S.** Afatinib increases sensitivity to radiation in non-small cell lung cancer cells with acquired EGFR T790M mutation. Oncotarget. 2015, 6(8): p.5832-5845.

222.   **Ninomiya, T., Takigawa, N., Ichihara, E., Ochi, N., Murakami, T., Honda, Y., Kubo, T., Minami, D., Kudo, K., Tanimoto, M., Kiura, K.** Afatinib prolongs survival compared with gefitinib in an epidermal growth factor receptor-driven lung cancer model. Molecular cancer therapeutics. 2013, 12(5): p. 589-597.

223.   **Schroit, A.J., Madsen, J., Nayar, R.** Liposome-cell interactions: in vitro discrimination of uptake mechanism and in vivo targeting strategies to mononuclear phagocytes. Chemistry and physics of lipids, 1986. 40(2-4): p. 373-393.

224.   **Chu, C.-J., Dijkstra, J., Lai, M.Z., Hong, K., Szoka, F.C.** Efficiency of cytoplasmic delivery by pH-sensitive liposomes to cells in culture. Pharmaceutical research. 1990, 7(8): p. 824-834.

225.   **Carvalho, T.C., Carvalho, S.R., McConville, J.T.** Formulations for pulmonary administration of anticancer agents to treat lung malignancies. Journal of aerosol medicine and pulmonary drug delivery. 2011, 24(2): p. 61-80.

226.   **Kim, I.-Y., Kang, Y.S., Lee, D.S., Park, H.J., Choi, E.K., Oh, Y.K., Son, H.J., Kim, J.S.** Antitumor activity of EGFR targeted pH-sensitive immunoliposomes encapsulating gemcitabine in A549 xenograft nude mice. Journal of Controlled Release. 2009, 140(1): p. 55-60.

227.   **Makinoshima, H., Takita, M., Matsumoto, S., Yagishita, A., Owada, S., Esumi, H., Tsuchihara, K.** Epidermal growth factor receptor (EGFR) signaling regulates global metabolic pathways in EGFR-mutated lung adenocarcinoma. Journal of Biological Chemistry. 2014, 289(30): p. 20813-20823.

228.   **Xie, S., Wang, C.** Expression of CAP1 and its association with lung cancer in the tumourigenesis and progression. In Respirology. (Vol. 22, pp. 111-112). 111 RIVER ST, Hoboken 07030-5774, NJ USA: WILEY.

229.   **Talaiezadeh, A., Shahriari, A., Tabandeh, M.R., Fathizadeh, P., Mansouri, S.** Kinetic characterization of lactate dehydrogenase in normal and malignant human breast tissues. Cancer cell international. 2015, 15(1): p. 19-28.

230.   **Koukourakis, M.I., Giatromanolaki, A., Simopoulos, C., Polychronidis, A., Sivridis, E.** Lactate dehydrogenase 5 (LDH5) relates to up-regulated hypoxia inducible factor pathway and metastasis in colorectal cancer. Clinical and Experimental Metastasis, 2005. 22(1): p. 25-30.

231.   **Koukourakis, M., Giatromanolaki, A., Sivridis, E., Bougioukas, G., Didilis, V., Gatter, K.C., Harris, AL.** Lactate dehydrogenase-5 (LDH-5) overexpression in non-small-cell lung cancer tissues is linked to tumour hypoxia, angiogenic factor production and poor prognosis. British journal of cancer. 2003, 89(5): p. 877-885.

232.   **Fantin, V.R., St-Pierre, J., Leder, P.** Attenuation of LDH-A expression uncovers a link between glycolysis, mitochondrial physiology, and tumor maintenance. Cancer cell. 2006, 9(6): p. 425-434.

233.   **Xie, S., Shen, C., Tan, M., Li, M., Song, X., Wang, C.** Systematic analysis of gene expression alterations and clinical outcomes of adenylate cyclase-associated protein in cancer. Oncotarget. 2017, 8(16): p. 27216-27239.

234.   **Yamazaki, Takamura, M., Masugi, Y., Mori, T., Du, W., Hibi, T., Hiraoka, N., Ohta, T., Ohki, M., Hirohashi, S., Sakamoto, M.** Adenylate cyclase-associated protein 1 overexpressed in pancreatic cancers is involved in cancer cell motility. Laboratory investigation. 2009, 89(4): p. 425-432.

235.   **Tan, M., Song, X., Zhang, G., Peng, A., Li, X., Li, M. Liu, Y., Wang, C.** Overexpression of adenylate cyclase-associated protein 1 is associated with metastasis of lung cancer. Oncology reports, 2013. 30(4): p. 1639-1644.

236.   **Nahar, K., Gupta, N., Gauvin, R., Absar, S., Patel, B., Gupta, V., Khademhosseini, A. Ahsan, F.** In vitro, in vivo and ex vivo models for studying particle deposition and drug absorption of inhaled pharmaceuticals. European journal of pharmaceutical sciences. 2013, 49(5): pp.805-818.

237.   **Massagué, J.** TGF-β signaling in development and disease. FEBS letters. 2012, 586(14): p. 1833.

238.   **Kubiczkova, L., Sedlarikova, L., Hajek, R., Sevcikova, S.** TGF-β–an excellent servant but a bad master. Journal of translational medicine. 2012, 10(1): p. 183-206.

239.   **Lebrun, J.-J.** The dual role of TGF β in human cancer: from tumor suppression to cancer metastasis. ISRN molecular biology. 2012, 2012: 381428.

240.   **Yang, X.F., Xu, Y., Qu, D.S. Li, H.Y.** The influence of amino acids on aztreonam spray-dried powders for inhalation. asian journal of pharmaceutical sciences. 2015, 10(6): pp.541-548.

241.   **Tawfeek, H., Khidr, S., Samy, E., Ahmed, S., Murphy, M., Mohammed, A., Shabir, A., Hutcheon, G. Saleem, I.** Poly (glycerol adipate-co-ω-pentadecalactone) spray-dried microparticles as sustained release carriers for pulmonary delivery. Pharmaceutical research. 2011, 28(9): pp.2086-2097.

242.   **González-Santiago, A.E., Mendoza-Topete, L.A., Sánchez-Llamas, F., Troyo-Sanromán, R., Gurrola-Díaz, C.M.** TGF-β1 serum concentration as a complementary diagnostic biomarker of lung cancer: establishment of a cut-point value. Journal of clinical laboratory analysis. 2011, 25(4): p. 238-243.

243.   **Goel, A., Baboota, S., Sahni, J.K., Ali, J.** Exploring targeted pulmonary delivery for treatment of lung cancer. International journal of pharmaceutical investigation. 2013, 3(1): p. 8-14.

244.   **Son, Y.-J., McConville, J.T.** Advancements in dry powder delivery to the lung. Drug development and industrial pharmacy. 2008, 34(9): p. 948-959.
245.   **Lu, D. Hickey, A.J.** Liposomal dry powders as aerosols for pulmonary delivery of proteins. AAPS PharmSciTech. 2005, 6(4): p. E641-E648.
246.   **Taylor, K.M. Fan, S.J.** Liposomes for drug delivery to the respiratory tract. Drug development and industrial pharmacy., 1993, 19(1-2): p. 123-142.
247.   **Chow, A.H., Tong, H.H., Chattopadhay, P., Shekunov, B.Y.** Particle engineering for pulmonary drug delivery. Pharmaceutical research. 2007, 24(3): p. 411-437.
248.   **Pulliam, B., Sung, J.C. Edwards, D.A.** Design of nanoparticle-based dry powder pulmonary vaccines. 2007, 4(6): p. 651-663.
249.   **Saluja, V., Saluja, V., Amorij, J.P., Kapteyn, J.C., De Boer, A.H., Frijlink, H.W. and Hinrichs, W.L.J.** A comparison between spray drying and spray freeze drying to produce an influenza subunit vaccine powder for inhalation. Journal of Controlled Release. 2010, 144(2): p.127-133.
250.   **Feng, A., Boraey, M.A., Gwin, M.A., Finlay, P.R., Kuehl, P.J., Vehring, R.** Mechanistic models facilitate efficient development of leucine containing microparticles for pulmonary drug delivery. International journal of pharmaceutics. 2011, 409(1-2): p. 156-163.
251.   **Li, H.-Y., Birchall, J.** Chitosan-modified dry powder formulations for pulmonary gene delivery. Pharmaceutical research. 2006, 23(5): p. 941-950.
252.   **Kato, Y., Onishi, H. Machida, Y.** Application of chitin and chitosan derivatives in the pharmaceutical field. Current Pharmaceutical Biotechnology. 2003, 4(5): p. 303-309.
253.   **Hamman, J.H., Schultz, C., Kotzé, A.F.** N-trimethyl chitosan chloride: optimum degree of quaternization for drug absorption enhancement across epithelial cells. Drug development and industrial pharmacy. 2003, 29(2): p. 161-172.
254.   **Amidi, M., Romeijn, S.G., Borchard, G., Junginger, H.E., Hennink, W.E., Jiskoot, W.** Preparation and characterization of protein-loaded N-trimethyl chitosan nanoparticles as nasal delivery system. Journal of Controlled Release. 2006, 111(1-2): p. 107-116.
255.   **Mao, S., Bakowsky, U., Jintapattanakit, A., Kissel, T.** Self-assembled polyelectrolyte nanocomplexes between chitosan derivatives and insulin. Journal of pharmaceutical sciences. 2006, 95(5): p. 1035-1048.
256.   **Vila, A., Sánchez, A., Janes, K., Behrens, I., Kissel,T., Vila Jato, J.L., Alonso, M.J.** Low molecular weight chitosan nanoparticles as new carriers for nasal vaccine delivery in mice. European Journal of pharmaceutics and biopharmaceutics. 2004,57(1): p. 123-131.
257.   **Bowman, K., Leong, K.W.** Chitosan nanoparticles for oral drug and gene delivery. International journal of nanomedicine. 2006, 1(2): p. 117-128.
258.   **Davis, S.S.** Delivery of peptide and non-peptide drugs through the respiratory tract. Pharmaceutical science & technology today. 1999, 2(11): p. 450-456.
259.   **Cheung, R.C.F., Ng, T.B., Wong, J.H., Chan, W.Y.** Chitosan: An update on potential biomedical and pharmaceutical applications. Marine drugs, 2015. 13(8): p. 5156-5186.
260.   **Grainger, C.I., Alcock, R., Gard, T.G., Quirk, A.V., van Amerongen, G., De Swart, R.L., Hardy, J.G.** Administration of an insulin powder to the lungs of cynomolgus monkeys using a Penn Century insufflator. International journal of pharmaceutics. 2004, 269(2), p.523-527.
261.   **Lee, S.L., Adams, W.P., Li, B.V., Conner, D.P., Chowdhury, B.A., Lawrence, X.Y.** In vitro considerations to support bioequivalence of locally acting drugs in dry powder inhalers for lung diseases. The AAPS journal. 2009, 11(3): p.414-423.
262.   **Naikwade, S.R., Bajaj, A.N., Gurav, P., Gatne, M.M., Soni, P.S.** Development of budesonide microparticles using spray-drying technology for pulmonary administration:

design, characterization, in vitro evaluation, and in vivo efficacy study. AAPS PharmSciTech. 2009, 10(3): p.993-1012.

263.	**Takeuchi, H., Thongborisute, J., Matsui, Y., Sugihara, H., Yamamoto, H., Kawashima, Y.** Novel mucoadhesion tests for polymers and polymer-coated particles to design optimal mucoadhesive drug delivery systems. Advanced drug delivery reviews. 2005, 57(11): p. 1583-1594.

264.	**Takeuchi, H., Yamamoto, H., Niwa, T., Hino, T., Kawashima, Y.** Enteral absorption of insulin in rats from mucoadhesive chitosan-coated liposomes. Pharmaceutical research. 1996. 13(6): p. 896-901.

265.	C**harnvanich, D., Vardhanabhuti, N. Kulvanich, P.** Effect of cholesterol on the properties of spray-dried lysozyme-loaded liposomal powders. AAPS PharmSciTech. 2010, 11(2): p. 832-842.

266.	**Karadag, A., Özçelik, B., Sramek, M., Gibis, M., Kohlus, R., Weiss, J.** Presence of electrostatically adsorbed polysaccharides improves spray drying of liposomes. Journal of food science. 2013, 78(2): p. E206-E221.

267.	**Lo, Y.-l., Tsai, J.-c. Kuo, J.-h.** Liposomes and disaccharides as carriers in spray-dried powder formulations of superoxide dismutase. Journal of Controlled Release. 2004, 94(2-3): p. 259-272.

268.	**Chougule, M., Padhi, B. Misra, A.** Development of spray dried liposomal dry powder inhaler of dapsone. AAPS PharmSciTech. 2008, 9(1): p. 47-53·

269.	**Kunda, N.K., Alfagih, I.M., Dennison, S.R., Tawfeek, H.M.,** Somavarapu, S., Hutcheon, G.A. and Saleem, I.Y. Bovine serum albumin adsorbed PGA-co-PDL nanocarriers for vaccine delivery via dry powder inhalation. Pharmaceutical research. 2015, 32(4), pp.1341-1353.

270.	**Zhang, T., Youan, B.-B.C.** Analysis of process parameters affecting spray-dried oily core nanocapsules using factorial design. AAPS PharmSciTech. 2010,11(3): p. 1422-1431.

271.	**Huang, W.H., Yang, Z.J., Wu, H., Wong, Y.F., Zhao, Z.Z., Liu, L.** Development of liposomal salbutamol sulfate dry powder inhaler formulation. Biological and Pharmaceutical Bulletin. 2010, 33(3): p. 512-517.

272.	**Duret, C., Wauthoz, N., Merlos, R., Goole, J., Maris, C., Roland, I., Sebti, T., Vanderbist, F., Amighi, K.** In vitro and in vivo evaluation of a dry powder endotracheal insufflator device for use in dose-dependent preclinical studies in mice. European Journal of Pharmaceutics and Biopharmaceutics. 2012, 81(3): p. 627-634.

273.	**Parlati, C., Colombo, P., Buttini, F., Young, P.M., Adi, H., Ammit, A.J., Traini, D.** Pulmonary spray dried powders of tobramycin containing sodium stearate to improve aerosolization efficiency. Pharmaceutical research. 2009, 26(5): p. 1084-1092.

274.	**Clark, A.R. Hollingworth, A.M.** The relationship between powder inhaler resistance and peak inspiratory conditions in healthy volunteers—implications for in vitro testing. Journal of aerosol medicine. 1993, 6(2): pp.99-110.

275.	**Wong, W., Crapper, J., Chan, H.K., Traini, D., Young, P.M.** Pharmacopeial methodologies for determining aerodynamic mass distributions of ultra-high dose inhaler medicines. Journal of pharmaceutical and biomedical analysis. 2010, 51(4), p.853-857.

276.	 **Kastner, E., Verma, V., Lowry, D., Perrie, Y.** Microfluidic-controlled manufacture of liposomes for the solubilisation of a poorly water soluble drug. International journal of pharmaceutics. 2015, **485**(1-2): p. 122-130.

277.	**Stevanovic, M. Uskokovic, D.** Poly (lactide-co-glycolide)-based micro and nanoparticles for the controlled drug delivery of vitamins. Current Nanoscience. 2009, 5(1): p. 1-14.

278.   **Li, H.-Y., Neill, H., Innocent, R., Seville, P., Williamson, I., Birchall, J.C.** Enhanced dispersibility and deposition of spray-dried powders for pulmonary gene therapy. Journal of drug targeting. 2003, 11(7): p. 425-432.

279.   **Sou, T., Kaminskas, L.M., Nguyen, T.H., Carlberg, R., McIntosh, M.P., Morton, D.A.** The effect of amino acid excipients on morphology and solid-state properties of multi-component spray-dried formulations for pulmonary delivery of biomacromolecules. European Journal of Pharmaceutics and Biopharmaceutics. 2013, 83(2): p. 234-243.

280.   **Learoyd, T.P., Burrows, J.L., French, E., Seville, P.C.** Chitosan-based spray-dried respirable powders for sustained delivery of terbutaline sulfate. European journal of pharmaceutics and biopharmaceutics. 2008, 68(2): p. 224-234.

281.   **Cevher, E., Orhan, Z., Mülazımoğlu, L., Şensoy, D., Alper, M., Yıldız, A., Özsoy, Y.** Characterization of biodegradable chitosan microspheres containing vancomycin and treatment of experimental osteomyelitis caused by methicillin-resistant Staphylococcus aureus with prepared microspheres. International journal of pharmaceutics. 2006, 317(2): p.127-135.

282.   **Tonon, R.V., Freitas, S.S., Hubinger, M.D.** Spray drying of açai (Euterpe oleraceae Mart.) juice: Effect of inlet air temperature and type of carrier agent. Journal of Food Processing and Preservation. 2011, 35(5): p. 691-700.

283.   **He, P., Davis, S.S., Illum, L.** Chitosan microspheres prepared by spray drying. International journal of pharmaceutics. 1999, 187(1): p. 53-65.

284.   **Wang, L., Zhang, Y., Tang, X.** Characterization of a new inhalable thymopentin formulation. International journal of pharmaceutics. 2009, 375(1-2): p. 1-7.

285.   **Chew, N.Y., Tang, P., Chan, H.K., Raper, J.A.** How much particle surface corrugation is sufficient to improve aerosol performance of powders?. Pharmaceutical Research. 2005, 22(1): p.148-152.

286.   **Lentz, B.R., Carpenter, T.J., Alford, D.R.** Spontaneous fusion of phosphatidylcholine small unilamellar vesicles in the fluid phase. *Biochemistry.* 1987, *26*(17): p.5389-5397.

287.   **Manca, M.L., Manconi, M., Valenti, D., Lai, F., Loy, G., Matricardi, P. and Fadda, A.M.** Liposomes coated with chitosan–xanthan gum (chitosomes) as potential carriers for pulmonary delivery of rifampicin. Journal of pharmaceutical sciences. 2012, *101*(2): p.566-575.

288.   **Kofuji, K., Akamine, H., Qian, C.J., Watanabe, K., Togan, Y., Nishimura, M., Sugiyama, I., Murata, Y., Kawashima, S.** Therapeutic efficacy of sustained drug release from chitosan gel on local inflammation. International journal of pharmaceutics. 2004, 272(1-2): p. 65-78.

289.   **Martinac, A., Filipović-Grcić, J., Perissutti, B., Voinovich, D., Pavelić, Z.** Spray-dried chitosan/ethylcellulose microspheres for nasal drug delivery: swelling study and evaluation of in vitro drug release properties. Journal of microencapsulation. 2005, 22(5): p. 549-561.

290.   **Filipović-Grčić, J., Perissutti, B., Moneghini, M., Voinovich, D., Martinac, A., Jalsenjak, I.** Spray-dried carbamazepine-loaded chitosan and HPMC microspheres: preparation and characterisation. Journal of pharmacy and pharmacology. 2003, 55(7): p. 921-931.

291.   **Cain, J.** An alternative technique for determining ANSI/CEMA standard 550 flowability ratings for granular materials. Powder Handling & Processing. 2002, 14(3): p. 218-220

292.   **Wu, X., Zhang, W., Hayes, D.J.r., Mansour, H.M.** Physicochemical characterization and aerosol dispersion performance of organic solution advanced spray-dried cyclosporine A multifunctional particles for dry powder inhalation aerosol delivery. International journal of nanomedicine. 2013, 8: p. 12691283.

293. **Duan, J., Vogt, F.G., Li, X., Hayes, D.J.r., Mansour, H.M.** Design, characterization, and aerosolization of organic solution advanced spray-dried moxifloxacin and ofloxacin dipalmitoylphosphatidylcholine (DPPC) microparticulate/nanoparticulate powders for pulmonary inhalation aerosol delivery. International journal of nanomedicine. 2013, 8: p. 3489-3505.

294. **Rabbani, N.R., Seville, P.C.** The influence of formulation components on the aerosolisation properties of spray-dried powders. Journal of controlled release. 2005, 110(1): p. 130-140.

295. **Slabbert, C., Du Plessis, L.H. Kotzé, A.F.** Evaluation of the physical properties and stability of two lipid drug delivery systems containing mefloquine. International journal of pharmaceutics. 2011, 409(1-2): pp.209-215.

296. **GRIT, M., ZUIDAM, N.J., UNDERBERG, W.J. CROMMELIN, D.J.** Hydrolysis of partially saturated egg phosphatidylcholine in aqueous liposome dispersions and the effect of cholesterol incorporation on hydrolysis kinetics. Journal of pharmacy and pharmacology. 1993, 45(6): pp.490-495.

297. **Frokjaer, S., Hjorth, E.L. Worts, O.** Stability testing of liposomes during storage. Liposome technology. 1984, 1: pp.235-245.

298. http://www.ema.europa.eu/docs/en_GB/document_library/EPAR__Product_Infor mation/human/002280/WC500152392.pdf.

299. **Viljoen, J.M., Steenekamp JH, Marais AF, Kotzé AF.** Effect of moisture content, temperature and exposure time on the physical stability of chitosan powder and tablets. Drug development and industrial pharmacy. 2014, 40(6): p. 730-742.

300. **Cervera, M.F., Cervera, M.F., Karjalainen, M., Airaksinen, S., Rantanen, J., Krogars, K., Heinämäki, J., Colarte, A.I. and Yliruusi, J.** Physical stability and moisture sorption of aqueous chitosan–amylose starch films plasticized with polyols. European journal of pharmaceutics and biopharmaceutics. 2004, 58(1): p. 69-76.

301. **Lim, L.Y., Khor, E. Ling, C.E.** Effects of dry heat and saturated steam on the physical properties of chitosan. Journal of Biomedical Materials Research Part A, 1999. 48(2): p. 111-116.

302. **Singh, D.J., Lohade, A.A., Parmar, J.J., Hegde, D.D., Soni, P., Samad, A., Menon, M.D.** Development of chitosan-based dry powder inhalation system of cisplatin for lung cancer. *Indian journal of pharmaceutical sciences.* 2012, *74*(6): p.521-526.

303. **Yang, J., Kim, Y.K., Kang, T.S., Jee, Y.K. and Kim, Y.Y.** Importance of indoor dust biological ultrafine particles in the pathogenesis of chronic inflammatory lung diseases. Environmental Health and Toxicology. 2017, 32: e2017021.

304. **Arora, S., Tyagi, N., Bhardwaj, A., Rusu, L., Palanki, R., Vig, K., Singh, S.R., Singh, A.P., Palanki, S., Miller, M.E., Carter, J.E., Singh, S.** Silver nanoparticles protect human keratinocytes against UVB radiation-induced DNA damage and apoptosis: potential for prevention of skin carcinogenesis. Nanomedicine: Nanotechnology, Biology and Medicine. 2015, 11(5): p. 1265-1275.

305. **Muralidharan, P., Malapit, M., Mallory, E., DonHayes, J.r., Mansour, H.M**. Inhalable nanoparticulate powders for respiratory delivery. Nanomedicine: Nanotechnology, Biology and Medicine. 2015, 11(5): p. 1189-1199.

306. **Tiwari, G., Tiwari, R., Sriwastawa, B., Bhati, L., Pandey, S., Pandey, P., Bannerjee, S.K.** Drug delivery systems: An updated review. International journal of pharmaceutical investigation. 2012, 2(1): p.2-11.

307. **Mahmud, M., Piwoni, A., Filipczak, N., Janicka, M., Gubernator, J.** Long-circulating curcumin-loaded liposome formulations with high incorporation efficiency, stability and anticancer activity towards pancreatic adenocarcinoma cell lines in vitro. PloS one. 2017, 11(12): e0167787.

308.   **Mayer, L.D., Tai, L.C., Ko, D.S., Masin, D., Ginsberg, R.S., Cullis, P.R., Bally, M.B.** Influence of vesicle size, lipid composition, and drug-to-lipid ratio on the biological activity of liposomal doxorubicin in mice. Cancer research. 1989, 49(21): p. 5922-5930.

309.   **Kan, P., Tsao, C.-W., Wang, A.-J., Su, W.-C., Liang, H.-F.** A liposomal formulation able to incorporate a high content of Paclitaxel and exert promising anticancer effect. Journal of drug delivery. 2011, 2011: 629234.

310.   **Chen, Y., Sun, J., Lu, Y., Tao, C., Huang, J., Zhang, H., Yu, Y., Zou, H., Gao, J., Zhong, Y.** Complexes containing cationic and anionic pH-sensitive liposomes: comparative study of factors influencing plasmid DNA gene delivery to tumors. International journal of nanomedicine. 2013, 8: p. 1573-1593.

311.   **Reddy, T.L., Garikapati, K.R., Reddy, S.G., Reddy, B.V., Yadav, J.S., Bhadra, U., Bhadra, M.P.** Simultaneous delivery of Paclitaxel and Bcl-2 siRNA via pH-Sensitive liposomal nanocarrier for the synergistic treatment of melanoma. Scientific reports. 2016, 6: p. 35223.

312.   **Koutsoulas, C., Pippa, N., Demetzos, C., Zabka, M.** Preparation of liposomal nanoparticles incorporating terbinafine in vitro drug release studies. Journal of nanoscience and nanotechnology. 2014, 14(6): p. 4529-4533.

313.   **Modi, S., Anderson, B.D.** Determination of drug release kinetics from nanoparticles: overcoming pitfalls of the dynamic dialysis method. Molecular pharmaceutics. 2013, 10(8): p. 3076-3089.

314.   **Yang, J.C.H., Wu, Y.L., Schuler, M., Sebastian, M., Popat, S., Yamamoto, N., Zhou, C., Hu, C.P., O'Byrne, K., Feng, J. and Lu, S.** Afatinib versus cisplatin-based chemotherapy for EGFR mutation-positive lung adenocarcinoma (LUX-Lung 3 and LUX-Lung 6): analysis of overall survival data from two randomised, phase 3 trials. The lancet oncology, 2015. 16(2): p. 141-151.

315.   **Li, H.Y., Seville, P.C., Williamson, I.J., Birchall, J.C.** The use of amino acids to enhance the aerosolisation of spray-dried powders for pulmonary gene therapy. The journal of gene medicine, 2005. 7(3): p. 343-353.

316.   **Li, H.Y., Seville, P.C., Williamson, I.J., Birchall, J.C.** The use of absorption enhancers to enhance the dispersibility of spray-dried powders for pulmonary gene therapy. The journal of gene medicine. 2005, 7(8): p. 1035-1043.

317.   **Li, H.-Y., Seville, P.C.** Novel pMDI formulations for pulmonary delivery of proteins. International journal of pharmaceutics. 2010, 385(1-2): p. 73-78.

318.   **Li, H.-Y., Song, X., Seville, P.C.** The use of sodium carboxymethylcellulose in the preparation of spray-dried proteins for pulmonary drug delivery. European Journal of Pharmaceutical Sciences. 2010, 40(1): p. 56-61.

319.   **Bosquillon, C., Rouxhet, P.G., Ahimou, F., Simon, D., Culot, C., Préat, V., Vanbever, R.** Aerosolization properties, surface composition and physical state of spray-dried protein powders. Journal of Controlled Release. 2004, 99(3): p. 357-367.

320.   **Seville, P.C., Learoyd, T.P., Li, H.Y., Williamson, I.J., Birchall, J.C.** Amino acid-modified spray-dried powders with enhanced aerosolisation properties for pulmonary drug delivery. Powder technology. 2007, 178(1): p. 40-50.

321.   **SHEU, T.Y., Rosenberg, M.** Microstructure of microcapsules consisting of whey proteins and carbohydrates. Journal of Food Science. 1998, 63(3): p. 491-494.

322.   **Luangtana-anan, M., Opanasopit, P., Ngawhirunpat, T., Nunthanid, J., Sriamornsak, P., Limmatvapirat, S. and Lim, L.Y.** Effect of chitosan salts and molecular weight on a nanoparticulate carrier for therapeutic protein. Pharmaceutical development and technology. 2005, 10(2): p. 189-196.

323.   **Zaru, M., Manca, M.L., Fadda, A.M., Antimisiaris, S.G.** Chitosan-coated liposomes for delivery to lungs by nebulisation. Colloids and surfaces B: Biointerfaces. 2009, 71(1): p. 88-95.

324. **Dubey, R.R., Parikh, R.H.** Two-stage optimization process for formulation of chitosan microspheres. AAPS PharmSciTech. 2004, 5(1): p. 20-28.

325. **Meenach, S.A., Vogt, F.G., Anderson, K.W., Hilt, J.Z., McGarry, R.C., Mansour, H.M.** Design, physicochemical characterization, and optimization of organic solution advanced spray-dried inhalable dipalmitoylphosphatidylcholine (DPPC) and dipalmitoylphosphatidylethanolamine poly (ethylene glycol)(DPPE-PEG) microparticles and nanoparticles for targeted respiratory nanomedicine delivery as dry powder inhalation aerosols. International journal of nanomedicine. 2013, 8: p.275-293.

326. **Yang, Y.M., Zhao, Y.H., Liu, X.H., Ding, F., Gu, X.S.** The effect of different sterilization procedures on chitosan dried powder. Journal of applied polymer science. 2007, 104(3): p.1968-1972.

327. **Photos, P.J., Bacakova, L., Discher, B., Bates, F.S., Discher, D.E.** Polymer vesicles in vivo: correlations with PEG molecular weight. Journal of Controlled Release. 2003, 90(3): p. 323-334.

328. **Ahmed, F., Pakunlu, R.I., Srinivas, G., Brannan, A., Bates, F., Klein, M.L., Minko, T., Discher, D.E.** Shrinkage of a rapidly growing tumor by drug-loaded polymersomes: pH-triggered release through copolymer degradation. Molecular pharmaceutics. 2006, 3(3): p. 340-350.

329. **Wang, H., Zhao, P., Su, W., Wang, S., Liao, Z., Niu, R., Chang, J.** PLGA/polymeric liposome for targeted drug and gene co-delivery. Biomaterials. 2010, 31(33): p. 8741-8748.

330. **Moretton, M.A., Cagel, M., Bernabeu, E., Gonzalez, L., Chiappetta, D.A.** Nanopolymersomes as potential carriers for rifampicin pulmonary delivery. Colloids and Surfaces B: Biointerfaces. 2015, 136: p. 1017-1025.

331. **Romero-Calvo, I., Ocón, B., Martínez-Moya, P., Suárez, M.D., Zarzuelo, A., Martínez-Augustin, O. and de Medina, F.S.** Reversible Ponceau staining as a loading control alternative to actin in Western blots. Analytical biochemistry. 2010, 401(2): p. 318-320.